Characterizing the Binding Potential, Activity, and Bioaccessibility of Peroxisome Proliferator Activated Receptor Gamma (PPARγ) Ligands in Indoor Dust

Mingliang Fang

Environment

Duke University

Date:_____

Approved:

_____

Heather M. Stapleton, Supervisor

_____

Thomas F. Webster

_____

Richard T. Di Giulio

_____

P. Lee Ferguson

_____

Heather B. Patisaul

Dissertation submitted in partial fulfillment of requirements

for the degree of Doctor of Philosophy

in Environment in the Graduate School of

Duke University

2015

ABSTRACT

Characterizing the Binding Potential, Activity, and Bioaccessibility of Peroxisome Proliferator Activated Receptor Gamma (PPARγ) Ligands in Indoor Dust

by

Mingliang Fang

Environment

Duke University

Date:_____

Approved:

_____

Heather M. Stapleton, Supervisor

_____

Thomas F. Webster

_____

Richard T. Di Giulio

_____

P. Lee Ferguson

_____

Heather B. Patisaul

An abstract of a dissertation submitted in partial

fulfillment of the requirements for the degree

of Doctor of Philosophy in Environment

in the Graduate School of

Duke University

2015

Abstract

Accumulating evidence is suggesting that exposure to some environmental contaminants may alter adipogenesis, resulting in accumulation of adipocytes, and often significant weight gain. Thus these types of contaminants are often referred to as obesogens. Many of these contaminants act via the activation (i.e. agonism) of the peroxisome proliferator activated receptor γ (PPARγ) nuclear receptor. To date, very few chemicals have been identified as possible PPARγ ligands. In the thesis, our goal was to determine the PPARγ ligand binding potency and activation of several groups of major semi-volatile organic compounds (SVOCs) that are ubiquitously detected in indoor environments, including flame retardants such as polybrominated diphenyl ethers (PBDEs) and Firemaster 550 (FM550), and other SVOCs such as phthalates, organotins, halogenated phenols and bisphenols. Additional attention was also given to the potential activity of the major metabolites of several of these compounds. Since the primary sink for many of these SVOCs is dust, and dust ingestion has been confirmed as an important pathway for SVOCs accumulation in humans, the potential PPARγ binding and activation in extracts from environmentally relevant dust samples was also investigated.

Previous studies have also shown that SVOCs sorbed to organic matrices (e.g., soil and sediment), were only partially bioaccessible (bioavailable), but it was unclear how bioaccessible these compounds are from indoor dust matrices. In addition, bioactivation of SVOCs (via metabolism) could exacerbate their PPARγ potency. Therefore, to adequately assess the potential risk of PPARγ activation from exposure to SVOC

mixtures in house dust, it is essential that one also investigates the bioaccessibility and bioactivation of these chemicals following ingestion.

In the first research aim of this thesis, the bioaccessibility and bioactivation of several important SVOCs in house dust was investigated. To accomplish this, Tenax beads (TA) encapsulated within a stainless steel insert were used as an infinite adsorption sink to estimate the dynamic absorption of a suite of flame retardants (FRs) commonly detected in indoor dust samples, and from a few polyurethane foam samples for comparison. Experimental results demonstrate that the bioaccessibility and stability of FRs following ingestion varies both by chemical and by matrix. Organophosphate flame retardants (OPFRs) had the highest estimated bioaccessibility (~80%) compared to brominated compounds (e.g. PBDEs), and values generally decreased with increasing Log K_{ow}, with <30% bioaccessibility measured for the most hydrophobic compound tested, BDE209. In addition, the stability of the more labile SVOCs that contained ester groups (e.g. OPFRs and 2-ethylhexyl-tetrabromo-benzoate (TBB)) were examined in a simulated digestive fluid matrix. No significant changes in the OPFR concentrations were observed in this fluid; however, TBB was found to readily hydrolyze to tetrabromobenzoic acid (TBBA) in the intestinal fluid in the presence of lipases.

In research aims 2 and 3, two commercially available high-throughput bioassays, a fluorescence polarization PPARγ ligand binding assay (PolarScreen™ PPARγ-competitor assay kit, Invitrogen, Aim 2) and a PPARγ reporter gene assay (GeneBLAzer PPARγ non-DA Assay, Invitrogen, Aim 3) were used to investigate the binding potency and activation of several groups of SVOCs and dust extracts with human PPARγ LBD;

respectively. In the PPARγ binding assay (Aim 2), most of the tested compounds exhibited dose-dependent binding to PPARγ. Mono(2-ethylhexyl) tetrabromophthalate (TB-MEHP), halogenated bisphenol/phenols, triphenyl phosphate and hydroxylated PBDEs were found to be potent or moderate PPARγ ligands, based on the measured ligand binding dissociation constant (Kd). The most potent compound was 3-OH-BDE47, with an IC_{50} of 0.24 μM. The extent of halogenation and the position of the hydroxyl group strongly affected binding. Of the dust samples tested, 21 of 24 samples showed significant PPARγ binding potency at a concentration of 3 mg dust equivalents (DEQ)/mL. In the PPARγ reporter assay (Aim 3), many SVOCs or their metabolites were either confirmed (based on previous reports) or for the first time were found to be potential PPARγ agonists with various potency and efficacy. We also observed that 15 of 25 dust extracts examined showed an activation percentage more than 8% (calculated activation threshold) of the maximal activation induced by rosiglitazone (positive control). In some cases, activation was as high as 50% of the rosiglitazone activation for the dust extracts with the highest efficacy. Furthermore, the correlation between the reporter assay and the ligand binding assay among the house dust extracts was significant and positive ($r = 0.7$, $p < 0.003$), suggesting the binding potency was predicting activation. In research aim 2, the effect of bioactivation on the PPARγ binding potency was also investigated. In vitro bioactivation of house dust extracts incubated with rat and human hepatic S9 fractions was used to investigate the role of in vivo biotransformation on PPAR gamma activity. The result showed that metabolism may

lead to an increased binding affinity, as a 3–16% increase in PPARγ binding activity was observed following bioactivation of the dust extracts.

In research aim 4, an effect-directed analysis (EDA) was used to identify compounds likely contributing to the observed PPARγ activity among the dust extract. Three dust extracts which showed significant PPARγ activity with approximately 25, 30, and 50% of the maximal response induced by rosiglitazone at the highest efficacy were fractionated using normal phase high-performance liquid chromatography (NP-HPLC) and each fraction was individually tested for PPARγ activity. Active fractions were then analyzed using gas-chromatography mass spectrometry (GC-MS) and possible compounds identified. Three dust extracts showed a similar PPARγ activity distribution among the NP-HPLC fractions. In the most active fractions, fatty acids (FAs) were identified as the most active chemicals. The concentrations of four FAs were measured in the house dust extracts, and the concentrations were found to be highly correlated with the observed PPARγ activity. These four FAs were also tested for PPARγ activity and found to be partial PPARγ agonists, particularly oleic and myristic acid. To tentatively identify sources of FAs, FAs in human/animal hair, dead skin cells, and two brands of cooking oil were analyzed. We found the same FAs in those samples and there concentrations were relatively abundant, ranging from 186 to 14,868 μg/g. Therefore, these results suggest that FAs are likely responsible for the observed PPARγ activity in indoor dust. Also, this is the first study reporting on the level of FAs in dust samples. The source of these FAs in dust may be either from the cooking or accumulation of human/animal cells in indoor dust.

In conclusion, this research demonstrates that many SVOCs ubiqutiously detected in house dust, and/or their metabolites, can be weak or moderate PPARγ ligands. In addition, chemical mixtures in house dust can effectively bind to and activate PPARγ. However, our results suggest FAs are probably responsible for these observations, and likely outcompeting the synthetic environmental contaminants present in the dust extract. Furthermore, bioactivation of contaminants present in house dust can potentially increase their affinity for PPARγ. And lastly, the bioaccessibility and stability of SVOCs in house dust after ingestion are likely to modulate the PPARγ activity in the environmental mixtures and should be considered in future risk assessments.

Contents

List of Tables

List of Figures

List of Abbreviations

15d-PJG2	15-Deoxy-D12,14-prostaglandin J2
2,4,6-TBP	2,4,6-tribromophenol
2,4,6-TCP	2,4,6,-trichlorophenol
2,4,6-TFP	2,4,6-trifluorophenol
2,4,6-TIP	2,4,6-triiodophenol
31d-PA	31-deuterated palmitic acid
3-OH-BDE47	3-hydroxide-2,2',4,4'-tetrabromodiphenyl ether
5-OH-BDE47	5-hydroxide-2,2',4,4'-tetrabromodiphenyl ether
6-OH-BDE47	6-hydroxide-2,2',4,4'-tetrabromodiphenyl ether
AMDIS	Automated mass spectral deconvolution and identification system
AA	Arachidic acid
ATV_{max}	Maximal activation%
AzA	Azelaic acid
BA	Behenic acid
BBP	Benzyl butyl phthalate
BC	Black carbon content
BDE47	2,2',4,4'-tetrabromodiphenyl ether
BDE99	2,2′,4,4′,5-pentabromodiphenyl ether
BEHF	Bis(2-ethylhexyl) fumarate
BPA	Bisphenol A
CDC	Centers for Disease Control and Prevention
CHO	Chinese Hamster Ovary
CYP1A	Cytochrome P4501A
DBP	Dibutyl phthalate
DCM	Dichloromethane
DDE	1,1-Dichloro-2,2-bis(p-chlorophenyl) ethylene
DEHP	Bis(2-ethylhexyl) phthalate
DEP	Diethyl phthalate
DEQ	dust equivalent quantity
DEQ	Dust equivalent quantity
DHA	Docosahexaenoic acid
Di-ITP	Di-isopropylated triaryl phosphates
DiNP	Diisononyl phthalate
DMSO	Dimethyl sulfoxide
DPP	biphenyl phosphate
DTT	DL-dithiothreitol
EDA	Effect-directed analysis
EI	Electron ionization
FB	Fluorescence background
F-BDE69	monofluorinated tetrabrominated diphenyl ether
FM550	Firemaster 550

FP	Fluorescence polarization
GC-MS	Gas chromatography mass spectrometry
GPC	Gel permeation chromatography
HDM	Hexadecanamide
ITP	isopropylated triphenyl phosphate
ITP	Isopropylated triaryl phosphates (Mixture)
LA	Lauric acid
LBD	Ligand-binding domain
LC-MS/MS	Liquid-chromatography mass spectrometry
Log K_{OA}	octanol-air partitioning coefficient
MA	Myristic acid
MDL	Method detection limit
MEHP	Mono(2-ethylhexyl) phthalate
MEHP	Mono(2-ethylhexyl)phthalate
Mono-ITP	Mono-isopropylated triaryl phosphates
MP	Polarization value
MRM	Multiple-reaction monitoring mode
MTB	Monobutyltin
NCI	Negative chemical ionization mode
NIST	National Institute of Standards and Technology
NOAEL	Non-observable adverse effect level
NP-HPLC	Normal phase high performance liquid chromatography
OA	Oleic Acid
ODM	Octadecanamide
OH-PBDEs	Hydroxylated polybrominated diphenyl ethers
OM	Oleamide
OPFRs	Organophosphate flame retardants
PA	Palmitic acid
PAHs	Polycyclic aromatic hydrocarbon
PBDE	Polybrominated diphenyl ether
PDA	Pentadecanoic acid
PentaBDE	Pentabrominated diphenyl ethers
PFCs	Perfluorinated chemicals
pKa	Acid dissociation constant
POA	Palmitoleic acid
PP	Piperine
PPARγ	Peroxisome proliferator activated receptor γ
PUF	Polyurethane foam
RP-HPLC	Reverse-phase HPLC
RXR	Retinoid X nuclear receptor
RT	Retention time
S/N	Signal-to-noise ratio
SA	Stearic acid

SRM	Standard Reference Material
SVOCs	Semi-volatile organic compounds
TA	Tenax beads
TBB/EH-TBB	2-ethylhexyl-2,3,4,5-tetrabromobenzoate
TBBA	2,3,4,5-tetrabromo benzoic acid
TBBPA	2,2′,6,6′-Tetrabromobisphenol A
TBEP	Tris(2-butoxyethyl) phosphate
TBMEHP	Tetrabromo mono(2-ethylhexyl)phthalate
TBPDP	Tert-butyl phenyl diphenyl phosphate
TBPH/BEH-TEBP	Bis(2-ethylhexyl) tetrabromophthalate
TBPP	Tris (4, tert-butyl-phenyl) phosphate
TBT	Tributyltin chloride
TBuP	Tributylphosphate
TCBPA	3,3′,5,5′-tetrachlorobisphenol A
TCEP	Tris(2-carboxyethyl)phosphate
TCIPP/TCPP	Tris (1-chloro-2-propyl) phosphate
TCPP	Tris (1-chloro-2-propyl) phosphate
TCS	Triclosan
TDCPP/TDCIPP	Tris(1,3-dichloro-2-propyl)phosphate
TIC	Total ion chromatography
TOC	Total organic carbon
TPP/TPHP	Triphenyl phosphate
TPPi	Triphenylphosphite
TPT	Triphenyltin chloride
Tri-ITP	Tri-isopropylated triaryl phosphates
β-NADPH	β-nicotinamide adenine dinucleotide 2′-phosphate reduced tetrasodium salt hydrate
15d-PJG2	15-Deoxy-D12,14-prostaglandin J2

1. Introduction

1.1 Overview of Research

Young children and infants in particular spend a majority of their time (> 95%) indoors where they are chronically exposed to semi-volatile organic compounds (SVOCs) in dust due to their high hand to mouth activity and crawling behavior. Several SVOCs commonly detected in indoor dust are considered "environmental obesogens", which are defined as chemicals that alter lipid homeostasis and fat storage, alter metabolic set points, or disrupt energy balance, resulting in fat accumulation and obesity. Several recent studies have suggested that perinatal exposure to obesogens may result in an increased odds of obesity in children as reviewed in (Amanda Janesick and Bruce Blumberg 2011). Examples of potential obesogens include phthalates (like DEHP), organotins, the flame retardant (FR) mixture Firemaster® 550 (FM550), perfluorinated chemicals (PFCs) and bisphenol A (BPA). Current research also suggests that many of these compounds act via a mechanism that includes cellular activation of peroxisome proliferator-activated nuclear receptors (PPARs). Many of these SVOCs are abundant in the house dust, and thus exposure to mixtures of these compounds may be associated with obesity or weight gain. Previous studies have also shown that SVOCs sorbed to organic matrices (e.g., soil and sediment), were only partially bioavailable, but it was unclear how bioavailable these compounds are from indoor dust. In addition, bioactivation of SVOCs (from metabolism) could exacerbate their PPARγ potency. Therefore, to adequately assess the potential risk of PPARγ activation from exposure to

SVOC mixtures in house dust, it is essential that one also investigate the bioaccessibility and bioactivation of those chemicals following exposure.

Based on these facts, I hypothesized that chemical mixtures in house dust have PPARγ activity. In addition, bioaccessibility and bioactivation of some of the SVOCs will modulate PPARγ activity in the house dust. Thus, the specific aims of this thesis are:

Aim 1: Examine the bioaccessibility of several SVOCs commonly detected in house dust using an *in-vitro* sorptive physiologically-based model. [Chapter 2];

Aim 2: Characterize the ligand binding activity of several SVOCs (individually), their metabolites, and extracts of indoor dust before and after bioactivation in human PPARγ. [Chapter 3];

Aim 3: Examine the transactivation of identified ligands in Aim 2 and extracts of indoor dust in human PPARγ. [Chapter 4];

Aim 4: Non-targeted screening of primary PPARγ ligands in house dust using Effect-Directed Analysis (EDA). [Chapter 5];

The remainder of this introduction provides brief background information on the PPARγ nuclear receptor, and a discussion of its natural and exogenous ligands. In addition, the environmental levels of these ligands, particularly in indoor environments, and potential human exposure to those ligands, along with their potential health risks, will be discussed. Also included is an overview of an effect-directed analysis (EDA), and the rationale for including this approach/methodology in this thesis.

1.2 Proliferator Activated Receptor (PPAR) Nuclear Receptor

PPARs are master transcriptional regulators controlling intracellular lipid flux and adipocyte proliferation and differentiation. Heterodimerized with the retinoid X receptor (RXR), PPARs serve as metabolic ligand sensors for a variety of hormones, dietary fatty acids, and their metabolites (Grün and Blumberg 2009). To date, three isoforms of PPARs, i.e., α (alpha), β/δ (beta), and γ (gamma), have been identified (Y Zhang et al. 2014). PPARα is primarily expressed in liver, kidney, heart, muscle, and adipose tissue. PPARβ is expressed in many tissues but markedly in brain, adipose tissue, and skin. And PPARγ is expressed in three forms through alternative splicing: γ1 expressed in virtually all tissues, including heart, muscle, colon, kidney, pancreas, and spleen; γ2 expressed mainly in adipose tissue (30 amino acids longer than γ1) and γ3 expressed in macrophages, large intestine, and white adipose tissue. In the absence of a ligand, PPARγ has the potential to remain silent by recruiting transcriptional co-repressors including nuclear receptor co-repressor (N-CoR) or SMRT (silencing mediator of retinoid and thyroid receptors). As shown in Figure 1, binding of agonist ligands to PPARγ triggers a conformation change that involves transcriptional co-activators, including members of the steroid receptor co-activator (SRC) family (McKenna and O'Malley 2002). The transcriptional co-activators and co-repressors can recruit histone-modifying enzymes, such as histone acetyltransferases (co-activators) and histone deacetylases (co-repressor) to DNA promoter region and form multiprotein complexes that could acetylate or deacetylate histone. .

A detailed review of PPAR functions has been described in several previous publications (Berger and Moller 2002; Lehrke and Lazar 2005; Michalik et al. 2006). In brief, the major role of PPARα is the regulation of energy homeostasis. In the liver, PPARα activates fatty acid and cholesterol catabolism, stimulates gluconeogenesis, heme, and ketone body synthesis, and is also involved in the control of lipoprotein assembly. Increased fatty acid oxidation by activated PPARα lowers circulating triglyceride levels, liver/muscle steatosis, and reduces adiposity, which in turn improves insulin sensitivity. In addition, PPARα agonists have demonstrated significant anti-inflammatory activities that probably play a role in their protective function in the cardiovascular system. PPARβ is necessary for placental and gut development and is also involved in the control of energy homeostasis by regulating fatty acid catabolism. Furthermore, PPARβ play an important role in the control of cell proliferation, differentiation, and is involved in tissue repair (e.g., wound healing process). In the meanwhile, PPARβ agonists can retard weight increase of animals exposed to high-fat diet and therefore maintain insulin sensitivity probably by stimulating skeletal muscle fatty acid catabolism and thermogenesis. PPARγ shows a similar anti-inflammation property with α and β. However, PPARγ plays a more important roles in adipose tissue differentiation and in maintaining adipocyte specific functions, including lipid storage in white and brown adipose tissues. PPARγ is also involved in glucose metabolism and pharmacological activation of PPARγ improves insulin sensitivity. In contrast to PPARα and β/δ which decrease or retard weight gain, agonists of PPARγ induce adipogenesis and increase lipid storage. Therefore, chemicals that specifically activate (agonize)

PPARγ and upregulate expression may promote weight gain and perhaps development of obesity.

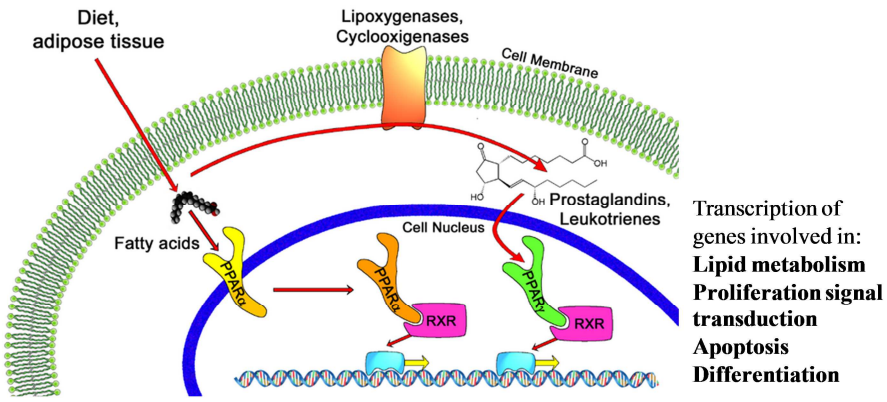

Figure 1. PPARs functional pathway (Redrawn from http://en.wikipedia.org/wiki/Peroxisome_proliferator-activated_receptor).

1.3 Natural Ligands of PPARγ

Studies investigating the crystallized structure of PPARγ have found that it exhibits flexible plasticity in the ligand-binding domain (PPARγ LBD), which allows it to accommodate a wide variety of ligands (Nolte et al. 1998). PPARγ was thought to be an orphan nuclear receptor, implying no specific endogenous ligands have been identified. Despite intensive research efforts, it remains to be determined whether PPARγ has a highly specific natural ligand or whether it is activated by the combined concentration of several weak ligands. A variety of chemicals have been suggested to be natural PPARγ ligands, including fatty acids and eicosanoids (Desvergne and Wahli 1999), components of oxidized low-density lipoproteins (Nagy et al. 1998), and oxidized alkyl phospholipids including lysophosphatidic acid (McIntyre et al. 2003) and nitrolinoleic acid (Schopfer et al. 2005). The prostaglandin J2 derivative, 15-deoxy-$\Delta^{12,14}$-PGJ2 (15d-

PJG2), does not naturally exist at sufficient concentrations to activate PPARγ in mammalian cells (Bell-Parikh et al. 2003). Several anti-diabetic drugs of the thiazolidinedione class such as rosiglitazone and pioglitazone also target PPARγ (Lu and Cheng 2010).

1.4 Emerging Exogenous Ligands of PPARγ

As shown in Figure 2, environmental contaminants including tributyltin (TBT), triphenyltin (TPT), and mono(2-ethylhexyl) phthalate bis(2-ethylhexyl) (MEHP) (a metabolite of the phthalate DEHP), have been shown to upregulate and stimulate several PPARs (Feige et al. 2007; Grün et al. 2006). Grün et al (2006) found that TBT induces the differentiation of adipocytes *in vitro* using murine 3T3-L1 cell model and increases adipose mass *in vivo* using mice and *Xenopus laevis* tadpoles. TBT was found to be a dual and nanomolar affinity ligand for both the RXR and the PPARγ. In the 3T3-L1 cell model, TBT significantly promotes adipogenesis and perturbs key regulators of adipogenesis and lipogenic pathways. It was also found that *in utero* exposure to TBT leads to significantly elevated lipid accumulation in adipose depots, liver, and testis of neonate mice and increased epididymal adipose mass in adults. In the amphibian *Xenopus laevis*, ectopic adipocytes form in and around gonadal tissues after TBT exposure. Therefore, it appears clear that some organotin compounds are "environmental obesogens" that promote adipogenesis through RXR and PPARγ activation. Developmental or chronic lifetime exposure to organotins may therefore act as a chemical stressor for obesity and related health disorders. Phthalate plasticizers are

another group of chemicals which can directly influence PPAR activity (Feige et al. 2007; Pereira-Fernandes et al. 2013). Previous studies have demonstrated that monoethyl-hexyl-phthalate (MEHP) could directly activate PPARγ and promote adipogenesis, albeit to a lower extent than the full agonist rosiglitazone. MEHP was found to induce activation of different PPARγ target genes, which requires recruitment of a specific subset of PPARγ co-regulators including Med1 and PGC-1alpha. Besides organotins and phthalates, accumulating evidence has suggested that FRs might represent an important class of compounds that may also bind to PPARγ and disrupt signaling. One halogenated monoester phthalate (tetrabromo mono(2-ethylhexyl)phthalate (TBMEHP), which is a possible metabolite of bis(2-ethylhexyl) tetrabromophthalate (TBPH), a primary component in the flame retardant mixture FM550, was also found to induce adipocyte differentiation in NIH 3T3 L1 cells, and activate both PPARα- and PPARγ-mediated gene transcription in NIH 3T3 L1 cells and FAO cells, respectively (Springer et al. 2012). A recent study found that 2,2,6,6′-tetrabromo bisphenol (TBBPA) and 3,3′,5,5′-tetrachlorobisphenol A (TCBPA), were also agonists of human, zebrafish, and Xenopus PPARγ (Riu et al. 2011). It was also found that the bulkier brominated BPA analogs had a greater capacity to activate PPARγ. In a follow-up study, TBBPA and TCBPA exposure in zebrafish led to significant weight gain (Riu et al. 2014). Both halogenated-BPAs, as well as TBBPA-sulfate induced lipid accumulation in zebrafish at the larval stage and also induced weight gain in juvenile zebrafish at 1 month age. In a recent study, perinatal exposure to the flame retardant mixture Firemaster 550 (FM550), a major replacement for pentabromodiphenyl ether (Penta-BDEs), resulted in a 20-30% weight

gain in both male and female rats relative to controls (Patisaul et al. 2013). Therefore, it is possible that several PPARγ ligands exist in this commercial mixture.

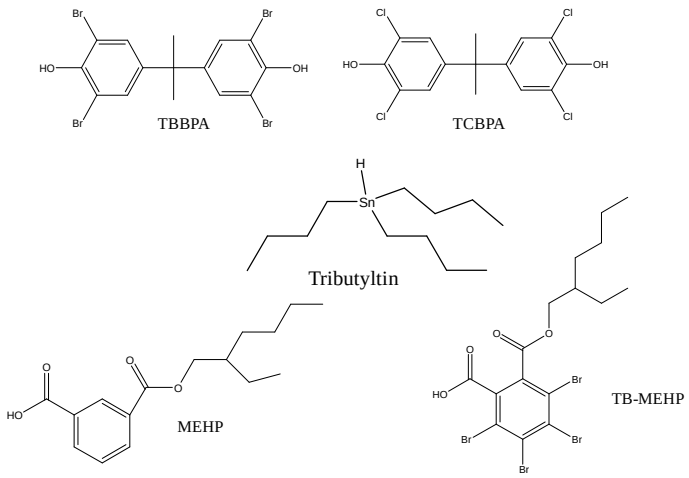

Figure 2: Examples of several exogenous ligands of PPARγ.

1.5 Children's Exposure to SVOC mixtures in Indoor Environment

It has now become clear that indoor dust is a primary sink for many SVOCs in indoor environments. Chemicals such as flame retardants (FRs), phthalates, and organotins are common additives applied to consumer products and construction materials. FRs are chemicals added to consumer and commercial products including textiles, carpeting, and electronics to reduce their combustibility. Most FRs contain either halogenated (e.g, chlorine and bromine) or organophosphate moieties. Among them, polybrominated diphenyl esters (PBDEs) were a major class of brominated FRs. There are three main commercial mixtures of PBDEs: PentaBDE, OctaBDE, and DecaBDE. The PentaBDE and OctaBDE mixtures have been phased out in the U.S. and banned in the European Union due to concerns about persistence, bioaccumulation, and toxicity

(Herbstman et al. 2010; Hites 2004). The fully brominated congener, decabromodiphenyl ether (BDE209) is the major PBDE congener present in the DecaBDE commercial mixture and has been voluntarily phased-out in the US in 2013 (EPA, 2009). Since the phase-out of PBDE commercial mixtures, additional types of FRs have been increasingly used as replacements. Potential replacements include decabromodiphenyl ethane (DBDPE), tetrabromobisphenol-A (TBBPA), bis(2,4,6,-tribromphenoxy)ethane (BTBPE), and several phosphate-based compounds (Covaci et al. 2011). In 2005, the Environmental Protection Agency (EPA) evaluated flame retardant alternatives for low-density polyurethane foam (PUF), in which PentaBDEs was previously widely used (EPA). The alternatives included Firemaster 550/552 (which includes bis(2-ethylhexyl)tetrabromophthalate (TBPH) and ethylhexyl-2,3,4,5-tetrabromobenzoate (TBB)) and some additional organophosphate flame retardants (PFRs) such as triphenyl phosphate (TPP), chloroalkyl phosphates (such as tris(1,3-dichloro-2-propyl) phosphate (TDCPP)), or alkylated triaryl phosphates (e.g., non chlorinated PFRs).

Phthalates are a group of synthetic chemicals added to plastics to increase their flexibility, transparency, durability, and longevity. High-molecular weight phthalates such as di-(2-ethylhexyl) phthalate (DEHP), butyl-benzyl phthalate (BBzP), di-isononyl phthalate (DiNP), and dioctyl phthalate (DOP) act primarily as plasticizers in the manufacture of polyvinyl chloride (PVC) building materials, floorings, food packaging and medical devices. Low-molecular weight phthalates such as diethyl phthalate (DEP), dimethyl phthalate (DMP), di-n-butyl phthalate (DnBP) and di-isobutyl phthalate (DiBP)

are mostly used in personal care products (Hauser and Calafat 2005). Organotin compounds (e.g., mono-, and di-organotins) are commercially applied as stabilizers in PVC and they suppress degradation by removing allylic chloride groups and by absorbing hydrogen chloride (Gajda and Jancso 2010). TBT compounds were once widely used as marine anti-biofouling agents painted on the vessel hull to improve the efficiency of ships. TPT derivatives are used as active components of antifungal paints and agricultural fungicides. TBT was reported to have biological effects (e.g., teratogenic, reproductive, immuno- and developmental toxicity) to marine life at a concentration of 1 nM and has been banned by the International Maritime Organization (IMO, 2002). However, TBT are crucially important starting materials or intermediates in the synthesis of monobutyltin (MBT) and dibutyltin (DBT) and is still found as a byproduct in commercial mixtures used in PVC (Gajda and Jancso 2010).

As many SVOCs including phthalates and FRs are not chemically bound to these components, they migrate out over time. SVOCs have physicochemical properties (high octanol-air partitioning coefficient Log K_{OA}) contributing to their high accumulation in dust. As a result, several of these reported environmental obesogens are ubiquitous and abundant in house dust (See Table 1), where human exposure can occur. Phthalates in particular have been measured in dust at concentrations as high as several mg/g dust. TPP, which is used as both a FR and plasticizer in commercial products, has also been detected as high as mg/g dust. Infants and young children spend a majority of their time (> 95%) indoors where they are chronically exposed to SVOCs present in dust due to

their increased hand to mouth activity and crawling behavior (US EPA, 2009). The EPA estimates that children ingest between 50 and 100 mg of dust per day indoors, implying that children are also receiving exposure to contaminants associated with those ingested dust particles. Furthermore, dust ingestion has been confirmed as a very important SVOC uptake pathway in many studies. For example, the level of PBDEs in the serum from toddlers and adults was significantly correlated with the levels of PBDEs in house dust, (Johnson et al. 2010; Stapleton et al. 2012a). Therefore, house dust is an environmentally relevant sample to investigate potential PPARγ disruption by SVOC mixtures.

Table 1: Reported concentrations of organic contaminants in US house dust (ng/g or ppb)

	Year Sampled	Sample #	% detect	Min	Median/Geomean	Max	Reference
DEHP (phthalate)	1999-2001	120	100	16,700	340,000	7,700,000	(Rudel et al. 2003)
DBP (phthalate)	1999-2001	120	98	<MDL	20,100	352,000	(Rudel et al. 2003)
BBP (phthalate)	1999-2001	120	100	3,870	45,400	1,310,000	(Rudel et al. 2003)
BDE47 (FR)	2009-2010	120	100	55	870	24,720	(Stapleton et al. 2012a)
BDE209 (FR)	2009-2010	120	100	441	2,574	76,130	(Stapleton et al. 2012a)
BPA (phenol)	1999-2001	120	86	<MDL	821	17,600	(Rudel et al. 2003)
TPP (FR&plasticizer)	2002-2007	50	98	<150	7,360	1,798,000	(Stapleton et al. 2009)
TDCPP (FR&plasticizer)	2002-2007	50	96	<90	1,890	56,090	(Stapleton et al. 2009)
TBPH (FR)	2010-2012	30	100	83	620	20,955	(H.M. Stapleton et al. 2014)

PFOA (PFC)	2000-2001	102	96	<10	296	1,960	(Strynar and Lindstrom 2008)
PFOS (PFC)	2000-2001	102	95	<9	761	12,100	(Strynar and Lindstrom 2008)
TBT (organotin)	2005-2006	24	75	<2	22	300	(Kannan et al. 2010)
MTB (organotin)	2005-2006	24	100	320	2,450	11,000	(Kannan et al. 2010)

1.6 Obesity Concerns in children and possible links to chemical exposure via PPARγ

As reviewed in (WHO, 2014) (Organization 2014), worldwide obesity has more than doubled since 1980. In 2014, 1.9 billion adults aged 18 years and over were overweight in 2014, and 13% of them were obese. Furthermore, 42 million children under the age of 5 were overweight or obese in 2013. Obesity has also become a serious epidemic in the US, especially for the young children and adolescent. For example, 17% of children between the ages of 2-19 are obese based on the report from the Centers for Disease Control and Prevention (CDC) (Ogden et al. 2012). The resulting health care costs were estimated to be over $140 billion in the US in 2008 (Finkelstein et al. 2009). The reasons for the obesity can be complex, including genetics, diet, and exercise. However, several recent studies have shown that prenatal exposures to "environmental obesogens" including BPA, phthalates, OTs and perflourinated compounds may increase the risk of obesity in children (Amanda Janesick and Bruce Blumberg 2011). Several studies found significant associations between urinary metabolites of phthalates and obesity (Wang et al. 2013).

High levels of several persistent organic pollutants (e.g., 1,1-Dichloro-2,2-bis(p-chlorophenyl) ethylene (DDE), hexachlorobenzene, and polybrominated diphenyl-ethers (PBDEs)) have also been found to be associated with obesity in humans (Tang-Peronard et al. 2011). One study found associations with BPA and another with phthalate metabolites, increasing concern that some chemicals may be acting as environmental obesogens. They may also modify the regulation of one's appetite, resulting in fat accumulation and obesity that many be contributing to the increasing prevalence of obesity in the US. It has been hypothesized that higher exposure to chemical contaminants during perinatal development leads to cellular reprogramming and metabolic disruption, which can lead to increased numbers of adipocytes and lipid content, and ultimately obesity, in children. A biological plausible explanation linking chemical exposures with adipogenesis has been reported by several researchers, particularly for the contaminants tributyltin (TBT) and DEHP (Feige et al. 2007; Grün et al. 2006). Both have been shown to upregulate and stimulate several PPARs, members of the nuclear receptor superfamily. As mentioned above, together with the RXR, PPARs serve as metabolic ligand sensors for a variety of hormones, dietary fatty acids, and their metabolites (Grün and Blumberg 2009). Chemicals that specifically activate (agonize) PPARγ and upregulate expression may promote the development of obesity. As mentioned above, children are continuously exposed to a "cocktail" of environmental contaminants including TBT, TPT, and MEHP (the metabolite of the phthalate DEHP), which all have been shown to upregulate and stimulate several PPARs. Therefore, it is

possible that co-exposure of those environmental obesogens could affect lipid metabolism and may promote the development of obesity in the children.

1.7 Bioactivation of SVOCs and its Health Effect

Chemicals carried into the body with ingested dust particles may be absorbed in the digestive system and metabolized via xenobiotic transformation systems. Several studies have found that metabolites can be more potent than their parent compounds in eliciting toxicity and endocrine disruption. In one previous study, hydroxylated polybrominated diphenyl ethers (OH-PBDEs) were found to be several orders of magnitude more potent than their parent compounds (PBDEs) in a thyroid hormone disruption assay (Butt et al. 2011). In another study, metabolically activated nonpolar contaminants in sediments were found to competitively bind to thyroid hormone transport proteins and increase transthyretin binding potency up to 100 times (Montaño et al. 2013). This study demonstrated that a more realistic in vitro risk characterization should include bioactivated nonpolar sediment fractions to prevent underestimation of its toxic potency in transthyretin binding. As for the PPARγ, several studies have also shown that the metabolites can be more potent than the parent compounds. For example, MEHP showed a much stronger PPARγ binding potency than its parent phthalate, DEHP, after biotransformation (Feige et al. 2007). Similarly, TBMEHP, a metabolite of TBPH, has also been reported to be an agonist for PPARs in mouse NIH 3T3 L1 preadipocyte cells, whereas TBPH was not (Springer et al. 2012). Therefore, it would be of great interest to investigate the effect of bioactivation on the PPARγ disruption by

SVOC mixtures. To date, very few in vitro bioactivation methods have been developed. The use of liver S9 or microsomal sub-cellular fractions has been used in several previous studies to study bioactivation (Montaño et al. 2012; Montaño et al. 2013) , though it often suffers form low rates of biotransformation of the parent compounds.

1.8 Bioaccessibility of SVOCs in Environmental Samples

Bioaccessibility is defined as the fraction of a chemical which can desorb from the ingested matrix during digestion process. In current exposure and risk assessments, 100% bioaccessibility is often assumed in assessing human exposure to SVOCs in house dust. However, previous studies have shown that SVOCs sorbed to organic matter cannot be completely released from these matrices and subsequently absorbed into the gastrointestinal tract (Costera et al. 2009; Lei et al. 2004). Therefore, understanding the bioaccessibility of SVOCs in dust is of great significance for adequate risk evaluations, including PPARγ disruption. More interestingly, the source of SVOCs in indoor dust is very complex, and can be either from SVOCs sorbed onto organic matter associated with dust, or weathered material/debris from commercial products (Webster et al. 2009). Therefore, SVOCs can have different fugacities (i.e. escaping tendencies) in different matrices, ultimately affecting their bioaccessibility after ingestion. Many factors of the matrix including organic carbon content, particle size and aging may also affect bioaccessibility (Wong and Bidleman 2011; Yu et al. 2012). Therefore, it is important to investigate compound-dependent and matrix-dependent bioaccessibility of SVOCs in dust.

In-vitro physiologically based extraction methods are predominately used in bioaccessibility studies because of their reduced cost/time and animal use. Various models have been proposed and most of them use simulated digestive fluid to sequentially, or continuously, extract contaminants within a matrix during relevant physiological residence times (Oomen et al. 2002). However, absorption in the gastro-intestinal tract is a dynamic process and traditional *in-vitro* methods might underestimate the bioaccessibility due to a failure to maintain and consider the concentration gradient, especially for very hydrophobic compounds. Recent studies found that sorption-assisted bioaccessible extractions using a silicon rod, an activated carbon impregnated silicon rod, or a C18 membrane as an "infinite sink" could increase the bioaccessibility of polycyclic aromatic hydrocarbons (PAHs) in sediment, and were more comparable with *in vivo* studies (Collins et al. 2013; Gouliarmou et al. 2013; Gouliarmou and Mayer 2012). Therefore, different in vitro bioaccessibility methods should be compared to find an effective method to evaluate SVOC bioaccessibility in dust.

Another knowledge gap is the stability of SVOCs in digestive fluids. Many SVOCs, including phthalates and emerging FRs, have more labile functional groups, such as phosphate and carboxylic esters, which could be vulnerable to nucleophilic reactions. The half-times of these esters in water (pH 7) vary significantly between chemicals, which can range from several minutes to years (Schwarzenbach et al. 2005). Furthermore, hydrolysis reactions might also be different across the dynamic pH conditions along the

human digestive system. In previous studies, DEHP was found to be hydrolyzed by intestinal enzymes very fast and very little of the orally ingested DEHP would have the opportunity to be absorbed as the parent compound (Albro 1986; Albro and Thomas 1973). Thus, it is also important to examine the stability of these less stable SVOCs in digestive fluids. This stability might also affect the PPARγ activity of those SVOCs. For example, PPARγ activity of di-ester phthalates might greatly increase if the ingested compounds could be converted to their mono-ester forms in the gastro-intestinal fluids.

1.9 Effect-directed Analysis

One of the key challenges environmental chemists and toxicologists are facing is the characterization and assessment of complex exposure scenarios that are typical for many environments. The most difficult and timely question is which chemical(s) in the mixture are responsible for the observed toxicity. The use of classic chemical–analytical techniques alone is not sufficient to address this issue. Specifically, analysis of the vast number of chemicals typically present in an environmental samples would not only be expensive but impossible due to limits in analytical methodologies. Therefore, approaches have been developed to combine chemical analysis with bio-analytical techniques that focus on a specific biological process. This type of method has been coined as an effect-directed analysis (EDA). Overall, EDA is a relatively recent technique utilizing iterative chemical separation, toxicity evaluation and qualitative chemical analysis to identify the chemical(s) exerting a specific toxicity in complex mixtures. To date, EDA has become a valuable approach to determine the agents

responsible for biological effects in various complex environmental samples (reviewed in (Brack et al. 2007; Brack and Schirmer 2003)). This strategy has been widely used in the sediment sample for dioxin-like compounds (Van den Berg et al. 1998) and estrogenic chemicals (Hilscherova et al. 2000; Hollert et al. 2005; Khim et al. 1999). For example, heterocyclic polyaromatic compounds, including dinaphthofurans, 2-(2-naphthalenyl)benzothiophene, methylated chrysene, and benz[a]anthracene, were identified and confirmed as major cytochrome P4501A (CYP1A)-inducing compounds in a contaminated sediment close to the industrial site of Bitterfeld (Germany) (Brack et al. 2007; Brack and Schirmer 2003). In one of my previous studies, EDA was successfully used to identify the active polycyclic aromatic hydrocarbon (PAHs) that explained the observed cardiotoxicity in zebrafish exposed to pore water from a Superfund site in Virginia (Fang et al. 2014a).

While numerous approaches to EDA exist in the literature, each method shares several common elements, namely, the extraction, enrichment and stepwise fractionation of an environmental mixture with manipulations directed by a specific bioassay response. Ultimately, the goal of EDA is to facilitate the identification of causative agents, through chemical analysis (e.g., mass spectrometry), responsible for observed toxic response(s) by reducing mixture complexity.

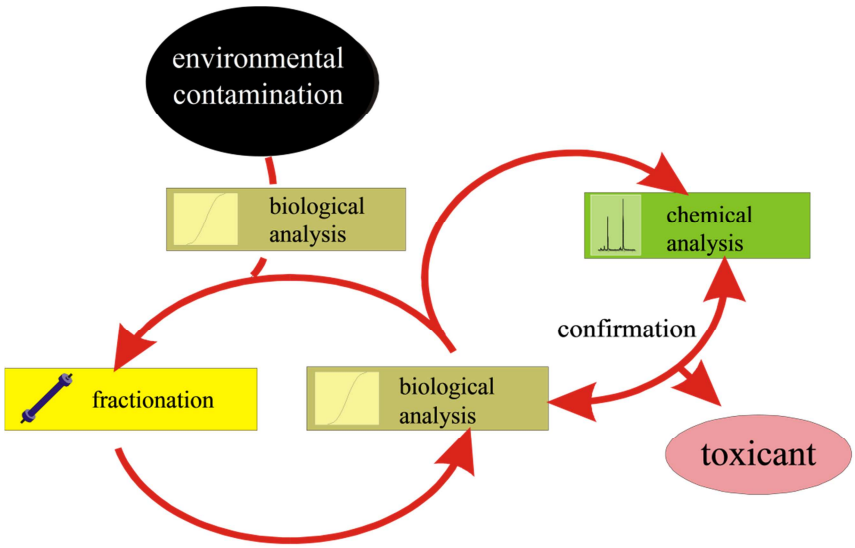

Figure 3: Principle of effect-directed identification of toxicants (Adapted from Brack et al., 2013)

As demonstrated in Figure 3, a complex sample (e.g., sediment, porewater, landfill leaches, air particulate matter, house dust extract, or soil extract) is first analyzed using one specific or a combination of multiple (non-target analysis) bioassays representing different modes of biological action. Parallel to the assessment of effects on specific biological processes, the general toxicity of a sample (e.g., cytotoxicity or cell viability for a cell-based bioassay) that could mask a specific response is run for comparison. If a sample has been identified with a significant biological activity, it will then be subjected to fractionation, separating the chemicals contained in it by, polarity, molecular weight, or any other physical–chemical property (Brack 2003). These fractions are then again tested for their potential to interfere with biological processes using the same mechanism-specific bioassay. A series of fractionation step might be repeated until the activity can be pinpointed to one or multiple specific fractions that contain the active chemicals. The active fractions are subjected to chemical analysis for suspected

compounds using mass spectrometry or other analytical instruments. Finally, a confirmation step in the EDA procedure uses a mass balance method to evaluate how much of the observed toxicity in the environmental sample could be explained by the mixture of identified toxicants (Brack 2003). Usually, a "mock" mixture with measured concentration of the identified compounds is prepared to evaluate the recovered toxicity.

1.10 Thesis Objective and Experiment Approach

The overall objective of this thesis research was to answer fundamental questions concerning whether the SVOCs in house dust affect PPARγ in vitro, and to determine which chemicals were driving the observed effect. A secondary goal was to explore the role of bioactivation and bioaccessibility on PPARγ activity in dust samples. The central hypothesis of this research is that chemical mixtures present in house dust have PPARγ activity. In addition, bioaccessibility and bioactivation will modulate PPARγ activity in house dust. Therefore, to adequately assess the potential risk of PPARγ activation from exposure to SVOC mixtures in house dust, it is essential that one also investigates the bioaccessibility and bioactivation of those chemicals following exposure. To test this hypothesis, the following three study aims and experimental approaches were designed and performed.

Aim 1: Examine the bioaccessibility of several SVOCs in house dust using an *in-vitro* sorptive physiologically-based model. The bioaccsessibility of SVOCs such as brominated FRs and OPFRs will be examined in both dust samples and commercial products. The influence of dust characteristics, including dust source and composition

(e.g. organic carbon content) will also be examined. Mathematical regression models will then be developed to explore the relationship between bioaccessibility and physico-chemical properties of tested SVOCs. Then the bioaccessibility of identified PPARγ in Aim 1 and the causal compounds in Aim 2 could be estimated. Furthermore, the stability of several less persistent SVOCs (e.g., organophosphate and carboxylic ester FRs) was investigated in the digestive fluid and its possible effect on the PPARγ activity was discussed [Chapter 2].

Aim 2: Characterize the ligand binding activity of several SVOCs (individually), their metabolites, and extracts of indoor dust before and after bioactivation in human PPARγ. The PPARγ ligand binding potential of several groups of SVOCs and their metabolites (e.g., phthalates, organotins, halogenated phenols, and major FRs), which are ubiquitously detected in house dust, will be tested using *in vitro* ligand binding assays. Dust samples before and after bioactivation with rat/human liver S9 fraction will also be examined for PPARγ ligand binding potential [Chapter 3];

Aim 3: Examine the transactivation of identified PPARγ ligands in Aim 2 and extracts of indoor dust in human PPARγ. In this aim, an *in vitro* PPARγ reporter assay was used to determine if the observed binding of pure chemicals or mixtures in house dust in Aim 2 indicates agonism of PPARγ. The correlation between this reporter assay and the ligand binding assay was also conducted. Furthermore, mixture effect of several important SVOCs, which were present in house dust and can activate human PPARγ, were investigated at environmentally relevant levels of exposure [Chapter 4];

Aim 4: Non-targeted screening of primary PPARγ ligands in house dust using EDA. In this aim, dust samples with significant PPARγ activity (identified in Aim 1) will be fractionated (based on polarity or size) and tested to determine which fraction contains the highest activity. After fractionation, a non-targeted analysis of the most responsive fractions using mass spectrometry will be performed to identify the "causative agents" in fractionated house dust samples [Chapter 5];

Chapter 6 discusses major findings and limitations of this research thesis and provides ideas for future research directions. It focuses special attention on how the data generated can advance our understanding of PPARγ disruption by SVOCs.

2. Evaluating the Bioaccessibility of Flame Retardants in House Dust Using an In Vitro Tenax Bead-Assisted Sorptive Physiologically Based Method[1]

Exposure to house dust is a significant source of exposure to flame retardant chemicals (FRs), particularly in the US. Given the high exposure there is a need to understand the bioaccessibility of FRs from dust. In this study, Tenax beads (TA) encapsulated within a stainless steel insert were used as the adsorption sink to estimate the dynamic absorption of a suite of FRs commonly detected in indoor dust samples (n=17), and from a few polyurethane foam samples for comparison. Organophosphate flame retardants (OPFRs) had the highest estimated bioaccessibility (~80%) compared to brominated compounds (e.g. PBDEs), and values generally decreased with increasing LogKow, with <30% bioaccessibility measured for BDE209. These measurements were in very close agreement with reported PBDE bioavailability measures from an in vivo rat exposure study using indoor dust. The bioaccessibility of very hydrophobic FRs (LogKow > 6) in foam was much less than that in house dust, and increasing bioaccessibility was observed with decreasing particle size. In addition, we examined the stability of more labile FRs containing ester groups (e.g. OPFRs and 2-ethylhexyl-tetrabromo-benzoate (EH-TBB)) in a mock-digestive fluid matrix.

---

[1]Fang ML, and Stapleton HM. Evaluating the Bioaccessibility of Flame Retardants in House Dust using an In Vitro Tenax Bead-Assisted Sorptive Physiologically Based Method. Environmental Science and Technology, 2014, 18;48(22):13323-30. doi: 10.1021/es503918m.

No significant changes in the OPFR concentrations were observed in this fluid; however, EH-TBB was found to readily hydrolyze to tetrabromobenzoic acid (TBBA) in the intestinal fluid in the presence of lipases. In conclusion, our study demonstrates that the bioaccessibility and stability of FRs following ingestion varies by chemicals and sample types and thus should be considered in exposure assessments.

2.1 Introduction

Flame retardants (FRs) are common additives applied to consumer products and construction materials. As additives they are not chemically bound to these components and over time they migrate out. Due to high octanol-air partitioning coefficient ($LogK_{OA}$), many FRs are ubiquitous and abundant in house dust (Dodson et al. 2012; Stapleton et al. 2012b), which is a known exposure for humans. Several studies have now found that house dust ingestion is one of the most important exposure pathways for FRs, especially for infants and toddlers (Johnson et al. 2010; Stapleton et al. 2012a). In current risk assessments, 100% bioaccessibility is often assumed when evaluating human exposure to FRs in house dust. However, previous studies have shown that hydrophobic organic compounds sorbed to organic matter (e.g., soil and sediment), cannot be completely released from these matrices and subsequently absorbed into the gastrointestinal tract (Costera et al. 2009; Lei et al. 2004). Therefore, understanding the bioaccessibility of FRs in dust is of great significance for adequate risk evaluations.

Though some studies have examined the bioaccessibility (i.e., the fraction which can desorb from the ingested matrix) of polybrominated diphenyl ethers (PBDEs) in house

dust (Huwe et al. 2008; Yu et al. 2012), no information is available for several new alternate FRs such as organophosphate FRs (OPFRs) and Firemaster®550 (FM550), which are the major replacements for the pentaBDE commercial formulations after their phase-out (Stapleton et al. 2011; Stapleton et al. 2012b). Furthermore, FRs in dust may have heterogeneous sources. FRs may be sorbed to organic material in the dust following partitioning from air, or be associated with debris in dust that results from product weathering (e.g. foam or plastic weathering). Using microscopic forensic methods, Webster et al. (2009) found that a strong bromine signal in a dust sample was associated with particles/debris suggestive of weathered commercial products. In another study using dust collected from a gymnasium, an abundance of polyurethane foam (PUF) debris was observed using scanning electron microscopy (Carignan et al. 2013a), again suggesting the FR signatures in dust may be associated with weathered materials/polymers. Infants or toddlers also tend to mouth toys or furniture made of PUF impregnated with FRs and phthalate additives. Therefore, it is important to evaluate the bioaccessibility of FRs from both dust particles and PUF material. However, to date, very few studies have investigated the bioaccessibility of FRs in commercial products.

In-vitro physiologically based extraction methods are predominately used in bioaccessibility studies due to the advantages of reduced cost/time and animal use. Various models have been proposed and most of them use simulated digestive fluid to sequentially, or continuously extract, contaminants within a matrix during relevant physiological residence times (Oomen et al. 2002). However, absorption in the gastro-

intestinal tract is a dynamic process and traditional *in-vitro* methods might underestimate the bioaccessibility due to a failure to maintain and consider the concentration gradient, especially for very hydrophobic compounds. Recent studies found that sorption-assisted bioaccessible extractions using a silicon rod, an activated carbon impregnated silicon rod, or a C18 membrane as an "infinite sink" could increase the bioaccessibility of polycyclic aromatic hydrocarbons (PAHs) in sediment, and were more comparable with *in vivo* studies (Collins et al. 2013; Gouliarmou et al. 2013; Gouliarmou and Mayer 2012). However, activated carbon impregnated silicon rods may be prone to back-extraction, and silicon rods needs large surface areas (~2 m) to ensure a high sorption capacity. Tenax beads (TA), a porous polymer adsorbent with desirable adsorption/desorption characteristics, have been validated as an effective method in the bioaccessibility evaluation due to their strong sorption capacity, easy back extraction and recycling use. A 6 hour TA extraction was widely used to predict the bioavailability of PAHs and pesticides in soils and sediments (Harwood et al. 2013; van der Heijden and Jonker 2009; Yu et al. 2012). Therefore, it seems feasible to predict that TA may also predict bioaccessibility of FRs in dust; however, to the authors' knowledge, no studies have investigated this potential application.

Another knowledge gap is the stability of FRs in digestive fluids. Due to stricter environmental health regulations and intense public awareness, the FR market has moved from persistent FRs like PBDEs to less persistent FRs such as OPFRs and FM550 (Dodson et al. 2012). These latter chemicals have more labile functional groups, such as phosphate and carboxylic esters, which could be vulnerable to nucleophilic reactions.

The half-times of these esters in water (pH: 7) vary significantly between chemicals, which could range from several minutes to years (Schwarzenbach et al. 2005). Furthermore, hydrolysis reactions might also be different across the dynamic pH conditions along the human digestive system. Thus, it is important to examine the stability of these less stable FRs in digestive fluids. Given these issues, the primary objectives of this study were to: (1) develop an effective TA-sorption assisted *in-vitro* physiologically based bioaccessible extraction method; (2) examine the bioaccessibility of OPFRs, FM550, and PBDEs in house dust samples; (3) test the bioaccessibility of several FRs in PUF and its dependence on particle size; and (4) investigate the stability of several less persistent FRs, e.g., OPFRs and components of FM550, in simulated digestive fluids.

2.2 Materials and Methods

2.2.1 Design of the TA-assisted bioaccessible extraction method

In our preliminary experiment, we found that the bile salts could precipitate the TA, which was probably due to the decreased tension force caused by the bio-detergent. Therefore, TA could not be used in the bioaccessible experiment until good separation from dust after incubation was achieved. In this study, TA beads (60~80 mesh, Supelco) were first cleaned by sonication using acetone:hexane (1:1, v/v) and sieved through 100 mesh (152 μm, USA standard testing sieve) to minimize the lost of small beads during the experiment. An insert was designed for use in this study (see Figure 19) that would contain the TA. A 100 mesh stainless steel material (Small Parts, Logansport, IN, USA) was cut into ~11 x 7 cm (length x width) dimensions. The mesh was rolled and fixed at

the ends with 0.4 mm copper wire. A half-cut 4 mL glass vial was inserted to one end as a cap. After loading TA (0.5 g), another pre-cleaned 4 mL vial was used as a cap on the other side. After incubation, the TA insert was rinsed thoroughly with deionized water to remove any dust residue attached to the TA, which were then collected in an aluminum weight boat. The rinsing water was combined with the colon fluid. Most of the dust remained in the colon fluid due to its smaller size (< 60 μm) and rinsing step could further separate TA from dust matrix. After collecting the beads, the insert was extracted together with the dust to guarantee that dust sticking to the stainless steel mesh insert could be recovered. Diffusion of methylene blue was used to confirm circulation of the digestive fluid across the stainless mesh and the result showed that the circulation was very efficient without any blockage. In this study we used a house dust Standard Reference Material (SRM) 2585 (National Institute of Standards and Technology (NIST), Gaithersburg, MD) to validate the method. One advantage was that a previous *in-vivo* study used SRM2585 to examine PBDE bioavailability in rats (Huwe et al. 2008), making it possible to compare the *in-vitro* and *in-vivo* data.

2.2.2 Dust and PUF preparation

Indoor dust samples (n = 17) collected during our previous studies (Stapleton et al. 2012a; H.M. Stapleton et al. 2014; Watkins et al. 2013) were used here to examine bioaccessibility in actual dust samples. Since most ingestible dust particles adhering to hands have a diameter less than 60 μm (Choate et al. 2006), all the dust used in this study was first sieved to < 53 μm. To investigate the factors affecting the bioaccessibility

in the house dust, total organic carbon (TOC), nitrogen, and hydrogen content were analyzed by Elemental Analyzer Vario MICRO Cube (Elementar). $LogK_{ow}$ values of PBDEs were taken from a previous study (Wania and Dugani 2003) and values for EH-TBB, BEH-TEBP and all the OPFRs were calculated using EPI suite (EPIWEB 4.1). PUFs treated either with TCDPP, FM550, or penta-BDEs were selected to study FR bioaccessibility in commercial products due to their frequent detection (Dodson et al. 2012; Stapleton et al. 2011; Stapleton et al. 2012b). To determine if particle size affected bioaccessibility, PUF samples were first freeze dried in liquid nitrogen and then scraped across a stainless mesh sieve with apertures of 500 μm, 250 μm and 106 μm in series. An attempt to further fragment the foam to < 53 μm failed due to very limited yield rate.

2.2.3 Physiologically based extraction of FRs in dust and PUFs

The procedure used here was modified from a recently developed colon-extended physiological based extraction method (Tilston et al. 2011) (See flow chart diagram in Figure 20). The composition of each type of simulated digestive fluid followed a previous published study (Gouliarmou et al. 2013) with the addition of porcine lipase (Type II, 100-400 units/mg protein using olive oil, Sigma Aldrich, St Louis, MO) at a final concentration of 1.6 mg/mL in the intestinal fluid. 50 mL glass centrifuge tubes were used for the incubation and fixed onto a rotatory device (RKVS, Appropriate Technical Resources, Inc., Laurel, MD), which was used to agitate the mixture with a speed of ~40 resolution per minute. The incubation was maintained at 37℃ in an oven (Precision, Thermo). Briefly, ~0.4 g house dust was incubated with 0.5 g TA as well as 45 mL pre-warmed simulated gastric fluid for 1.5 hours. Then sodium carbonate ($NaHCO_3$) was

added to adjust pH to ~6.5 and bile salts (bovine and ovine, Sigma Aldrich), lipases, and pancreatin (porcine, 8 USP, Sigma Aldrich) were added to prepare the intestinal fluid. After incubating for ~4 hours, TA insert was taken out and dust was separated from intestinal fluid by centrifugation at 1000 × *g* for 10 min. Then TA insert was reinstalled and the colon fluid was added, followed by incubation for ~16 hours. Bead collection is described above and dust was separated by centrifugation. The experiments with the PUF (~20 mg for each incubation) were conducted in a similar manner as the dust samples except that a different method was used to separate foam particles from the digestive fluid. Centrifugation did not work well due to the resuspension of foam particles. Instead, the digestive fluid was filtered through glass wool packed in a 15 mL serological borosilicate glass pipette. The glass wool containing the foam particles was recovered by pumping air into the pipette from the bottom.

2.2.4 Hydrolysis experiments for OPFRs and FM550

The FM550 commercial mixture (Great Lakes Chemical, West Lafayette, IN) and OPFRs including tris(2-chloroethyl) phosphate (TCEP), TDCIPP, and tris (1-chloro-2-propyl) phosphate (TCIPP) dissolved in methanol were spiked into 100 mL gastric fluid, intestinal fluid, and colon fluid stored separately in amber glass bottles to obtain a final concentration ~200 ng/mL for each compound. An additional 1.5 mL of methanol was added to increase the solubility of hydrophobic compounds like EH-TBB and BEH-TEBP in the mixtures. Glass coated stir bars were used to minimize the sorption onto the coating material. 1 mL aliquots (in duplicate) were transferred to 6 mL pre-cleaned glass

tubes at selected sampling times (from 0 to 20 hours) and the reaction was immediately quenched by adding 100 μL 6 M HCl. One aliquot was spiked with a monofluorinated tetrabrominated diphenyl ether (F-BDE69), deuterated TDCIPP (d-TDCIPP), and d-TPHP as surrogates to quantify EH-TBB/BEH-TEBP, and other OPFRs; respectively. The other aliquot was spiked with 2,3,5 triiodo-benzoic acid (TIBA; 98%, Sigma Aldrich, St. Louis, MI) to quantify the metabolite TBBA from EH-TBB. Both aliquots were warmed at 50 ℃ for 15 minutes to further denature the protein. Parent compounds were extracted using liquid-liquid extraction with hexane: ethyl acetate (1:1) three times. The analysis TBBA followed the method in a previous study (Roberts et al. 2012). Briefly, the sample was extracted with acetone:water (1:1, v/v), evaporated, and cleaned using an Agilent-OPT SPE column . One control (without lipase and pancreatin, but with FR spike) was run alongside to observe the effect of lipases on the hydrolysis of OPFRs and FM550. After confirming the formation of TBBA from EH-TBB in the intestinal fluid, a further measurement of the bioaccessibility of TBBA was assessed to determine if this metabolite could be absorbed during the residence time in the intestinal tract. TBBA was spiked into simulated intestinal fluids with two different pH values (5.7 and 8.0) and 0.6 g TA was added. Aliquots of 1 mL fluid were transferred to 6 mL borosilicate tubes at different sampling time and the concentration of TBBA was analyzed in each sample.

2.2.5 Chemical Analysis

A detailed chemical analysis of FRs in dust/foam, TA, and digestive fluid are described in the Appendix A Chemical Analysis.

2.2.6 Data Analysis and Quality Control

Bioaccessibility in this study was calculated using the following equation: *Bioaccessibility = 1- (FRs remaining in dust (or foam) after incubation/ the sum of FRs measured in the dust (or foam), TA and digestive fluid)*. SRM2585 was used as the reference material to observe the intra-day (n = 3) and inter-day variability (n = 3). The relative standard deviation of both was less than 15% for most compounds. In the foam extraction, duplicate samples were prepared for each sample. The recoveries of F-BDE69, ^{13}CBDE209, and OPFR surrogate standard ranged from 65-120%, 50-110% and 71-115%; respectively, during sample solvent extraction and cleanup. All statistical analyses were conducted using SigmaPlot 12.0 software, testing hypotheses at $\alpha = 0.05$, and all tests were two-tailed. When comparing the aging effect in dust samples, a two factor *ANOVA* analysis was used.

2.3 Result and Discussion

2.3.1 Performance of the TA-assisted method

To validate the sorption efficiency of PBDEs and less hydrophobic OPFRs by TA, sorption kinetics of the FRs were first investigated in the three digestive fluids by spiking in the pure chemicals. Solutions of high and low levels of OPFRs and PBDEs (in methanol) were spiked into each digestive fluid with a final concentration ~2 μg/mL and ~10 ng/mL for each FR, which could represent the level of FRs in foam and house dust; respectively. Additional methanol was added to make a final concentration of 1% methanol in the digestive fluid to increase the solubility at the initiation of the experiment. Duplicates of 0.5 mL were collected at various incubation time points, chemically analyzed and averaged. As shown in Figure 22, the majority of the FRs

partitioned from the digestive fluid into the TA within 2 hours of incubation, especially in the gastric and intestinal fluid for both the high and low dosed levels. The sorption kinetics of OPFRs and BDE209 in the low level spike (~10 ng/mL) was not shown due to high background levels of those chemicals and non-detection of several later time points. It did appear that the sorption of higher molecular weight PBDEs, such as BDE209, was slower than for the lower molecular weight congeners, and sorption of FRs in the intestinal fluid appeared to occur more quickly than in the gastric and colon fluid. This might be due to the presence of high levels of bile salts, which could increase the solubility and diffusion of hydrophobic FRs. Even for the less hydrophobic TCEP (logKow~1.78), more than 90% of the spiked TCEP partitioned to the TA after a 6 hour incubation. Therefore, considering the average residence time in the human digestive tract, sorption of the FRs to the TA will not be a rate limiting step for the FRs studied here.

To test the efficacy of separation between TA and dust using this method, the recovered mass of SRM2585 (n=3) and TA (n=3) following the incubation was recorded. Triplicate incubations of SRM2585 without TA was also run alongside the samples for comparison. As shown in Figure 21, more than 94% of the added TA (by mass) could be recovered using the designed TA trap. The recovery of the dust incubated with TA was no different than the one without TA; however, the mass of dust recovered was low overall (~60%). The low recovery may be due to the loss of either inorganic carbon in the acidic gastric fluid or dissolved organic matter in the fluid.

2.3.2 Comparison between in-vitro and in-vivo using SRM2585

The bioaccessibility of FRs in SRM2585 was compared using digestive fluid with and without TA employed as an infinite sink (see **Figure 4**). No significant difference between the two methods was observed for several less hydrophobic OPFRs such as TCEP, TCIPP, and TDCIPP. However, large differences were observed for hydrophobic compounds such as EH-TBB, BEH-TEBP and PBDEs. For example, the bioaccessibility of BDE47 in SRM 2585 was ~80% using the TA method, but was only ~10% using only digestive fluid. In general, the bioaccessibility of FRs in SRM2585 using the TA method was several folds higher than the method without the infinite sink, especially for the fairly hydrophobic compounds. Lepom et al. (Lepom et al. 2013) also measured bioaccessibility of PBDEs in SRM2585 using an *in vitro* incubation method without including an infinite sink and the average bioaccessibility for the tri- to hepta-BDEs ranged from 27 to 42%, and BDE209 was about 10% (range 7 to 14 %), which were slightly higher than the values measured in this study without TA, but lower than that measured with TA. To further validate the method, an *in-vivo* data set on the net absorption efficiency of several PBDEs (calculated as the fraction of the ingested chemical that was not excreted via the feces) in rats exposed to SRM2585, was also included for comparison (Huwe et al. 2008). As seen in **Figure 4**, the *in vivo* net absorption data are quite comparable with the bioaccessibility measure using the TA method. These findings confirm several recent studies (Collins et al. 2013; Gouliarmou et al. 2013; Gouliarmou and Mayer 2012) that inclusion of an infinite sink could maintain

the concentration gradient between matrices and fluid, and is essential in evaluating the bioaccessibility of fairly hydrophobic organic compounds ($LogK_{ow} > 5$).

The distribution of several FRs among the four different compartments (i.e., GI fluid, colon fluid, dust, and TA) was also investigated (Figure 23). For BDE47 and 99, most of the mass either sorbed to the TA or remained in the dust matrix, which could be explained by the higher hydrophobicity of those chemicals. However, for less hydrophobic compounds such as TCEP and TCIPP, ~ 20% of the total mass was partitioned into the intestinal fluid, which was slightly higher than the measured value in the sorption efficiency experiment using the spiking method (Figure 23). Therefore, the fraction of these chemicals ($LogK_{ow} < 4$) in the fluid should also be considered even with the presence of an infinite sink.

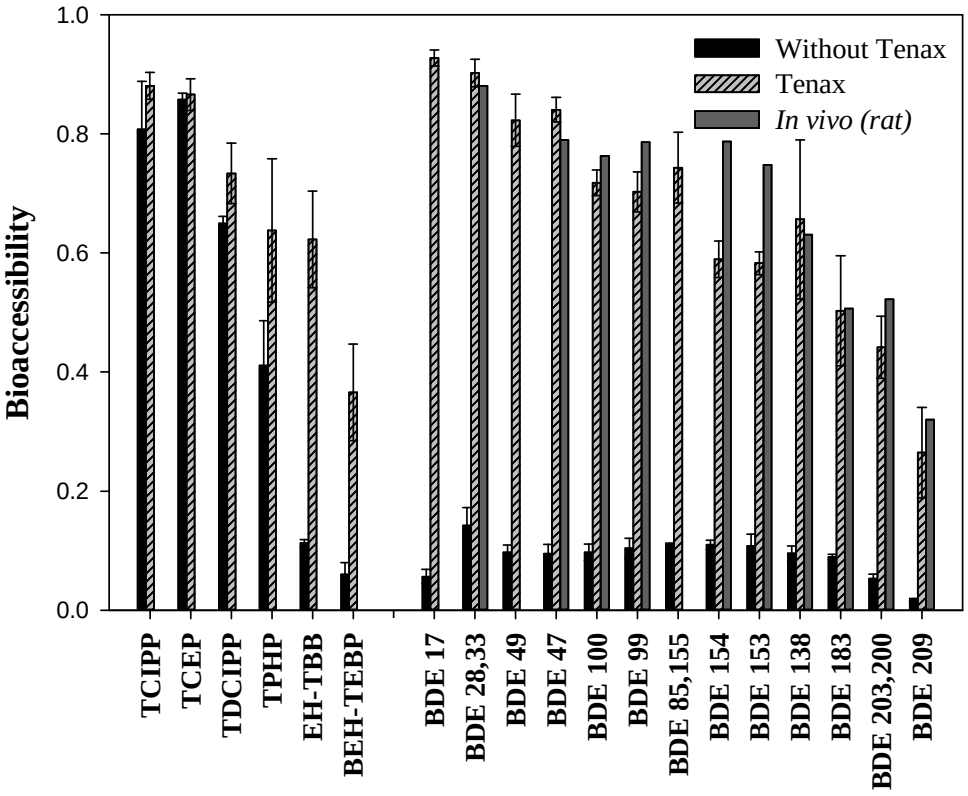

Figure 4: Measured bioaccessibility of OPFRs, EH-TBB, BEH-TEBP, and PBDEs in SRM2585 sieved to < 53 micron (n = 3) with and without TA-assisted extractions. The net absorption rate of several PBDEs in a previous *in vivo* study using *Sprague–Dawley* rats dosed with SRM2585 was also included as comparison (Huwe et al. 2008). Error bar represents standard deviation of triplicates.

2.3.3 Bioaccessibility of FRs in house dust (n=17)

After validating the TA method, the bioaccessibility of FRs in 17 different dust samples was investigated. FRs were well detected in those dust samples and the concentration were shown as follows: Σ_{10}BDEs (BDE 17, 28/33, 49, 47, 100, 99, 85/155, 154, 153, and 138, range: 150–76,540 ng/g dust, GM: 1,700 ng/g dust); BDE209 (range: 370–86,000 ng/g dust, GM: 1,720 ng/g dust); TCEP (range: non-detected–6,935 ng/g dust, GM: 360 ng/g dust); TDCIPP (range: non-detected–54,010 ng/g dust, GM: 1,620 ng/g dust); TCIPP (range: non-detected–65,820 ng/g dust, GM: 3,510 ng/g dust); TPHP (range: non-detected–1,532,000 ng/g dust, GM: 6,520 ng/g dust); EH-TBB (range: non-detected–3,500 ng/g dust, GM: 1,020 ng/g dust), and BEH-TEBP (range: non-detected–17,600 ng/g dust, GM: 530 ng/g dust). The calculated bioaccessibility of the FRs in individual dust samples can be found in **Table 4**; average values are presented in **Figure 5**. OPFRs, including TCEP, TCIPP, TDCIPP, and TPHP, are highly bioaccessible and 80% of the measured compounds in the house dust can be readily desorbed into the digestive fluid. In contrast, the bioaccessibility of PBDEs varied among congeners. The bioaccessibile fraction was over ~60% for the lower molecular weight PBDEs, such as tri-penta-BDE congeners, but it decreased to ~25% for the higher molecular weight compounds,

particularly BDE209. The bioaccessibility of EH-TBB was ~50% and BEH-TEBP was similar to BDE209.

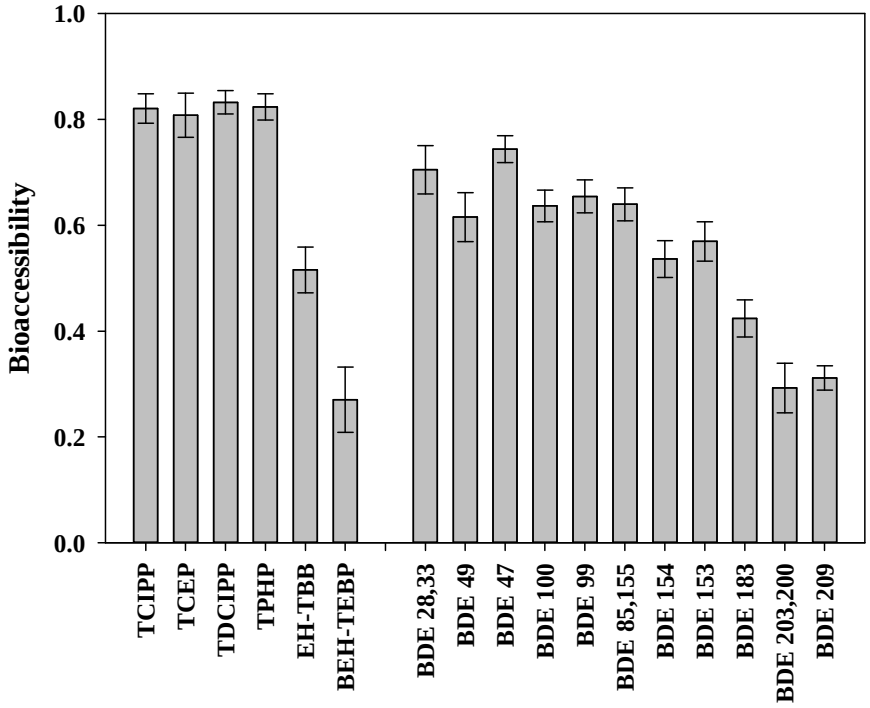

Figure 5: Average estimated bioaccessibility (%) of FRs in 17 dust samples. Error bar represents the standard error (n=17).

2.3.4 Factors affecting the bioaccessibility of FRs in dust

The FRs investigated here have a wide range in molecular weight, solubilities and partitioning properties, which likely influence their bioaccessibility. As shown in **Figure 6**, a general decreasing trend in bioaccessibility was observed with increasing LogKow. It should be noted that LogKow for some chemicals (e.g, OPFRs and EH-TBB/BEH-TEBP) were estimated using EPI suite (EPIWEB 4.1) while some (e.g., PBDEs) were based on experimental measures (Wania and Dugani 2003). The different sources for the K_{ow} values may explain why EH-TBB is a relative outlier in this relationship (Figure 6). However, overall the LogKow value was a good predictor of the bioaccessibility of the

FR chemicals. No difference in the bioaccessibility was observed for FRs with LogKow values <5, but a reverse relationship was observed for FRs with LogKow values >5. A two resistance model in absorption has been proposed in a previous study (McLachlan 1994). One resistance is the organic barrier (e.g, TA) with lipid like properties while the second is an aqueous barrier. At low LogKow values the lipid barrier provides the dominant resistance for absorption, which is independent of LogKow. However, as LogKow increases, diffusive transport through the aqueous barrier becomes increasingly limited and the absorption decreases. The relationship between K_{ow} and bioaccessibility observed in this study was very similar to a previous *in vivo* study in cows assessing the PBDE absorption potential (Kierkegaard et al. 2009). However, Lepom et al. (Lepom et al. 2013) reported that the bioaccessibility of individual PBDE congeners did not appear to be correlated with degree of bromination for tri- to hepta-BDEs using an *in vitro* method. And Ruby et al. (Ruby et al. 2002) did not find any correlation between bioaccessibility of polychlorinated dibenzodioxins/furan (PCDD/Fs) in soil and the degree of chlorination using a different *in vitro* method. In this study, the bioaccessibility of PBDEs in SRM2585 using the traditional incubation method (without TA) also did not show a decreasing trend for tri-hepta BDEs either. These findings suggest that the measured bioaccessibility is very method-dependent.

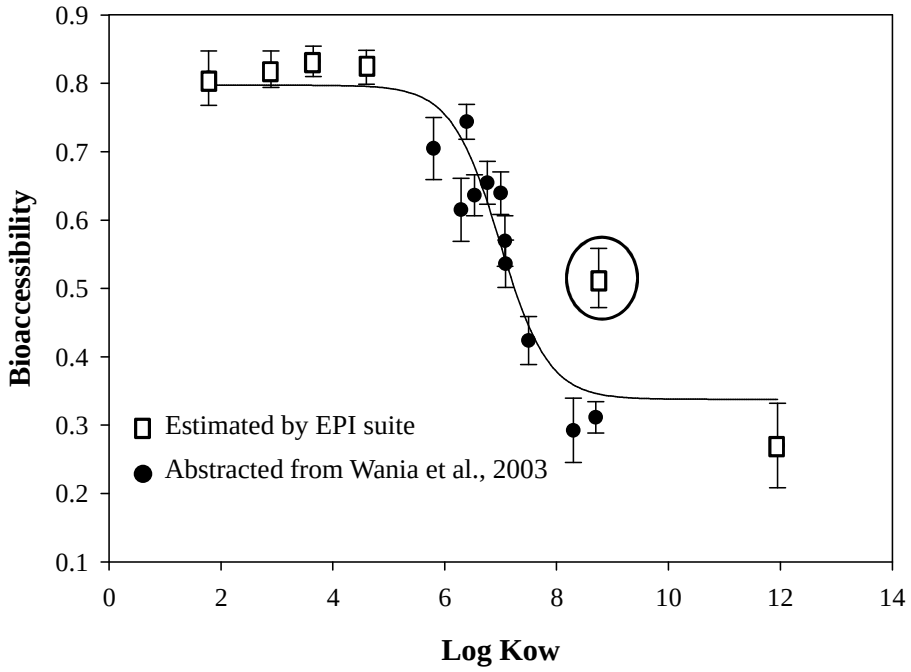

Figure 6: The relationship between bioaccessibility and hydrophobicity (LogK_{ow}) of the FRs in 17 house dust samples. The circled symbol represents EH-TBB. Error bar represents the standard error (n=17).

Dust samples from different sampling years were also analyzed to examine the potential effect of aging on the bioaccessibility of FRs, as previous studies have shown that aging could reduce the bioaccessibility of hydrophobic compounds in soils and sediments (Luo et al. 2012; Wong and Bidleman 2011). In these previous studies, the mobility of hydrophobic compounds sorbed to organic matter was reduced with aging of the soils/sediments. As shown in Figure 24, the bioaccessibility of dust samples collected in 2006 (n=7) was significantly different from those collected in 2010 (n=10; $p <$ 0.001, two-way *ANOVA*). Significantly higher bioaccessibility of TCIPP, EH-TBB, BEH-TEBP, BDE100, BDE183, and BDE200/203 was observed in the dust samples collected in 2010. However, BDE209 was not significantly different between the two groups, which

might be explained by the fact that most of BDE209 in the dust may be associated with weathered polymers from commercial products, and not from sorption onto dust particles directly (Webster et al. 2009). These results suggest for the first time that aging could decrease the bioaccessibility of some FRs in dust.

Since organic carbon content and composition of dust may also affect bioaccessibility, we investigated the relationship between these variables. No significant relationships were observed with TOC (Figure 25), or ratios of C/N, and C/H in the dust. In a previous study in soils, no particular relationship between TOC, black carbon content (BC), and bioaccessibility of PAHs was observed either (Collins et al. 2013). Due to the complexity and heterogeneity of the source for dust, it might be difficult to establish a model to effectively predict the bioaccessibility of one compound in the dust based on its composition.

2.3.5 Bioaccessibility of FRs in PUFs and size effect

Because dust samples may also contain small pieces of PUF from furniture, we also investigated the bioaccessibility of FRs directly from FR-treated PUF. Measured concentrations of FRs in three PUF samples were 1.8, 2.4, and 4.3 mg/g PUF for TDCIPP, Σ_{10}BDEs, and FM550 (the sum of EH-TBB and BEH-TEBP); respectively. As the FRs are more highly concentrated in the PUF relative to the dust, the mass of TA used in the incubations with PUF (0.6 g TA) was increased to reduce the likelihood of saturation. Also, no difference was observed using either 0.6 g or 1.0 g TA in a bioaccessibility test for FM550 impregnated foam (data not shown), suggesting 0.6 g TA can serve as an infinite sink of FRs from the foam. Microscopic imaging of the three size fractions

showed that PUF could be effectively fragmented into micro-foam particles (**Figure 26**), which also showed a similar shape with those identified in dust collected from a gymnasium (Carignan et al. 2013a).

The measured bioaccessibility of TDCIPP, pentaBDEs, and EH-TBB/BEH-TEBP in PUFs, as well as their fragmented foam particles, are shown in **Figure 7**. TDCIPP was quite bioaccessible (~70–80%) in the PUF, similar to the dust samples, and no particle size effect was observed. The bioaccessibility of PBDEs in the PUF was also related to hydrophobicity (i.e. LogKow), similar to the dust. Bioaccessibilty ranged from 20-40% for the tri- and tetra-BDEs and less than 10% for the penta- and hexa-BDEs. The bioaccessibility of EH-TBB and BEH-TEBP was less than 10% and no bioaccessible BEH-TEBP was observed in the non-fragmented foam (i.e. the PUF cube). An effect with particle size was observed with the higher molecular weight FRs, in which higher bioaccessibility was observed in the smaller particle size fractions (< 250 μm and < 100 μm) for both PBDEs and FM500 impregnated foam. The smaller particles have a larger total surface area and likely can facilitate the transport of FRs from the PUF to the digestive fluid. Here, the bioaccessibility of the more hydrophobic FRs in the foam was much less than what was observed in the dust samples, which might be due to lower fugacities of these chemicals in the PUF. PUF has a stronger retention capacity for semi-volatile organic chemicals and has been widely used as adsorbent in air monitoring for these types of compounds. A similar result was observed in an *in-vivo* study with earth worms, where the bioaccumulation factor in worms fed PUF was several times lower

than that of worms fed PBDEs in spiked soil (Gaylor et al. 2013). Therefore, our results suggest that the bioaccessibility of more hydrophobic FRs in PUF is lower than in dust.

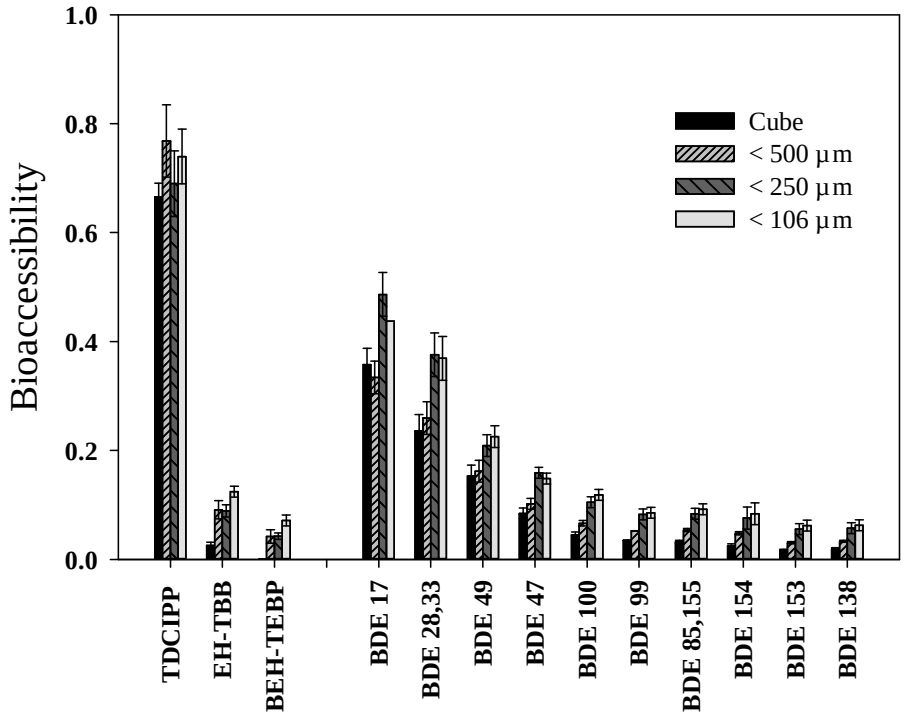

Figure 7: Estimated bioaccessibility of OPFRs, FM550, and PBDEs in three respective PUF samples with different particle sizes. Error bar represents the standard deviation of duplicate foam samples. Cube represents the whole piece of foam with a weight of ~20 mg.

2.3.6 Hydrolysis of OPFRs, EH-TBB and BEH-TEBP

We also investigated potential degradation of the more labile FRs during the incubation process. After incubating the FRs directly with three digestive fluids over a physiological residence time, no significant drop in the OPFR concentration was observed (**Figure 27**), suggesting negligible hydrolysis or degradation of OPFRs occurred in the digestive fluid. In contrast, ~70% of the initial EH-TBB concentration

disappeared after incubating with the intestinal fluid for 20 hours (**Figure 8**), which was not observed in either the gastric fluid or colon fluid. BEH-TEBP, another component in FM550, did not show any hydrolysis during the incubation (**Figure 8**). This observation was consistent with our previous study investigating the *in-vitro* metabolism of EH-TBB and BEH-TEBP in human and rat sub-cellular hepatic fractions (Roberts et al. 2012). Due to the similar pH range in the colon fluid and intestinal fluid, it was hypothesized that an enzyme in the intestinal fluid could hydrolyze EH-TBB in the intestinal fluid. Two enzymes (lipases and pancreatins) were added to the intestinal fluid in this study. The lipase, which is a type of esterase, can perform essential roles in the digestion, transport and processing of dietary lipids such as triglycerides (a carboxylic ester) to small fatty acids (Svendsen 2000). The pancreatin purchased in this study is a mixture of several digestive enzymes composed of amylase, lipase and protease. EH-TBB is a carboxylic ester and we therefore hypothesized that lipases in the intestinal fluid could degrade EH-TBB. To test this hypothesis an intestinal fluid mixture without lipases and pancreatins was prepared and incubated with EH-TBB. No decrease in the EH-TBB concentration was observed (**Figure 28**), supporting our hypothesis that the enzymes were mediating the transformation of EH-TBB. Subsequent experiments tested the degradation of EH-TBB with two different lipase concentrations, 1.6 mg/mL and 10 mg/mL, since the efficacy of porcine lipase used in this study may be much weaker than human lipase (Carrière et al. 2005). No difference was observed with the two different lipase concentrations (data not show). In previous studies, di-ethylhexyl phthalate (DEHP) was found to be hydrolyzed by rat lipases in several tissues, and the

quantitative data on rates of phthalate ester hydrolysis by intestinal enzymes suggested that low amounts of orally ingested DEHP would have little opportunity to be absorbed as the parent compound (Albro 1986; Albro and Thomas 1973).

The EH-TBB degraded in these experiments was transformed to tetrabromobenzoic acid (TBBA), which was confirmed using liquid chromatography tandem mass spectrometry (LC-MS/MS). As shown in **Figure 8**, increasing amounts of TBBA were observed with time. A mass balance analysis showed that TBBA was the major metabolite of EH-TBB in the intestinal fluid (~73% of EH-TBB degraded). TBBA was found as the major metabolite of EH-TBB in our *in-vitro* study (Roberts et al. 2012) and has been identified as a potential urinary biomarker for FM550 exposure (Hoffman et al. 2014b). Though little toxicity has been reported for this compound, TBBA has found to be a possible moderate peroxisome proliferator activated receptor (PPARγ) ligand (Fang et al. 2015). Since TBBA was rapidly formed, we also investigated the bioaccessibility of TBBA in the intestine or colon after hydrolysis. Due to the induction effect of the bromine atoms on the molecule, the estimated acid dissociation constant (pKa) of TBBA is 2.3 (using the Hammett Equation (Schwarzenbach et al. 2005)) and thus pH may influence the fate of TBBA. In our study, we tested the bioaccessibility of TBBA at two extreme pH values in the intestinal fluid (pH: 5.3 and 8) (Fallingborg 1999). TBBA was spiked into the digestive solution with a final concentration of ~1 μg/mL. At both pH values, the concentration of the TBBA did not change with time, suggesting that there is no absorption by TA (**Figure 29**). This result was not unexpected, since nearly all of the TBBA will be deprotonated at pH >5. *In vivo* absorption might not occur in the intestine

if no active transportation was involved. Overall, the hydrolysis experiment in this study revealed that more labile FRs can undergo transformation in the digestive fluid prior to absorption and should be considered in further exposure/risk assessment. However, it should be noted that this *in-vitro* method only included a limited set of enzymes and also did not include other factors such as microfloral activity, which could also affect absorption and fate in the gastrointestinal tract.

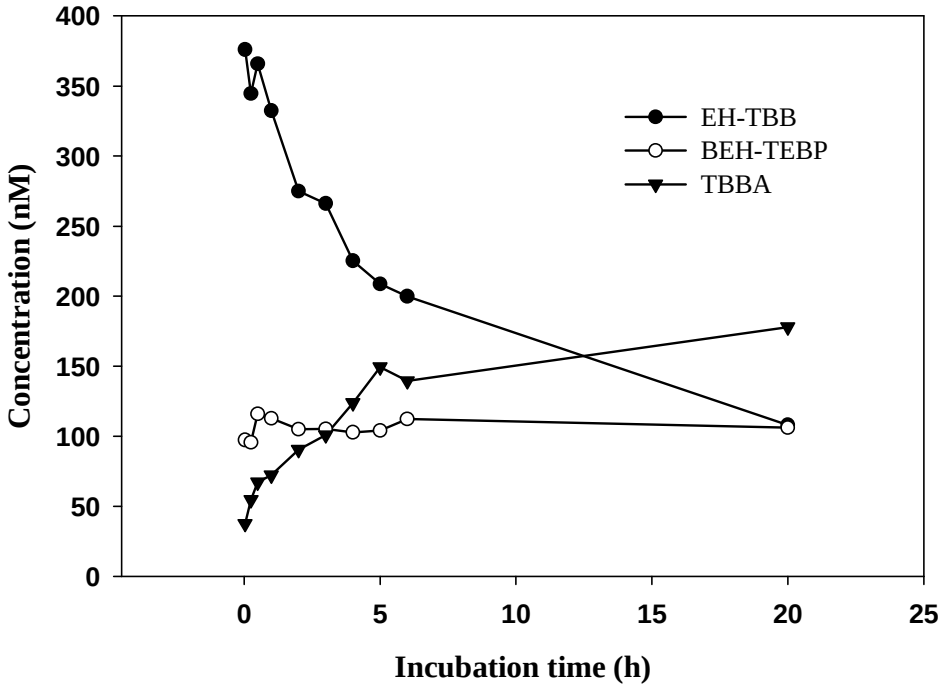

Figure 8: Concentration (nM) of spiked EH-TBB and BEH-TEBP and the formation of TBBA incubated with 1.6 mg procine lipases/mL intestinal fluid at 37 ℃ and pH~7 at different sampling time. Each value was the average of duplicate samples at each sampling time.

2.3.7 Environmental Implication

In this study, an *in vitro* bioaccessibility test using TA as an adsorption sink was developed and our results are very comparable to an *in vivo* study, confirming several

recent findings that the use of an infinite sink is necessary in evaluating *in vitro* bioaccessibility. The bioaccessibility of FRs varied greatly between compounds/matrices and it should be considered in future exposure and risk assessments, particularly for highly hydrophobic compounds (LogKow > 5). The results of this study also showed that less hydrophobic FRs such as OPFRs are quite bioaccessible in both dust and in PUF, suggesting a higher risk of exposure for those compounds, despite the fact that they are generally less bioaccumulative. To date, the stability of the ingested organic contaminants in the gastro-intestinal tract was not well studied, although metabolism after absorption has been a focus of several studies. In this study, EH-TBB was found to be readily transformed into TBBA in the presence of intestinal enzymes. Due to the abundance and variety of enzymes present in the digestive fluid, more labile organic contaminants with low ingestion rates might not be absorbed into the body as parent compounds. This may be an important consideration as chemical industries shift from producing persistent/bioaccumulative chemicals to less persistent forms. However, it should be noted that the *in vitro* artificial digestive fluid in the present study could not completely resemble human or rodent digestive fluids. For example, the role of microflora on the metabolism and absorption should be considered in future studies.

3. Characterizing the Peroxisome Proliferator–Activated Receptor (PPARγ) Ligand Binding Potential of Several Major Flame Retardants, Their Metabolites, and Chemical Mixtures in House Dust[1]

Accumulating evidence has shown that some environmental contaminants can alter adipogenesis and act as obesogens. Many of these contaminants act via the activation of the peroxisome proliferator activated receptor γ (PPARγ) nuclear receptor. Our goal was to determine the PPARγ ligand binding potency of several major flame retardants, including polybrominated diphenyl ethers (PBDEs), halogenated phenols and bisphenols, and their metabolites. Ligand binding activity of indoor dust and its bioactivated extracts were also investigated. A commercially available fluorescence polarization ligand binding assay (PolarScreenTM PPARγ-competitor assay kit, Invitrogen) was used to investigate the binding potency of flame retardants and dust extracts to human PPARγ LBD. Rosiglitazone was used as a positive control. Most of the tested compounds exhibited dose-dependent binding to PPARγ. Mono(2-ethylhexyl) tetrabromophthalate (TB-MEHP), halogenated bisphenol/phenols, and hydroxylated PBDEs were found to be potent PPARγ ligands. The most potent compound was 3-OH-BDE47, with an IC_{50} of 0.24 μM. The extent of halogenation and the position of the hydroxyl group strongly affected binding.

---

[1]Fang ML, Webster TF, and Stapleton HM. Characterize the PPARγ Ligand Binding Potential of Several Major Flame Retardants, Their Metabolites, Indoor Dust and Bioactivated Dust. Environmental Health Perspective, 2014, doi:10.1289/ehp.1408522.

In the dust samples, 21 of the 24 samples tested showed significant binding potency at a concentration of 3 mg dust equivalent (DEQ)/mL. A 3–16% increase in PPARγ binding potency was observed following bioactivation of the dust using rat hepatic S9 fractions. Our results suggest that several flame retardants are potential PPARγ ligands, and that metabolism may lead to increased binding affinity. The PPARγ binding activity of house dust extracts at levels comparable to human exposure warrants further studies into agonistic or antagonistic activities and their potential health effects.

3.1 Introduction

According to a report from the Center for Disease Control and Prevention (CDC), 17% of children between 2 and 19 years of age are obese in the US, and the health care costs associated with obesity were estimated to be more than $140 billion in the US in 2008 (Ogden et al. 2012). While genetics, diet, and exercise all contribute to obesity, recent studies have shown that prenatal exposures to "environmental obesogens" including bisphenol A, phthalates, organotins and perflourinated compounds may increase the risk of obesity in children (A. Janesick and B. Blumberg 2011). Several studies found significant associations between urinary metabolites of phthalates and obesity (Wang et al. 2013). High levels of several persistent organic pollutants (e.g., DDE, hexachlorobenzene, and polybrominated diphenyl-ethers (PBDEs)) have also been found to be associated with obesity in humans (Tang-Peronard et al. 2011).

Current research suggests that several of the obesogenic compounds act via a mechanism involving activation of peroxisome proliferator-activated nuclear receptors

(PPARs) during perinatal development (A. Janesick and B. Blumberg 2011). PPARs are master transcriptional regulators controlling intracellular lipid flux and adipocyte proliferation and differentiation. Heterodimerized with the retinoid X receptor, PPARs serve as metabolic ligand sensors for a variety of hormones, dietary fatty acids, and their metabolites (Grün and Blumberg 2009). Chemicals that specifically activate PPARγ and upregulate expression may promote the development of obesity. Studies investigating the crystal structure of PPARγ with thiazolidinedione drugs have found that it exhibits flexible plasticity in the ligand-binding domain (PPARγ LBD), which allows it to accommodate a wide variety of ligands (Nolte et al. 1998). The endogenous ligands of PPARγ include polyunsaturated fatty acids, prostanoids, and oxidized fatty acids. Several anti-diabetic drugs of the thiazolidinedione class such as rosiglitazone target PPARγ (Lu and Cheng 2010) and weight gain is often a side effect (Ness-Abramof and Apovian 2005). Environmental contaminants including tributyltin (TBT), triphenyltin (TPT), and mono(2-ethylhexyl) phthalate bis(2-ethylhexyl) (MEHP) (a metabolite of the phthalate DEHP), have been shown to upregulate and stimulate several PPARs (Feige et al. 2007).

Flame retardants (FRs) are a class of compounds that have been used in large volumes over the past few decades to reduce the flammability of textiles, polymers and resins. Accumulating evidence has suggested that FRs might represent an important class of compounds that could bind to PPARγ and disrupt signaling. A recent study found that 2,2,6,6′-tetrabromo bisphenol (TBBPA) and 3,3′,5,5′-tetrachlorobisphenol A (TCBPA), were agonists of PPARγ (Riu et al. 2011). In our recent studies, Firemaster 550

(FM550), a FR replacement for pentabromodiphenyl ethers (Penta-BDEs), activated PPARγ and initiated adipocyte differentiation *in vitro* (Pillai et al. 2014), which may explain why perinatal exposure to FM550 in rats lead to obesity and glucose sensitivity (Patisaul et al. 2013). Therefore, further investigation of PPARγ-targeted disruption by FRs is warranted.

Several organophosophate compounds are also structurally similar to PPARγ exogenous agonists. For example, tributylphosphate (TBuP) and tris(2-butoxyethyl) phosphate (TBEP) are structurally similar to TBT. The PPARγ ligand triphenyl phosphate (TPP) and its antioxidant analogue triphenylphosphite (TPPi) resemble TPT. Many of the PBDE metabolites (i.e., hydroxylated PBDEs and halogenated phenols) are structurally similar to TBBPA, which was shown to be a PPARγ ligand. Therefore, it would be of great interest to investigate whether these structurally similar compounds could also act on PPARγ.

Indoor dust is a primary sink for additive chemicals applied to consumer products, and many of the reported environmental obesogens are found abundantly in house dust. For example, DEHP was detected in all dust samples analyzed with a geometric mean concentration of 340,000 ng/g (Rudel et al. 2003), and organotins are also commonly detected (Kannan et al. 2010). Three of the four chemicals in FM550 were widely detected in house dust samples in the US (Dodson et al. 2012; H.M. Stapleton et al. 2014). Young children in the US spend a majority of their time (>95%) indoors where they are chronically exposed to FRs due to increased hand to mouth activity (U.S. EPA

2009). Therefore, it is important to investigate the PPARγ binding potency of environmentally relevant house dust samples.

Little attention has also been given to the effect of bioactivation on PPARγ disruption. Several studies have revealed that metabolites can be more potent endocrine disruptors than the parent compounds. For example, the metabolite MEHP exhibited much stronger PPARγ binding potency than its parent compound, DEHP (Feige et al. 2007). Tetrabromo mono(2-ethylhexyl)phthalate (TBMEHP), a metabolite of bis(2-ethylhexyl) tetrabromophthalate (TBPH), has also been reported to be an agonist for PPARs in mouse NIH 3T3 L1 preadipocyte cells, whereas TBPH was not (Springer et al. 2012). The chemicals present in ingested house dust are absorbed into the digestive system and can be metabolized to chemicals with more polar functional groups. Therefore, it is important to determine whether PPARγ binding potency of contaminants changes with metabolism.

The primary goals of this study were to: 1) characterize the binding potency of several major FRs such as PBDEs (and their metabolites) using a human protein–ligand binding assay; 2) test the PPARγ binding activity of indoor dust extracts; and 3) examine the effect of *in vitro* bioactivation on the PPARγ binding potency of dust extracts.

3.2 Materials and Methods

3.2.1 Chemicals

The tested compounds included FM550 (and their metabolites), several PBDE congeners (and their metabolites), halogenated phenols and bisphenols. All the

abbreviation was shown in Appendix B Abbreviation. Rosiglitazone and MEHP were used as positive controls. The chemical structures of all the tested compounds are shown in Appendix Figure 30. 2,2',4,4'-tetrabromodiphenyl ether (BDE-47) and 2,2′,4,4′,5-pentabromodiphenyl ether (BDE-99), their metabolites [i.e., 3-OH-BDE-47, 5-OH-BDE-47, 6-OH-BDE-47, 5′-OH-BDE-99, and 6′-OH-BDE-99], and TBBPA (98%) were purchased from AccuStandard (New Haven, CT). 2,4,6-tribromophenol (2,4,6-TBP, 99%), 2,4,6-triiodophenol (2,4,6-TIP, 97%), 2,4,6-trifluorophenol (2,4,6-TFP, 99%), 2,4,6,-trichlorophenol (2,4,6-TCP, 98%), TPP (99%), diphenyl phosphate (DPP, 99%), rosiglitazone (98%), triclosan (> 97%), TBT (96%), TBEP (94%), TPPi (97%), DL-dithiothreitol (DTT, >99%), β-nicotinamide adenine dinucleotide 2′-phosphate reduced tetrasodium salt hydrate (β-NADPH, >93%), magnesium chloride (hexa-hydrates, >99%), and dextran (Leuconostoc spp., MW: 6,000 to 10,000) were purchased from Sigma-Aldrich (St Louis, MO). TPT (95%) was purchased from ACROS Organics (NJ, USA). TCBPA (98%) was purchased from TCI America (Portland, OR). The metabolic product TBBA (estimated > 98% purity by H1-NMR) was synthesized by the Duke Small Molecule Synthesis Facility. TBMEHP was a gift from Dr. Kim Boekelhide's group at Brown University. MEHP (98%) was purchased from Wako Pure Chemical Industrials, Ltd (Osaka, Japan). A commercial standard of FM 550 was supplied by Great Lakes Chemical (West Lafayette, IN), a company owned by Chemtura (Philadelphia, PA). ITP commercial mixture was purchased from one manufacturer in China. All solvents and other materials were of HPLC grade.

3.2.2 Chemical Analysis

To investigate the elution profile of chemicals in the gel permeation chromatography (see Appendix, Operation of Gel Permeation Chromatography), DEHP, MEHP, TBBPA, TBBA and other tested compounds were quantitatively analyzed by either liquid chromatography tandem mass spectrometry (Agilent 6410 Triple Quad LCMS) or gas chromatography coupled with mass spectrometry detector (GC-MSD). The details of the parameter used in this study were described in Table 5.

3.2.3 PPARγ Competitive Binding Assay

A detailed description of the PPARγ binding assay is shown in Appendix B PPARγ Competitive Binding Assay. Briefly, a commercially available high-throughput ligand binding assay (PolarScreen™ PPARγ-competitor assay kit, Invitrogen) was used to investigate the binding potency of tested compounds to PPARγ LBD. The kit uses the human-derived recombinant PPARγ-LBD tagged with a N-terminal GST-tag and a selective fluorescent PPARγ ligand (PPARγ Green). A SpectraMax M5 plate reader was used in fluorescence polarization (FP) mode with 485 nm excitation and 535nm emission wavelength. To measure ligand binding, we quantified polarization (mP) of the bound protein using the following equation:

$$mP = 10^3 * (I_p - I_s)/(I_p + I_s) \quad [1]$$

where I_p and I_s are the fluorescence intensity of emissions that are parallel (P) and perpendicular (S) to the excitation light; respectively (Rossi and Taylor 2011).

3.2.4 Dust sample dosing

Extracts of indoor dust samples (n=23) collected from our previous studies and a dust Standard Reference Material (SRM 2585, National Institute of Standards and Technology (NIST), Gaithersburg, MD) were tested for ligand binding potential. The indoor dust samples were investigator-collected from the main living areas of homes for Group A (Stapleton et al. 2012a) and D (H. M. Stapleton et al. 2014). Dust samples in Group B were collected from gymnastics studios (Carignan et al. 2013b). Dust samples in Group C were investigator collected from office environments (Watkins et al. 2013), and Group E were participant-collected dust samples from the main living area as reported in Hoffman et al. (2014). All dust samples were extracted with acetone:hexane (1:1, v/v) using sonication, and then concentrated, filtered and reconstituted in dimethyl sulfoxide (DMSO). Fluorescence background (FB) from the dust matrix was initially observed in the dust extracts (observed by spiking the incubation buffer solution with the extract but without PPARγ LBD and PPARγ Green). Therefore, the dust extracts were cleaned and diluted prior to measuring the PPARγ ligand binding activity. As shown in Appendix Figure 31 (a), a FB dose-response of SRM 2585 was observed and dilution greatly reduced the FB from the dust matrix. In this study, gel permeation chromatography (GPC, Environgel GPC system (Waters, Milford, CA, USA)) cleanup, which can partially remove large molecular weight (MW) compounds containing fluorophores, was used to clean the extracts (See Appendix B Operation of Gel Permeation Chromatography and Table 6). To minimize FB, further dilution was performed until no obvious FB (i.e., < 5% intensity of the complex consisting of 1.25nM PPAR-Green and 38nM PPARγ LBD) was observed. Following GPC cleanup and

dilution, a single concentration of 3 mg dust equivalent quantity (DEQ)/mL PPARγ assay medium was prepared to qualitatively investigate the relative PPARγ binding potency of the dust samples and a full dose-response of one potent dust extract was investigated. To quantitatively estimate the effect of FB on the polarization values (mP), we spiked the positive control (rosiglitazone, 12.5μM) into several different dose levels of a SRM2585 extract previously cleaned by GPC to measure the ligand binding activity relative to the pure standard.

3.2.5 Bioactivation of dust samples

The influence of biotransformation on ligand binding activity was assessed by incubating dust extracts in a pooled liver S9 fraction prepared from Sprague Dawley rats (Gibco, Grand Island, NY). Bioactivation was assessed in 7 of the 23 dust samples (one dust sample was tested in triplicate while the others were tested once due to dust mass limitations) and in SRM 2585 (n=3). The 7 dust samples were from Group A (Samples 5,7,8), B (Samples 9,10) and C (Samples 11,12). The influence of biotransformation was also investigated using pure chemical standards. DEHP (100μM) and a mixture (MIX) containing 1μM each of FM550, isopropylated triaryl phosphate (ITP), BDE47, BDE99, and DEHP were evaluated for binding activity before and after bioactivation. A detailed description of the method is shown in Appendix B Bioactivation of Dust Samples and S3. Briefly, dust samples were bioactivated by incubation with an S9 fraction (1 mg protein/mL), extracted, and cleaned by dextran-assisted liquid-liquid extraction and phenolic extraction. An additional sample of each dust extract was incubated with inactive S9 fraction (by adding 150 μL of ice-cold 6 M HCl before incubation) to serve as

a control. To test the efficacy of metabolism, MEHP, which is a metabolite of DEHP in house dust, was used as a marker compound to optimize the incubation method (See Figure 33). To compare the bioactivation difference between rodents with human, a pooled human liver S9 (CellzDirect, Durham, NC) was also used to bioactivate SRM2585.

3.2.6 Data Analysis

IC_{50} values and dissociation constants were calculated to compare the potency of binding. In this competitor study, the dose-response curve was depicted as ligand-binding, three parameter sigmoidal dose-response model in the ''Regression Wizard'' in SigmaPlot 12.0 (Systat Software Inc., Chicago, IL):

$$y = min + (max - min)/(1 + 10^{(\log IC_{50} - x)}) \quad [2]$$

where y is the measured polarization value (mP); x is the log of the compound concentration; max is the mP of the DMSO control or the maximum mP of the tested compounds; min is the the basal mP when reference agonists completely inhibit the binding between PPARγ LBD and PPAR-Green. Since min was not zero and varied between batches, high doses of rosiglitazone (10 μM) were run alongside each batch to roughly calculate the $min_{norminal}$. The dissociation constants were calculated according to the following equation (Lin et al. 1999):

$$IC_{50}/[\text{PPARγ Green}] = K_{d,ligand}/K_{d,probe}, \quad [3]$$

where $K_{d,probe}$ is the dissociation constant calculated from titration of 1.25 nM PPARγ Green with added PPARγ-LBD concentration.

3.2.7 Statistical Analyses

All statistical analyses were conducted using SigmaPlot 12.0 (Systat Software Inc.), testing hypotheses at $\alpha = 0.05$, and all tests were two-tailed. When comparing the binding potencies of the dust extracts, all the FP values of the dust samples were normalized to the procedural blank. Then a one way *ANOVA* was conducted and Newman-Keuls *post-hoc* test was used to identify which dust extracts were significantly different from the procedural control. When comparing the PPARγ binding activity before and after metabolism, all the data were normalized to the mP of the S9 control and student *t*-test was used to test the difference between active S9 and inactive S9 for the dust samples with triplicate incubations. For the bioactivated dust (n = 6) with single measurements, paired *t*-test was conducted. Quality control is described in Appendix B Quality Assurance/Quality Control.

3.3 Results

3.3.1 Performance of the FP assay

We used rosiglitazone as a positive control in the ligand binding assay. As shown in Table 2, the IC_{50} of rosiglitazone was 0.23 μM. The FP range was more than 120 mP, indicating a good dynamic range for the dose-response. A PPARγ-LBD titration curve was also investigated by varying the protein concentration in 1.25 nM PPAR-Green (See Figure 34). In this study we used 38 nM of the PPARγ-LBD, which was in the linear range of the titration curve, providing a calculated K_d of 20 nM. A "U" shaped dose-

response curve was observed for some tested compounds, which was probably due to limited solubility and precipitation of the compounds. Under such circumstances, the FP values of the concentration on the right side of the "U" shape were discarded for data analysis and partial dose-response curves were analyzed. The primary challenge of this assay was the fluorescence interference from the dust matrix in the extracts. As shown in Appendix Figure 31 (a), GPC cleanup can reduce the FB significantly, which suggests that macromolecules might be resulting in the observed interference. After further dilution, a dose of 3 mg DEQ/mL was used for the dust samples. In the matrix-spiked rosiglitazone test, the binding activity of rosiglitazone was completely masked at high matrix background (12.5 mg DEQ/mL) (See Figure 35). The FB of house dust increased the fluorescence intensity of emission parallel (P) to the excitation plane more than that perpendicular (S) to the excitation plane, which resulted in the increased mP. It is impossible to completely eliminate the background interference, and exhaustive cleanup increases the possibility of analyte loss. We estimate that at the dosing concentration used in this study (3 mg DEQ/mL), the binding potency of house dust might be actually be underestimated by 5-10% due to the fluorescence interference from dust matrix (see Appendix Figure 35). Overall, we conclude that the FP assay was appropriate and efficient to evaluate the binding potency of the tested compounds and dust extracts. The dose-response curves of the tested compounds were shown in Appendix Figure 36 and the calculated IC_{50} together with K_d was listed in Table 2.

Table 2: IC_{50} Values, Dissociation Constants (K_d), and the Relative Potency by setting Rosiglitazone as 1

Parent Compounds* and Metabolites		IC_{50} (μM)	K_d (μM)	Relative Potency
Rosiglitazone		0.23	0.12	1.0000
TBB		NA	NA	NA
	TBBA	42.0	22.10	0.0055
TBPH		NA	NA	NA
	TBMEHP	0.64	0.34	0.3594
DEHP		NA	NA	NA
	MEHP	3.80	2.00	0.0605
TPP		40.0	20.87	0.0058
	DPP	627	327.13	0.0004
ITP		60.0	31.30	0.0038
TPT		1.72	0.90	0.1337
TPPi		>1,250	>652.17	<0.002
TBT		0.30	0.16	0.7667
TBuP		137	71.48	0.0017
TBEP		103	53.74	0.0022
BPA		NA	NA	NA
TCBPA		5.18	2.70	0.0444
TBBPA		1.49	0.78	0.1544
2,4,6–TFP		NA	NA	NA
(Continued)				
2,4,6–TCP		100	52.17	0.0023
2,4,6–TBP		36.3	18.94	0.0063
2,4,6–TIP		1.84	0.96	0.1250
BDE–47		>12	>6.25	<0.16
	3–OH BDE47	0.24	0.13	0.9583

	5–OH BDE47	3.09	1.61	0.0744
	6–OH BDE47	>10.0	>5.22	<0.023
BDE–99		NA	NA	NA
	5′–OH BDE99	30.0	15.65	0.0077
	6′–OH BDE99	>50	>26.09	<0.0046
Triclosan		12.5	6.52	0.0184

NA–No effect at 250μM; * The chemicals in bold represent the parent compounds.

3.3.2 FM550 metabolites

Using this assay, we recently demonstrated that while the organophosphate components in FM550 did bind to PPARγ, the brominated components, TBB and TBPH, did not (Pillai et al. 2014). We also investigated the binding affinities of potential metabolites of the individual FM550 components [See Figure 9 (a)]. We found that the metabolites of TBB and TBPH, TBBA and TBMEHP (Roberts et al. 2012), respectively, can bind PPARγ effectively. As shown in Table 2, TBBA was found to be a moderately potent ligand of PPARγ with an IC_{50} of 42 μM. The binding of TBMEHP was particularly potent with an IC_{50} of 0.64 μM, which was much lower than the well-known PPARγ agonist MEHP (3.8 μM) and comparable to PPARγ binding pharmaceutical compound rosiglitazone (IC_{50}: 0.23 μM). The metabolite of TPP (IC_{50}: 40 μM), DPP (IC_{50}: 627 μM), was one order of magnitude less potent than its parent compound.

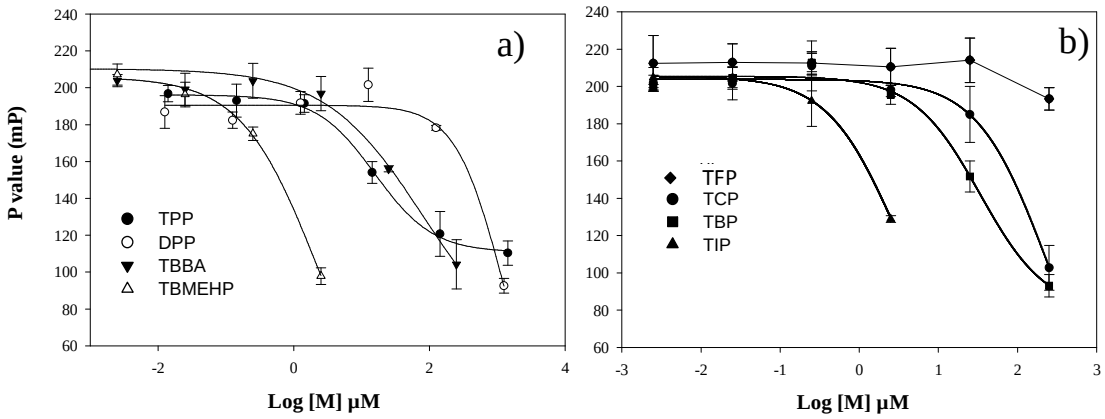

Figure 9: FP value (mP) of 1.25 nM PPAR–Green as a function of a) added TPP, and several FM550 metabolites including DPP, TBBA and TBMEHP and b) added 2,4,6–TFP, TCP, TBP and TIP concentration in 40 µL of 38 nM PPARγ LBD. Values represent the average of the triplicates, and error bars represent standard deviation.

3.3.3 Halogenated phenols/bisphenols

Phenols and biphenol compounds with different degrees of halogenations were also tested for binding with PPARγ. A dose-response relationship was observed for all the tested phenols except 2,4,6-trifluorophenol (2,4,6-TFP). Potency increased with size of the halogen in order of F<Cl (IC_{50}:100 µM)<Br (IC_{50}: 36.3 µM)<I (IC_{50}: 1.84 µM) [see Figure 9 (b) and Table 2]. A significant FB was observed for TIP at concentrations over 10µM. A similar trend in binding with halogenation was observed for TBBPA (IC_{50}:1.49 µM) and TCBPA (IC_{50}: 5.18µM), which are known PPARγ ligands; however, BPA did not exhibit any binding. Triclosan, which is largely applied in personal care products, also exhibited PPARγ binding with an IC_{50} of 12.5µM.

3.3.4 BDE and BDE metabolites

The binding activity of BDEs was very poor. The calculated IC_{50} for BDE47 was >12μM, and no binding was observed for BDE99 at any dose tested. However, some of the OH-BDEs were found to be very potent ligands of PPARγ (See Table 2). The BDE47 metabolite 3-OH-BDE47 (IC_{50}: 0.24μM) showed a similar binding capacity with the positive control rosiglitazone, followed by 5-OH-BDE47 with a calculated IC_{50} of 3.09μM. In contrast 6-OH-BDE47 and 6-OH-BDE99 were not active ligands for PPARγ. The calculated IC_{50} for 5-OH-BDE 99 was 30μM.

3.3.5 Organophosphate/phosphite analogues of organotin

As shown in Table 2, TBuP, TBEP, TPPi, and TPP were found to bind to the *PPARγ LBD*; however, the IC_{50} varied greatly between the compounds. TBuP (IC_{50}: 137μM) and TBEP (IC_{50}: 103μM) were two orders of magnitude less potent than TBT (IC_{50}: 0.3μM). However, we also observed that TBuP could completely inhibit the binding between the probe and the PPARγ LBD at the high concentration (2,500μM, see Appendix Figure 36). TPPi was much less potent at binding than TPP (IC_{50}: 40 μM) and TPT (IC_{50}: 1.72μM) with an IC_{50} >1,250μM.

3.3.6 Binding activity of dust samples

Significant PPARγ binding activity of the dust samples at a concentration of 3 mg DEQ/mL was observed for 21 of the 24 dust samples tested (see Figure 10). No significant binding was observed for SRM2585. High variability was observed between the dust samples. Ten of the dust extracts competitively inhibited the binding between

the PPARγ LBD and PPARγ Green by more than 40% of the control. The binding potency of those dust extracts was only slightly lower than the positive control (12.5μM of rosiglitazone), which could completely inhibit the binding between the PPARγ and Green probe. Dust (DS) 6, which demonstrated a high binding potency, was selected to quantitatively evaluate the binding potency, and a clear dose-response relationship was observed [see Figure 37 (a)]. The calculated IC_{50} of DS6 was approximately 0.37 mg DEQ/mL. We also observed differences in binding potency among dust extracts from different sources. For example, the dust extracts from Groups A and D, which were collected from main living areas in homes, showed a higher binding affinity with PPARγ than other groups (see Figure 10). In contrast, the Group B samples collected from gymnastic studios did not show any obvious binding.

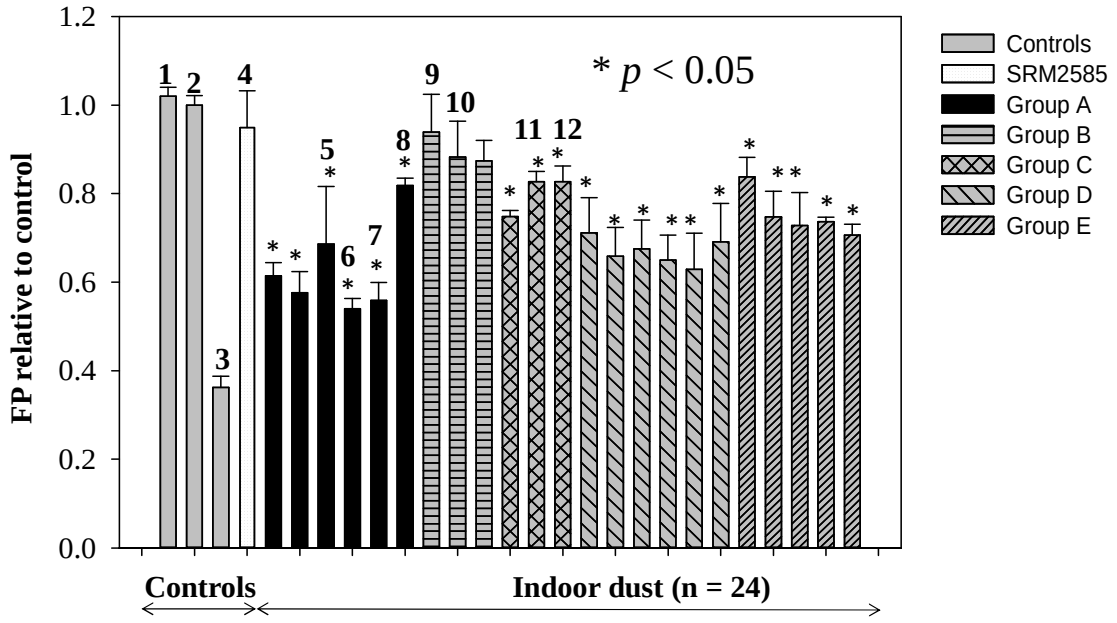

Figure 10: FP value (mP) of 24 dust samples with a concentration of 3 mg dust/mL relative to the procedure dust blank in 40μL of 38 nM PPARγ LBD and 1.25 nM PPAR–Green. "1" represents DMSO control. "2" represents procedure blank. "3" represents the positive control of 12.5μM rosiglitazone. "4" represents SRM2585 and "6" is the DS6 used for dose–response. "5" and "7–12" represents the dust extracts which were used in the bioactivation. Values represent average of the triplicates and error bar represents standard deviation.

3.3.7 Bioactivated dust samples

No difference in ligand activity was observed between the extracts of active and inactive S9 fractions alone (i.e., S9 control, see Figure 11). A slight increase in the potency of PPARγ binding was observed after bioactivation of 100μM DEHP (n=3), and the bioactivated MIX (n=3), which was about a ~5% increase in binding (i.e., ~10 mP). Bioactivated SRM2585 using rat liver S9 fraction was significantly more potent with an approximately 16% (i.e., 40 mP) increase in inhibition. A similar increase (~18%) was observed in SRM2585 incubated with the human liver S9 fraction, suggesting similar bioactivation effects on PPARγ binding. In DS5, a significant increase (~13%) in the binding was also found after bioactivation. A slight increase (3–10%) was also observed in other incubated dust samples. A paired *t*-test including all the dust samples with single incubations revealed that bioactivated dust samples showed significantly stronger binding potency with PPARγ than dust samples incubated with inactive S9 fraction ($p < 0.01$). To quantitatively observe the change with different doses, a dose-response analysis was conducted to investigate the binding potency of the MIX, bioactivated MIX, and SRM2585. A partial dose-response curve was observed because the dust matrix or

S9 co-extracts interfered with polarization at high doses [see Appendix Figure 31 (c) and (d)]. As shown in Appendix Figure 37 (b), higher inhibition potency was observed for the bioactivated MIX in the dynamic range of the dose-response curve. Bioactivated SRM2585 also showed a dose response curve [see Appendix, Figure 37 (c)], although no inhibition was observed for the nonactivated extract [see Figure 10 (a)]. Thus our data indicate that PPARγ binding potency of dust samples increases after metabolism.

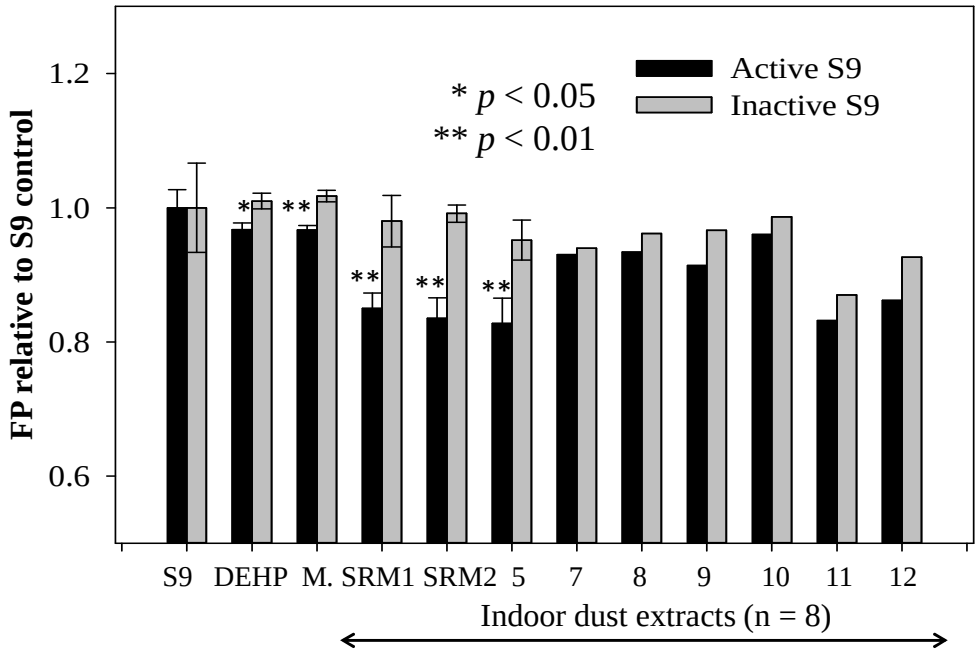

Figure 11: Competitive PPARγ binding potency of rat liver S9 control, DEHP, Mixture (M.), SRM 2585 and other 6 dust samples (100 mg) by incubation with S9 and inactive S9 fraction with a concentration of 1mg protein/mL in a final volume of 3 mL. All data were normalized with the mP of S9 control. M. includes 5μM FM550, ITP, BDE–47, BDE–99, and DEHP. SRM1 and SRM2 represent the incubation of SRM2585 with rat liver S9 and human liver S9, respectively. The dosing concentrations were 3mg DEQ/mL, 6 mg DEQ/mL, 2μM and 100μM for SRM2585, other dust samples, M., and DEHP; respectively. Values represent average of the triplicates and error bar represents standard deviation. Symbols without error bars represent one incubated sample.

3.4 Discussion

PPARγ is a master nuclear receptor that regulates lipid metabolism, cell proliferation signal transduction, apoptosis, and differentiation. Until now, few environmental contaminants have been shown to significantly bind and activate PPARγ signaling. This study was designed to test the PPARγ binding potency of several major FRs including FM550, and PBDEs, and their metabolites using a ligand-binding competitor assay. Furthermore, the PPARγ binding of SVOCs structurally similar to known PPARγ agonists, such as organotins and halogenated bisphenols, was examined. The binding potency of house dust samples and their bioactivated extracts was also examined. To our knowledge, very few studies have been conducted to investigate PPARγ disruption in environmentally relevant dust samples. However, it should be noted that no definitive conclusions can be drawn from this PPARγ binding data as to whether these samples would lead to transactivation of PPARγ.

Data presented here is consistent with data reported in previous studies based on a luciferase gene reporter cell line assay. The *in vitro* binding of FM550 and its components

were consistent with the Cos-7 luciferase reporter assay, indicating that TPP was the major contributor to the PPARγ binding in the commercial mixtures (Pillai et al. 2014). The relative potency of TBBPA and TCBPA tested in this study was also similar to the results of the HGELN-GAL-PPAR assay reported by (Riu et al. 2011). Therefore, our study showed that this direct protein–ligand binding competitor assay could be used as an effective alternative method in the early screening of PPARγ ligands.

In this study, we found that several of the tested chemicals or their metabolites can competitively bind with the PPARγ LBD. The calculated IC_{50} values and K_d of the tested compounds with the PPARγ-LBD varied considerably. Most of the previously reported potential PPARγ ligands (e.g., TBBPA, TCBPA, TB-MEHP, TBT, and TPT) were confirmed in this study using a different bioassay. To the best of our knowledge, many of the compounds tested here, including halogenated phenols, several hydroxylated metabolites of PBDEs and FM550, TBuP, TBEP and TPPi were shown for the first time to have PPARγ binding activity. Although some of the tested compounds (e.g., TBEP and TBuP) showed weaker PPARγ binding potency, these compounds may yet be of great concern because of their ubiquitous detection in indoor environments, with levels up to μg-mg/g (Van den Eede et al. 2011).

Our study also revealed that metabolites of many FRs can be more potent than their parent compounds. PBDEs are a group of FRs that has increased public health concerns for decades due to potential disruption of thyroid hormone regulation and neurodevelopment (Noyes et al. 2011). BDE-47 and -99, which were predominant

components of the banned PentaBDE commercial mixture that are still widely detected in the environment, did not show strong binding potency to PPARγ. However, OH-BDEs, which are formed through cytochrome P450-mediated oxidative metabolism of BDEs, were observed in the present study as potent PPARγ ligands. The metabolite 3-OH-BDE-47 exhibited a comparable binding potency to the drug rosigilitazone. 5-HO-BDE-47, which is one of the most abundant metabolites of BDE-47 (Qiu et al. 2007), also showed a very strong binding potency. Due to their high potency, further studies on the role of OH-BDEs in PPARγ signaling disruption should be investigated. Although the other two major components of FM550, TBB and TBPH, did not show any binding activity, their metabolites (TBMEHP and TBBA) can be potent ligands of PPARγ. While TBMEHP is not readily metabolized from its parent TBPH by enzymes in human hepatic S9 fractions or microsomes in our previous *in-vitro* studies (Roberts et al. 2012), the other major metabolites (i.e., DPP and TBBA) have been frequently identified in human urine samples (Cooper et al. 2011; Hoffman et al. 2014b; Meeker et al. 2013). To date, little toxicological information has been reported for TBBA, and further studies on its potential to disrupt PPARγ should be investigated.

Our results also highlight several characteristics that may increase binding potency to PPARγ. First, halogenation, especially bromination, increases the potency of PPARγ binding, which was confirmed by the specific binding activities of halogenated phenols and bisphenols. The flame retardant 2,4,6-TBP showed a similar binding potency with TPP. Our structure-activity relationship experiments showed that the inhibition potency

generally increased with increasing halogen molecular weight (i.e., I > Br > Cl > F), which suggests that non-specific hydrophobic interactions (i.e., Van der Waals force) with the PPARγ binding pocket favor binding. These findings are consistent with studies investigating T4-TTR binding affinity and deiodination activity inhibition (Meerts et al. 2000). A similar trend was also observed for TCBPA and TBBPA, which was consistent with a previous study suggesting that bulkier compounds bind more strongly with PPARγ (Riu et al. 2011). The IC_{50} of TB-MEHP was one order of magnitude lower than the IC_{50} of MEHP, which suggests that halogenation supports binding. All these findings indicate that the large ligand binding pocket of PPARγ can readily accommodate the addition of bulky bromine or chlorine. Therefore, PPARγ signaling disruption may be a major concern for FRs because most FRs are halogenated. Second, we also found that the number of halogens and the position of the hydroxyl group affect PPARγ binding. In this study, a dose-response relationship for BDE-47 was observed, but no binding was observed with BDE-99. Suzuki et al. (2013) also observed a dose- response relationship between PPARγ2 and BDE-47 with a 5% induction concentration of 10μM using a human osteosarcoma (U2OS) cell-based reporter assay (Suzuki et al. 2013), but no activity was observed for other BDEs. The variable IC_{50} values of BDEs and OH-BDEs suggest that the OH-BDEs with a *meta* hydroxyl group exhibited stronger PPARγ binding potency than OH-BDEs with an *ortho* substituted hydroxyl group. Among all the OH-BDEs tested, 3-OH-BDE-47 showed the most similar structure to the known PPARγ agonist TBBPA, with a *meta*-substituted hydroxyl group and two adjacent bromine atoms. Lastly, we observed that the PPARγ binding potency differed greatly for

chemicals with similar structures. Organophosphates were more potent than the organophosphites, but both were much less potent than the organotins, which suggests that some other chemical feature, perhaps the electron density of the tin atom, might play an important role in the binding. Alternatively, this also may be related to the relative solubilities of the compounds.

To date, few toxicological studies have investigated potential health effects from environmentally relevant house dust samples, which are more insightful than exposures of pure chemicals with regards to human exposure. Because many SVOCs bind to dust in the indoor environment, dust samples were tested for the PPARγ binding potency in this study. Binding activity was observed in most of the dust samples (21 out of 24 dust samples) and differences were observed between groups of dust extracts. To date, no characterization of the chemical composition in the dust samples from different sources has been conducted. In our previous study, FRs especially PBDEs in the dust from gymnasium (Carignan et al. 2013a), were found at least one order of magnitude higher concentrations than levels in residential dust, suggesting those FRs might not be the primary contributor to the PPARγ binding. However, the small sample size and heterogeneity of the house dust samples prevent any solid conclusions from being made. Also, the binding potency of the house dust in this study might be underestimated due to FP interference from the dust matrix. Young children spend most of their time indoors and are exposed to house dust via frequent hand-to-mouth behavior. Therefore, tests on dust samples are needed to determine the public health concerns for exposures

to contaminant mixtures present in dust. The USEPA estimates that children ingest between 50–100 mg/dust day (U.S. EPA 2009) . In one of the most potent dust samples, an IC_{50} of 0.37 mg DEQ/mL was observed. Therefore, our data suggest that environmentally relevant dust exposures might interact with PPARγ *in vivo*.

We also investigated the bioactivation of dust samples to increase understanding of the potential activity *in vivo* following metabolism. Stronger binding potency was observed in the bioactivated dust samples compared with the raw dust extracts. Bioactivation could transform the hydrophobic chemicals into more polar metabolites by adding polar groups such as –OH and –COOH, which might increase the binding interaction with the LBD through hydrogen bonds. It might be possible that several compounds such as TBB, TBPH, PBDEs, and DEHP in dust could be metabolized to PPARγ active ligands after incubation, which was supported by the increased binding potency of the prepared MIX containing these chemicals. While the effect of bioactivation was only on the order of less than ~20%, it is possible that *in vivo* metabolism would lead to higher binding activity. Chemicals in the human body would have a half-life that is longer than our two-hour incubation, and would lead to longer contact time with xenobiotic metabolizing systems in the body. Therefore, bioactivation should be considered when evaluating potency of environmental chemicals and potential human health risks.

3.5 Conclusion

In conclusion, this study showed that many of the tested compounds or metabolites are potential PPARγ ligands. Significant binding activity of environmentally relevant dust samples was also observed with high frequency. We also observed that bioactivation could increase the binding potency of chemical mixtures in the ingested dust. Further work is needed to determine which components in the dust samples are acting as ligands. A limitation of this study is that ligand binding does not necessarily indicate agonism of the receptor, leading to transcriptional events. Ligands can be agonists (full or partial) or competitive antagonists. To confirm the health effects of the identified PPARγ ligands, further studies using cell-based reporter assays that can distinguish between agonism and antagonism should be conducted.

4. Activation of Human Peroxisome Proliferator-Activated Nuclear Receptors (PPARγ) by Semi-Volatile Compounds (SVOCs) and Chemical Mixtures in Indoor Dust

In our recent study, several semi-volatile compounds (SVOCs) were found to be competitive ligands for human peroxisome proliferator-activated nuclear receptor gamma (PPARγ). We also observed significant binding from chemicals extracted from house dust at a concentration of 3 mg dust equivalent (DEQ)/mL. Our goal was to determine if the observed binding of pure chemicals or mixtures in house dust indicates agonism of PPARγ. A commercially available reporter gene assay (GeneBLAzer PPARγ non-DA Assay, Invitrogen) was used to investigate the PPARγ activation of groups of possible PPARγ ligands and house dust extracts. Many SVOCs or their metabolites were either confirmed or for the first time were found to be weak or moderate PPARγ agonists. We also observed that 15 of 25 dust extracts showed an activation percentage more than 8% of the maximal activation induced by rosiglitazone. In some cases, activation was as high as 50% of the rosiglitazone activation for the most potent dust extracts. Furthermore, there was a significant and positive correlation ($r = 0.7$, $p < 0.003$) between this reporter assay and our previous ligand binding assay tested on dust extracts. Our results suggest that many SVOCs ubiquitous in house dust, or their metabolites, are possible PPARγ agonists. Chemical mixtures present in house dust can activate human PPARγ in a transfected cell culture system at environmentally relevant levels of exposure, and further research is needed to identify the primary chemical(s) driving this activity.

4.1 Introduction

Peroxisome proliferator-activated nuclear receptor gamma (PPARγ) is a master nuclear receptor that regulates lipid metabolism, cell proliferation, apoptosis, and differentiation. Recently, many environmental contaminants have been shown to activate PPARγ, leading to increased adipogenesis in cell cultures an in vivo. Those chemicals include several organotins (tributyltin (TBT) and triphenyltin (TPT)), and mono(2-ethylhexyl) phthalate bis(2-ethylhexyl) (MEHP) (a metabolite of the phthalate DEHP), both of which were shown to upregulate and stimulate PPARγ (Feige et al. 2007; Grün et al. 2006). Several recent studies have suggested that flame retardants (FRs) and phthalates might represent important classes of compounds that could bind to and activate PPARγ. For example, 2,2′,6,6′-tetrabromo bisphenol (TBBPA),3,3′,5,5′-tetrachlorobisphenol A (TCBPA) and triphenyl phosphate (TPP), were identified as partial agonists of PPARγ (Pillai et al. 2014; Riu et al. 2011).In another study, benzyl butyl phthalate (BzBP) and butyl paraben showed significant activation of PPARγ and adipogenesis using cell culture assays (Pereira-Fernandes et al. 2013) . Therefore, it was of great significance to further identify new "chemical obesogens" and investigate their potential health effect.

In our recent study, more than 20 SVOCs, primarily including FRs and some of their metabolites, were tested for PPARγ binding potential using a fluorescence polarization ligand binding assay (PolarScreenTM PPARγ-competitor assay kit, Invitrogen) (Fang et al. 2015). Due to the accumulation of SVOCs in indoor dust, the PPARγ binding

potential was also investigated in house dust extracts. In that study, several organophosophate compounds such as tributylphosphate (TBuP) and tris(2-butoxyethyl) phosphate (TBOEP) which are structurally similar to tributyltin (TBT), showed significant binding potential, though much weaker than TBT. Many of the PBDE metabolites (i.e., hydroxylated PBDEs and halogenated phenols) could also effectively bind to PPARγ. As for the house dust, 21 of 24 dust samples tested showed significant PPARγ binding potency at a concentration of 3 mg dust equivalent (DEQ)/mL. However, ligand binding does not necessarily indicate agonism of the receptor, leading to transcriptional events. Therefore, it would be of great interest to investigate whether those identified possible PPARγ ligands or the chemicals in house dust could activate PPARγ.

To follow up on our previous study, PPARγ activation using cell-based reporter assays was used in this study. Chemicals which have been identified as possible PPARγ ligands were tested for PPARγ activation. Furthermore, several other groups of chemicals such as phthalates and triaryl phosphates which are ubiquitous in house dust were also included. The aryl phosphates with isopropyl or tert-butyl substitutions were similar to TPP in chemical structure and used as important components in FRs and plasticizers. Therefore, it is of great interest to study the PPARγ activation by those chemicals and investigate the structure-dependent activity. Also, the PPARγ activation by house dust extracts was also examined. According to the US EPA Exposure Factors Handbook (2009) , children are assumed to ingest 50 mg of dust per day, and dust ingestion has been increasingly identified as an important pathway for the uptake of

organic contaminants. Therefore, investigating PPARγ activation using environmentally relevant house dust samples could be of more value in estimating real-world exposure and possible health effects.

4.2 Materials and Methods

4.2.1 Tested Compounds

Most of the tested compounds were the identified PPARγ ligands in our previous study (Fang et al. 2015). The abbreviation and structures of all the tested compounds are shown in Table 3, Appendix Tested Compounds (C.1) and Figure 39. In general, those chemicals included FM550 (and their metabolites), tri-aryl phosphates, 2,2',4,4'-tetrabromodiphenyl ether (BDE47 and its metabolites), phthalates, halogenated phenols and bisphenols. Type II diabetes drug rosiglitazone was used as positive controls. An endogenous PPARγ ligands 15-Deoxy-D12,14-prostaglandin J2 (15d-PJG2) was also run as comparison.

4.2.2 House Dust Extracts

The house dust extracts were from our previous PPARγ binding assay (Fang et al. 2015). In brief, the indoor dust samples were investigator-collected from the main living areas of homes for Group A (Stapleton et al. 2012a) and D (Stapleton et al. 2014). Dust samples in Group B were collected from gymnastics studios (Carignan et al. 2013b). Dust samples in Group C were investigator-collected from office environments (Watkins et al. 2013), and Group E were participant-collected dust samples from the main living area as reported in Hoffman et al. (2014) (Hoffman et al. 2014a). All dust samples were extracted

with acetone:hexane (1:1, v/v) using sonication, and then concentrated, filtered, cleaned by gel permeation chromatography [GPC, Environgel GPC system (Waters, Milford, CA, USA)] and reconstituted in DMSO. A final stock with a concentration approximately 2000 mg DEQ dust/mL DMSO was prepared for PPARγ reporter assay.

4.2.3 PPARγ Reporter Assay

A commercially available reporter gene assay (GeneBLAzer PPARγ non-DA Assay, Invitrogen) was used to investigate the PPARγ activation of groups of possible PPARγ ligands and house dust extracts. The details of the assay are fully described in the Appendix, PPARγ reporter assay and cell viability assay. Amalar Blue assay which was prepared from resazurin was used for the cell variability test.

4.2.4 Data Analysis

After subtraction of fluorescence background from cell-free wells, the response ratio (RR) of fluorescence intensity at 460 versus 530 nm (designated as 460:530 nm) was calculated. All of the observed PPARγ activation by the chemicals or house dust extracts was normalized to the maximal response of rosiglitazone, and this activation percentage (Activation%) was used to describe the potency/efficacy of the samples. Activation% was calculated using the following equation:

$$\text{Activation\%} = (RR_{Compound} - RRDMSO)/(RR_{rosiglitazone} - RRDMSO)*100 \quad [1];$$

$RR_{Compound}$, RR_{DMSO} and $RR_{rosiglitazone}$ were the florescence response ratio of 460:530 nm in the tested compounds, DMSO control and maximal response of rosiglitazone; respectively.

For most tested chemicals and dust extracts, the activation% was less than 30%. As suggested for the weak agonists (Pereira-Fernandes et al. 2013), an activation threshold (LAT) is proposed based on the limit of quantification (LOQ) used in analytical chemistry techniques to assure the biological meaning of statistically significant effects. In this study, LAT is based on the variation of the DMSO control and calculated as the average DMSO value + 10*SD of the solvent control over all experiments. The result showed that activation% less than 8% was not thought to be significantly different from the DMSO control. To compare the potency/efficacy between compounds, maximal activation% (ATVmax), the concentration inducing the maximal activation [ATV]max, non-observable adverse effect level (NOAEL), and the concentration inducing 15% (EC_{15}) and 20% (EC_{20}) activation was reported in this study. Specifically, EC15 and EC20 were used for the potency and maximal activation was used to describe the efficacy. For the mixture such as ITP, FM550 and BPDP, the weighted molecular weight was calculated based on the composition. The statistical analyses and quality control are detailed in the Appendix.

4.3 Results

4.3.1 PPARγ reporter assay performance

Rosiglitazone was used as a positive control and showed a clear dose-response curve in the transactivation assay (Figure 12e). The calculated EC_{50} was approximately 5.5 nM, which was lower than that in the PPARγ ligand binding assay (EC_{50}: 349 nM). It was also 1-2 orders of magnitude more sensitive than reported in previous studies which used

either a human osteosarcoma (U2OS) cell-based reporter assay (EC_{50}: 52 nM) (Suzuki et al. 2013) or a Chinese Hamster Ovary (CHO) cell line luciferase reporter assay system (EC_{50}: 225 nM) (Belcher et al. 2014). Clear dose-response relationship were observed for 28 of the 35 tested compounds and are shown in **Figure 11** and **Table 3**. An inverted U-shaped non-monotonic concentration response relationship was observed for several of the compounds tested. Belcher et al. (2014) also observed non-monotonic relationships for several weak PPARγ agonists which he partially attributed to cytotoxicity. In this study, reduced cell viability was suggested based on results from an Alamar Blue cell viability assay. Most of the chemicals tested showed some cytotoxicity at concentrations >10μM. In some cases, there was no evident difference between the control and treated cells when evaluated for viability using the Alamar Blue assay. However, the proliferation of cell appeared to be hindered under microscopic examination (see Appendix Figure 40); cells were characterized by smaller proliferation colonies compared to control samples. Morphologically, HEK293 cells exposed to dosed chemicals or high concentrations of dust extracts displayed an enlarged round shape, losing cell-cell contact, in contrast with control cultures dominated by an elongated star-shaped cell morphology. A similar observation has been reported in a previous study (Pomati et al. 2006).

4.3.2 Organophosphates

As shown in Figure 12a, PPARγ activation varied greatly with slight changes in the chemical structure. The maximal activation of those chemicals followed the order:

TBPP~ TPPi ~Mono-ITP~Di-ITP<Tri-ITP<TPP< BPDP. The commercial mixture BPDP and TPP began to activate PPARγ at about 0.4μM and showed the highest PPARγ activation of approximately 60% and 42% relative to controls; respectively. Among the isopropylated ITP isomers, tri-ITP began to activate PPARγ at 1.2μM and showed the highest maximal activation of 41% at the dosing concentration of 33μM, while all three did not show any obvious activation at low doses (<1.2μM). Highly reduced cell viability was observed for mono-ITP and di-ITP compared with tri-ITP at high doses (33 and 100μM). The phosphite analogue of TPP, TPPi was much weaker than TPP, with the maximal activation of 12%. A clear dose-response curve was observed for TBOEP and TBuP, which analogous to TBT in structure. In general, the activation was much less potent than TBT. TBuP activated PPARγ at 0.4μM and the maximal activation was 23%. TBOEP with a maximal activation just above the activation threshold (LAT) at 11μM was weaker than TBuP. 15d-PJG2 is considered an endogenous PPARγ ligand and by comparison it showed potent PPARγ activation, which began to activate PPARγ at 0.01μM and had a maximal activation of 85% of rosiglitazone.

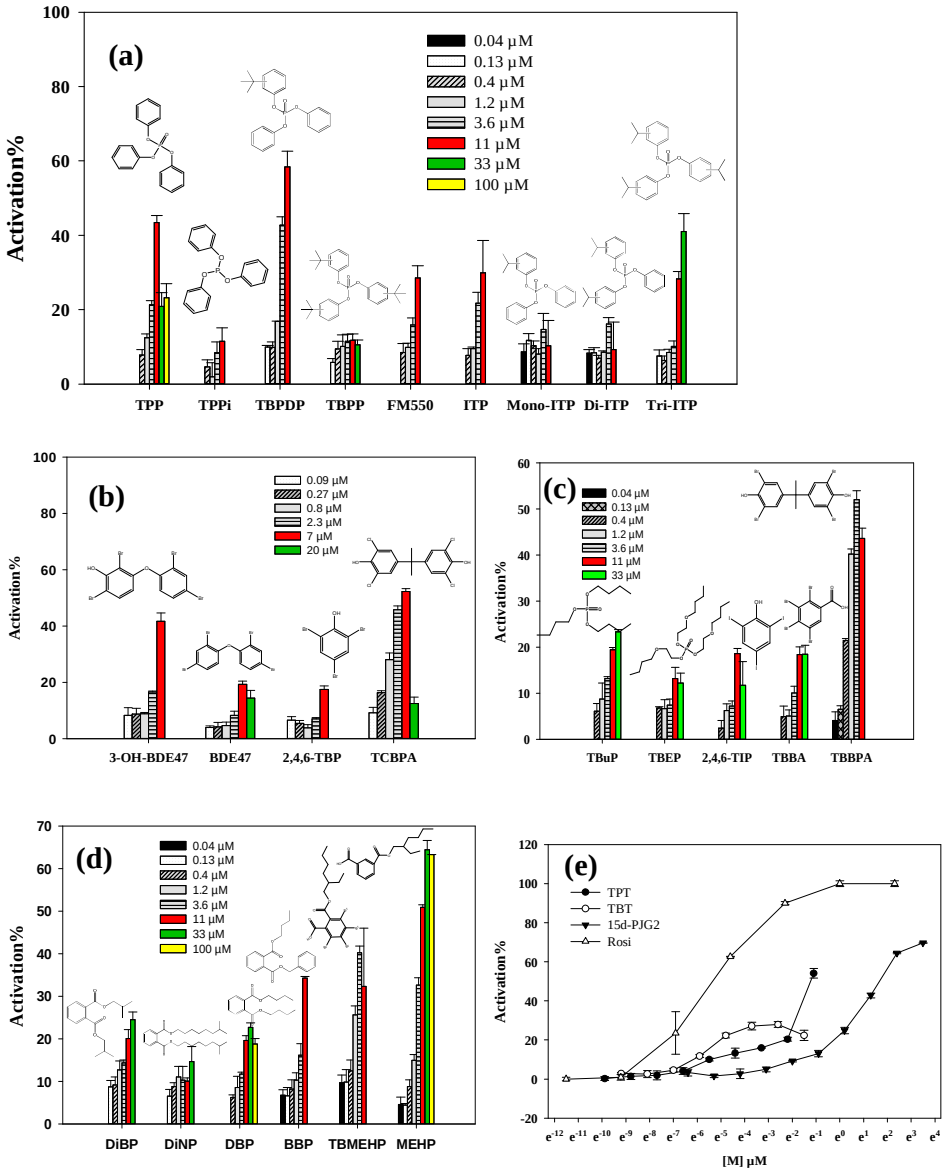

Figure 12: Dose-response relationship of PPARγ activation by: a) TPP and its related compounds; b) and c) phenols/ bisphenols and TBT analogs; d) phthalates and some metabolites; and e) potent PPARγ ligands including TPT, TBT, 15d-PJG2, and rosiglitazone. Values represent the average of the triplicates, and error bars represent standard deviation.

Table 3: Summary of PPARγ activation by test compounds using HEK293 PPARγ reporter assay.

Chemicals	Acronym	ATV_{max}	[ATVmax] (µM)	NOAEL (µM)	EC_{15} (µM)	EC_{20} (µM)	Efficacy *

Triphenyl phosphate	TPP	43%	11	0.4	2.12	3.27	++++
Triphenyl phosphite	TPPi	12%	11	1.2	NA	NA	+
Tert-butyl phenyl diphenyl phosphate	BPDP	58%	11	0.4	1.09	1.59	+++++
Tris (4, tert-butyl-phenyl) phosphate	TBPP	12%	11	0.4	NA	NA	+
Firemaster 550 (Mixture)	FM550	28%	11	1.2	3.23	6	++
Isopropylated triaryl phosphates (Mixture)	ITP	30%	11	1.2	2.28	3.32	+++
Mono-isopropylated triaryl phosphates	Mono-ITP	15%	3.6	1.2	3.6	NA	+
Di-isopropylated triaryl phosphates	Di-ITP	16%	3.6	1.2	3.25	NA	+
Tri-isopropylated triaryl phosphates	Tri-ITP	41%	33	1.2	5.7	7.76	++++
Tributyl phosphate	TBuP	23%	33	0.4	5.86	13.35	++
Tri(2-butoxyethanol) phosphate	TBOEP	13%	11	3.6	NA	NA	+
2,4,6-triiodinated phenol	2,4,6-TIP	20%	11	0.4	8.72	11	++
2,3,4,5-tetrabromobenzoic acid	TBBA	20%	33	1.2	8.16	33	++
2,2′,6,6′-tetrabromobisphenol A	TBBPA	52%	11	0.13	0.32	0.41	+++++
3-hydroxide-2,2',4,4'-tetrabromodiphenyl ether	3-OH-BDE47	42%	7	0.8	2.01	2.993	++++
6-hydroxide-2,2',4,4'-tetrabromodiphenyl ether	6-OH-BDE47	<10%	NA	NA	NA	NA	NA
2,2',4,4'-tetrabromodiphenyl ether	BDE47	20%	7	0.8	5.2	7	++
2,4,6-tribrominated phenol	2,4,6-TBP	18%	7	0.8	5.89	NA	+

3,5,3',5'-tetrachlorobisphenol A	TCBPA	52%	7	0.09	0.23	0.47	+++++
triclosan	TCS	<10%	NA	NA	NA	NA	NA
Diisobutyl phthalate	DiBP	25%	33	0.4	4.47	11.1	++
Diisononyl phthalate	DiNP	15%	33	0.4	33	NA	+
Dibutyl phthalate	DBP	23%	33	0.4	6.73	13.6	++
Benzylbutyl phthalate	BBP	34%	10	0.13	2.94	4.81	+++
Mono-(2-ethyhexyl) tetrabromophthalate	TBMEHP	40%	3.3	0.13	0.53	0.78	++++
Mono(2-ethylhexyl)phthalate	MEHP	65%	100	0.13	1.26	2.12	+++++
Bis(2-ethylhexyl) phthalate	DEHP	NA	NA	NA	NA	NA	NA
Bis(2-ethylhexyl) fumarate	BEHF	<10%	NA	NA	NA	NA	NA
Triphenyltin Chloride	TPT	54%	0.33	0.0003	0.004	0.01	+++++
Tributyltin Chloride	TBT	28%	0.07	0.0005	0.004	0.006	+++++
15-Deoxy-$D^{12,14}$-prostaglandin J2	15d-PJG2	85%	33	0.01	0.51	0.74	+++++
Rosiglitazone	Rosi.	100%	0.93	0.00001	0.00132	0.0005	+++++

*+ 8%-20% (**ATV_{max}**); ++ 20-30%; +++ 30-40%; ++++ 40-50%; +++++ >50%

4.3.3 Halogenated phenols/bisphenols

Of the tested phenol/bisphenols, TCBPA and TBBPA were the most potent, which was consistent the recent finding by Riu et al. (2011). In our previous study, 3OH-BDE47, TBBA, 2,4,6-TBP, and 2,4,6-TIP were identified as potential PPARγ ligands. In the PPARγ reporter assay, clear dose-response activation was observed for these chemicals, which began to act on PPARγ at micro-molar level. 3OH-BDE47 started to activate

PPARγ at 0.8μM and show the highest PPARγ activation, ~40%, at the highest dose (7μM), which was similar to the effect caused by TCBPA, though the latter had a much lower EC_{15}. However, no activation was observed for 6-OH-BDE47, suggesting the position of the hydroxyl group affects the PPARγ binding and activation, which was similar to the observation in our previous PPARγ ligand-binding assay (Fang et al. 2015). TBBA, which is a metabolite of a brominated benzoate in FM550 also showed a clear PPAR activation at high concentration with a maximal activation of 20% at 11μM. Triclosan, which showed moderate binding potency in our PPARγ binding assay (Fang et al. 2015), did not initiate any activation of PPARγ in this study.

4.3.4 Phthalates and their metabolites

A clear dose-response relationship was observed for BzBP, DiBP, DBP and DiNP, while no activation was observed for DEHP. The relative efficacy of PPARγ activation was: BzBP>DiBP~DBP> DiNP>DEHP. BzBP was the most potent (EC_{15}: 2.94μM) among all the parent phthalates with a maximal activation of 34%, which was consistent with the results reported in a previous study (Pereira-Fernandes et al. 2013). The phthalate monoesters TBMEHP and MEHP, which are the metabolites of TBPH and DEHP, respectively, were much stronger than the parent phthalate and showed moderately potent activation of PPARγ. MEHP began to activate PPARγ at 0.13μM and the maximal activation was 65%. TBMEHP showed a stronger activation than MEHP at lower dosing range, but lower activation at higher dose due to the reduced viability at higher dosing

levels. Another phthalate replacement DBHF did not display any obvious PPARγ activation.

4.3.5 PPARγ activation by dust samples

We found that 15 of the 25 tested dust extracts showed a clear dose-response relationship with the maximal activation at levels significantly higher than the activation threshold (LAT). In general, significant PPARγ activation was observed at ~100 μg DEQ dust/mL and there was a significant concentration-response trend within those 15 samples. In some cases, the activation was as high as 50% of rosiglitazone. No significant activation was observed for the house dust reference material SRM2585. High variability was also observed in dust extracts from different sources. For example, the dust extracts from Groups A and D, which were collected from main living areas in homes, showed a higher binding affinity with PPARγ than other groups (see Figure 13). In contrast, Group B samples collected from gymnastic studios did not show any obvious activation.

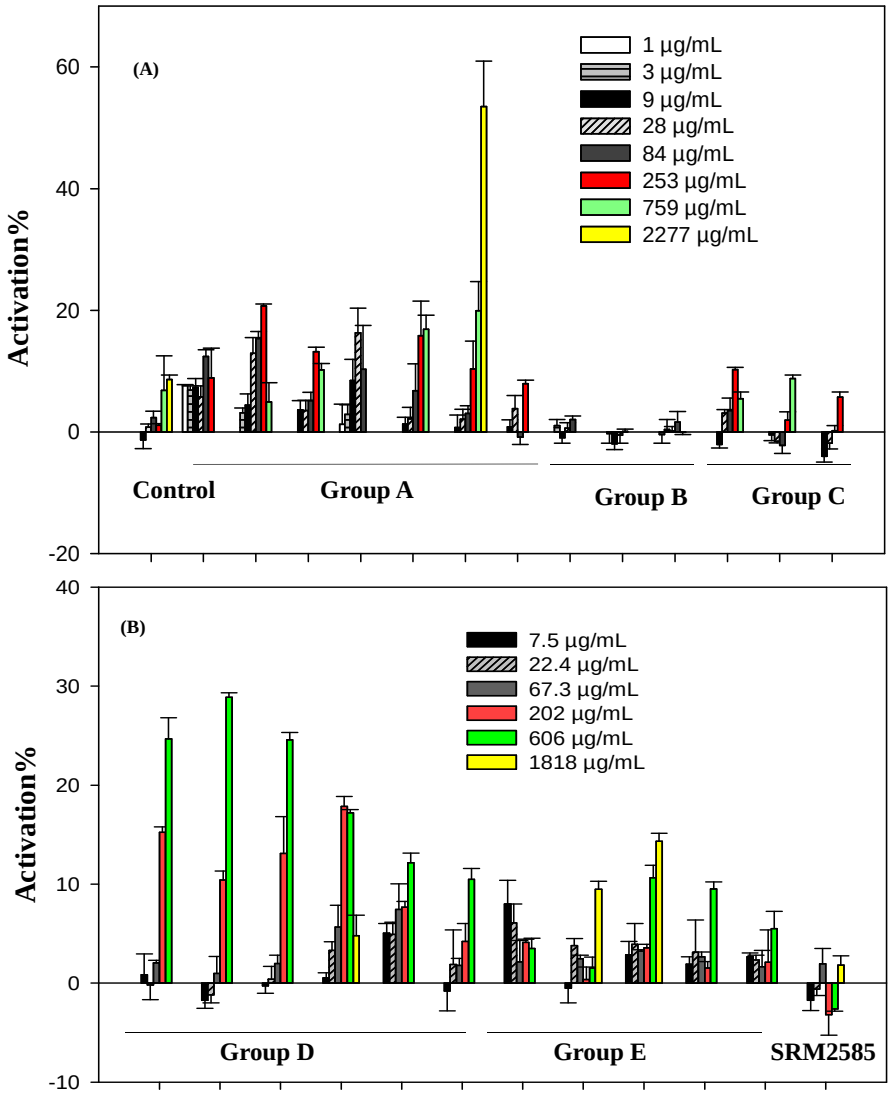

Figure 13: Dose-response relationship of PPARγ activation by 25 house dust extracts. Dust was groups with different sources. Control is the procedural blank. Values represent the average of the triplicates, and error bars represent standard deviation.

4.3.6 Correlation between ligand-binding assay and reporter assay

Data from our previous paper (Fang et al. 2014) reporting PPARγ ligand binding potency was compared with data generated in this study on PPARγ activation to

determine if the relative potencies were significantly correlated. For the individual chemicals investigated, no obvious correlation was observed between ligand binding and activation (data not shown), suggesting that binding does not necessarily induce activation. However, a significant and positive correlation (r=0.7, p<0.003) was observed between PPARγ binding and PPARγ activation for the house dust extracts (Figure 14), suggesting that the binding observed in the dust mixtures are primarily producing agonistic effects.

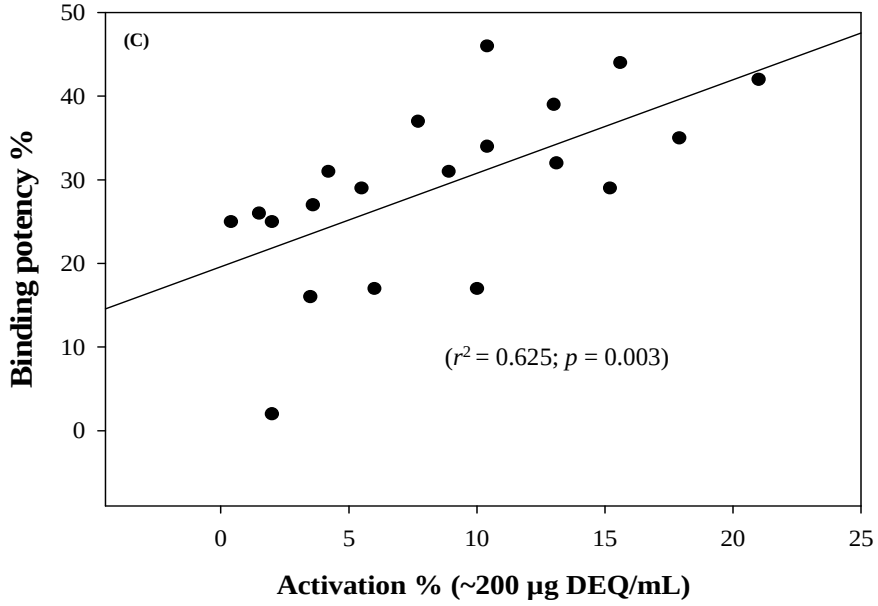

Figure 14. Correlation between PPARγ activation% at a dose of 200 µg dust/mL in the reporter assay and ligand competitive binding potency% of PPARγ-LBD assay at a dose of 3 mg dust/mL.

4.4 Discussion

Until now, few environmental contaminants have been shown to significantly bind and activate PPARγ signaling. In our recent study, several SVOCs and/or their metabolites were found to competitively bind to PPARγ (Fang et al. 2015). Furthermore, significant binding potency was observed for 21 of 24 dust samples. To follow up this study, PPARγ activation reporter assay was used to determine whether the binding potency observed led to activation of PPARγ. In this study, 28 of 35 tested chemicals were found to be weak to moderate agonists and showed a significant dose-response relationship. Most of the previously reported potential PPARγ partial agonists (e.g., TBBPA, TCBPA, TB-MEHP, TPP, TBT, and TPT) were confirmed in this study using a different bioassay. To the best of our knowledge, several of the compounds tested here, including halogenated phenols, hydroxylated metabolites of PBDEs (i.e., 3OH-BDE47) and FM550 (i.e., TBBA), TBDPD, tri-ITP and TBuP, were shown for the first time to have the potential to activate PPARγ.

The result in this study demonstrates that the structure is very important in PPARγ activation and slight changes in the chemical structure can alter the activation significantly. For example, activation of compounds with a similar structure to TPP was compared. The result showed that TPP was more potent than its organophosphite form, but both were much less potent than the organotins. The isopropylated form of TPP was also less potent in activating PPARγ, suggesting the isopropylated branch might decrease the binding and activation. Alternatively, this also may be related to the relative solubility of the compounds or cytotoxicity of those chemicals, shielding

potential effects at higher dose. However, it was interesting to find that the BPDP commercial mixture was more potent than TPP in PPARγ activation. In the BPDP mixture, TPP, BPDP isomers, di-butylphenyl phosphate, and tri-butylphenyl phosphate account for approximately 35%, 49.1%, 14.4%, and 1% of the total (MRIGlobal 2012). The higher activity in this commercial mixture suggested that BPDP isomers or di-butylphenylphosphate could be more potent than TPP. Due to the lack of purified BPDP isomer standards, it is impossible to confirm this hypothesis in this study. BPDP is of interest because it is used as a FR and is also commonly used as additives to lubricants, hydraulic fluids, and plastics (Institute. 1979). BPDPIn contrast, a pure chemical standard of TBPP, the tri-tert-butyl substituted isomer, did not show much activation, suggesting the substitution and number of branches strongly affects the binding potential. The comparison between TPP and its analogs also make the contribution of TPP in FM550 and ITP clearer, since the role of other ITPs could not be excluded in previous studies (Belcher et al. 2014; Pillai et al. 2014). FM550 consists of 2-ethylhexyl-2,3,4,5-tetrabromobenzoate (TBB, ~30%) and bis (2-ethylhexyl) tetrabromophthalate (TBPH, ~8%), TPP (~17%) and ITPs (~45%) (Klosterhaus S. 2009; Stapleton et al. 2008). The ITP component is a complex flame retardant mixture containing TPP and ortho-, meta-, and para-substituted isomers of mono-, di-, tri-,and tetra-ITPs, which are believed to comprise approximately 32, 10, 2.4, and 0.4% of FM550, respectively (Klosterhaus et al., 2009). Considering the percentage of TPP in FM550 and ITP, it is very possible that TPP is the major contributor to PPARγ activation in both commercial mixtures.

In this study, several other FRs or their metabolites were identified as weak PPARγ agonists. BDE47 demonstrated some PPARγ activation. Several recent studies have increasingly identified BDE47 as a possible "environmental obesogen". Induction of adipocyte differentiation by BDE47 in 3T3-L1 Cells had been observed (Tung et al. 2014). Global gene expression analysis in 3T3-L1 cells exposed to low doses of BDE-47 induced adipocyte differentiation through various mechanisms that include PPARγ2 gene induction (Kamstra et al. 2014). Suzuki et al. (2013) also observed a dose-response relationship between PPARγ2 and BDE-47 with a 5% induction concentration of 10μM using a U2OS reporter assay. In this current study, 3OH-BDE47, which is a metabolite of BDE47, was found to moderately activate PPARγ at a high dose (~40% activation at 7μM), suggesting it may be more potent than the parent BDE-47. In the previous PPARγ binding study, 3-OH-BDE-47 exhibited a comparable binding potency to rosiglitazone (Fang et al. 2015). Though the activation was not as potent, it was still more potent than its parent compound. Therefore, it might be interesting to confirm if the PPARγ activation with BDE47 was due to hydroxylated metabolites present in the incubations. 2,4,6-TBP, which was used as a fungicide or FR product, also showed a weak activation of PPARγ. 2,4,6-TBP has been widely detected in environmental samples and has been identified as a potential thyroid-disrupting compound in indoor dust (Suzuki et al. 2008). TBBA, the metabolite of a brominated benzoate present in FM550, also showed a clear PPAR activation at higher concentrations, and was recently reported as a good biomarker of exposure to FM550, being detected frequently in urine samples (Butt et al. 2014; Hoffman et al. 2014b). In a rodent study, perinatal exposure to FM550 in lead to

obesity (Patisaul et al. 2013), and it is possible that the observed weight gain may be linked to PPARγ activation by either TPP or TBBA, and should be a focus of future research.

Several phthalates were also identified as PPARγ agonists in this study. Though phthalate metabolites such as MEHP and mono-benzyl phthalate have been identified as PPARγ agonists and observed to stimulate differentiation of 3T3-L1 adipocytes (Hurst and Waxman 2003), few studies on the parent compounds have been conducted. Generally, the tested phthalates in this study were much less potent than the monoester phthalate such as MEHP. However, BBzP itself was identified as a partial agonist of PPARγ with the maximal activation of 34% and the EC_{15} of 2.94μM, which was very comparable with TPP and consistent with another recent study (Pereira-Fernandes et al. 2013). Concern over the link between phthalate exposure and PPARγ activation has been increasing in recent years and several studies found significant associations between urinary metabolites of phthalates and obesity in human populations with specific age, gender or race/ethnicity groups (Trasande et al. 2013; Wang et al. 2013; Y Zhang et al. 2014)

Here we report for the first time that house dust extracts have the potential to activate PPARγ. In this study, 15 out of 25 tested dust samples showed significant PPARγ activation higher than activation threshold (LAT) (i.e., >8% activation compared to rosiglitazone). Furthermore, the correlation between the reporter assay and ligand binding assay was significant and positive (r=0.7, $p<0.003$), suggesting that the binding

observed in the dust mixtures were primarily producing agonistic effects. To our knowledge, very few studies have been conducted to investigate PPARγ disruption in environmentally relevant dust samples, and this is the first time agonistic effects from mixtures of chemicals present in house dust extracts were found. Suzuki et al. (2013) observed PPARγ antagonistic effect in 9 out of 13 dust extracts, which was in contrast with findings reported here. Several reasons could be used to explain these contrasting results. First, the reporter assay in this study was more sensitive than the U2OS cell-based reporter assay used by Suzuki et al. For example, the IC_{50} for rosiglitazone was 52 nM in U2OS reporter assay, while it was 5.5 nM for the assay used in this study. Another possible difference is the different DNA domains, i.e., PPARγ1 and PPARγ2, that were used in the two studies. The U2OS cell line was transfected with PPARγ2, while in our study the cell line was transfected with PPARγ1. Furthermore, observing antagonistic effects does not necessarily imply that agonists are absent in a sample. For most antagonistic assays, a full agonist such as rosiglitazone is added and the antagonistic effect is determined by increasing the concentration of your substrate to determine if it reduces the activation. Therefore, weak or partial agonists can be "antagonist" when combined with the full agonist by competitively binding. It could also be possible that both agonists and antagonists were in the house dust mixtures and further investigation should be conducted.

Great variance of PPARγ activation was observed in the dust sample from different sources. To date, no characterization of the chemical composition in the dust samples

from different sources has been conducted. In our previous study, PBDEs in dust samples collected from gymnasiums (Carignan et al. 2013a), were found to contain at least one order of magnitude higher concentrations than levels in residential dust. This suggests that the PBDEs are not the primary contributor to the PPARγ activation. However, the small sample size and heterogeneity of the house dust samples prevent any solid conclusions from being made.

4.5 Conclusion

This study was a follow-up investigation to our PPARγ binding research on SVOCs and chemical mixtures in house dust. Many SVOCs or their metabolites were for the first time found to be weak or moderate PPARγ agonists, which increased the family of "environmental obesogens". Clear PPARγ activation was also observed in 15 of the 25 house dust extracts, suggesting possible PPARγ disruption by the house dust exposure. Further study should be conducted to identify the causal chemicals that are the primary contributor to the PPARγ activation in the house dust.

5. Effect-Directed Analysis of Human Peroxisome Proliferator-Activated Nuclear Receptors (PPARγ) ligands in Indoor Dust

Agonism of human peroxisome proliferator-activated nuclear receptor gamma (PPARγ) was recently observed in 15 of 25 samples of indoor dust extracts at environmentally relevant exposure levels, yet the active components in these mixtures have not been identified. The goal of this study was to use analytical separation methods and mass spectrometry to identify the active compounds leading to PPARγ agonism in the dust extracts. An effect-directed analysis (EDA) approach was used to identify the primary contributors of PPARγ activity in the dust extracts. Three dust extracts showing significant PPARγ activity were fractionated with normal phase high-performance liquid chromatography (NP-HPLC) and each fraction was tested individually for PPARγ activity. Active fractions were analyzed using gas-chromatography mass spectrometry (GC-MS) and possible compounds were identified by comparison to a mass spectral database and by using authentic standards. Three dust extracts showed a similar PPARγ activity distribution in the NP-HPLC fractions. In most active fractions, fatty acids (FAs), including oleic acid, stearic acid, palmitic acid and myristic acid, were the primary chemicals identified. Chemical measurements of the FAs in 35 house dust extracts suggested a very positive and significant correlation with the observed PPARγ activity. To tentatively identify sources of FAs in the dust, FAs were quantified in several samples of human/animal hair, dead skin cells, and cooking oil. FAs were abundant in all samples and data indicate that all of these may be sources to indoor dust. Our study showed that FAs are likely driving the observed PPARγ activity in the indoor dust.

Furthermore, this is the first study to report on levels of FAs in indoor dust and our analyses suggest the FAs may be derived from cooking process or human/animal hair and cells.

5.1 Introduction

Peroxisome proliferator-activated nuclear receptors (PPARγ) is a master nuclear receptor that regulates lipid metabolism, cell proliferation signal transduction and cell differentiation (Lehrke and Lazar 2005). To date, several environmental contaminants have been shown to significantly bind and activate PPARγ signaling. Several well-established model chemicals include tributyltin (TBT), triphenyltin (TPT), and mono(2-ethylhexyl) phthalate bis(2-ethylhexyl) (MEHP) (a metabolite of the bis(2-ethylhexyl) phthalate or DEHP), which have been shown to upregulate and stimulate several PPARs (Feige et al. 2007; Grün et al. 2006). More recently, 2,2′,6,6′-tetrabromo bisphenol (TBBPA), 3,3′,5,5′-tetrachlorobisphenol A (TCBPA), and triphenyl phosphates (TPP) were identified as partial agonists of PPARγ (Pillai et al. 2014; Riu et al. 2011). As these chemicals are ubiquitously detected in indoor dust, PPARγ binding and activation of chemicals present in indoor dust extracts was recently investigated (Fang et al. 2014b; Fang et al. 2015). Using a PPARγ reporter assay, we found that 15 of 25 dust extracts tested displayed significant activation (more than 10% of the maximal activation induced by rosiglitazone) and a clear increase in activation with increasing dose. In some cases, activation was as high as 50% for the most potent dust extracts. The observed PPARγ activity could either be driven by some known PPARγ agonists, such

as phthalates, TPP, and organotins, or some unknown ligands. Therefore, further research is needed to identify the primary chemical(s) driving the PPARγ activity in the indoor dust.

Effect-directed analysis (EDA) is a technique utilizing chemical separation, bioassay evaluation and qualitative chemical analysis to identify the chemical(s) leading to a specific biological response in complex mixtures. EDA usually includes the extraction, enrichment and stepwise fractionation of an environmental mixture with manipulations directed by a specific bioassay response. Chemicals in active fractions can then be identifed through chemical analysis (e.g., mass spectrometry). To date, EDA has become a valuable approach to identify chemicals responsible for biological effects in various complex environmental samples (reviewed in (Brack et al. 2007)).

In the present study, our goal was to identify the active chemicals leading to PPARγ activity in indoor dust extracts. To this end, we first fractionated three dust extracts that showed relatively high PPARγ activity, and then subsequently tested the activity in each fraction. The active fractions were scanned using mass spectrometry and possible chemicals were identified. To confirm those possible candidates, the concentration of those chemicals in dust samples was measured and a correlation analysis was conducted with PPARγ activity in the dust extracts. The potential sources of those candidate chemicals were also investigated.

5.2 Materials and Methods

5.2.1 Chemicals

Most of the chemicals used in this study were described in previous studies (Fang et al. 2014b; Fang et al. 2015). Besides, oleic acid (OA, ≥ 99%), palmitic acid (PA, ≥ 99%), stearic acid (SA, ≥ 98.5%), myristic acid (MA, ≥ 99%), 31-deuterated palmitic acid (31d-PA, 99%), tris(2-carboxyethyl)phosphate (TCEP, 97%), tris (1-chloro-2-propyl) phosphate (TCPP), and tris(1,3-dichloro-2-propyl)phosphate (TDCPP) were purchased from Sigma-Aldrich (St Louis, MO). 4-monochlorophenol (98%) was supplied from TCI America (Boston, Massachusetts). All solvents and other materials were of HPLC grade. All the cell culture reagents were from Life Technology Inc. (Grand Island, NY).

5.2.2 Sample preparation

The indoor dust extracts were from our previous PPARγ binding and reporter assay (Fang et al. 2014b; Fang et al. 2015). In brief, the indoor dust samples were collected from the main living areas of homes for Group A, D and E. Dust samples in Group B and C were collected from gymnastics studios and office environments; respectively. All dust samples were extracted with acetone:hexane (1:1, v/v) using sonication, and then concentrated, filtered, cleaned by gel permeation chromatography [GPC, Environgel GPC system (Waters, Milford, CA, USA)]. Half of the extracts were reconstituted in dimethyl sulfoxide (DMSO) for bioassay test and the other half was stored for the EDA. After finding that fatty acids (FAs) might be the potential PPARγ ligands in the 25 dust extracts, 10 more dust samples from Group D and E were prepared and tested without using GPC cleanup to eliminate the concern that chemical composition might be changed after multiple cleanup steps. To identify the possible source of FAs in the indoor dust, animal hairs (n=3) from dog, cat, and human were collected from donors.

Furthermore, dandruff was collected as the dead skin cells by brushing the scalp using a solvent-cleaned wooden comb. Two common cooking vegetable oil (soybean) and one cod fish liver oil (ISI BRANDS INC., American Fork, UT) were purchased from market. All study protocols were approved by the NIEHS Institutional Review Board, and participants provided informed consent. To analyze FAs in those samples, ~0.01 g hair samples or dandruff were spiked with 31d-PA and extracted using the same method of indoors dust samples. Oil samples were diluted with acetone, spiked with 31d-PA, and directly analyzed.

5.2.3 PPARγ Reporter Assay

As described in our previous study (Fang et al. 2015), PPARγ reporter assay (GeneBLAzer PPARγ non-DA Assay, Invitrogen) was used as the bioassay to investigate the PPARγ activation of indoor dust extracts and their NP-HPLC fractions. Amalar blue assay prepared from resazurin was used for the cell variability test. The PPARγ activity in the indoor dust after fractionation was expected to be decreased due to the separation of the active chemical mixtures. To ensure the PPARγ activity after the fractionation, two higher doses (4,200 and 1,400 μg dust equivalent quantity (DEQ)/mL) were used in the bioassay. Also, less cyto-toxicity was observed after the fractionation step which was probably due to the separation of the toxic compounds in the dust matrix and thus high doses could be used.

5.2.4 Fractionation Procedures

Fractionation of indoor dust extracts was achieved using a normal phase high performance liquid chromatography (NP-HPLC) system consisting of an Waters 1525

Binary HPLC pump (Milford, CA) equipped with a degasser and 2.5 mL injection loop and a Supelcosil LC-Diol column (250×10 mm, 5 μm particle size). To figure out the elution profile and optimize the gradient elution, a mixture including several typical flame retardants or their metabolites, halogenated phenols, phthalate metabolites, and organotin chloride was prepared and fractionated (Table 7). Those chemicals covered a wide range of physicochemical properties such as logKow values and some of them were known PPARγ agonists including TBBPA, phthalates, TPP, and organotins. Therefore, the elution profile could also help preliminarily evaluate the PPARγ activity contribution of several targeted compounds in the dust fractions. During optimization, 1 min fraction of the chemical mixture was collected and analyzed by mass spectrometry as described in the Chemical Analysis. Finally, the following gradient elution with a total running time of 53 mins was used: isocratic elution with hexane for 5 min, followed by gradient elution to 100% dichloromethane (DCM) within 15 min, then maintain 100% DCM for 2 minutes, then followed by another gradient elution to 100% acetone within 15 mins, and finally flush the column with 100% methanol for 16 mins. A flow rate of 5 mL min^{-1} was used during the entire fractionation. Three dust extracts (i.e., Dust I, II and III), which showed high PPARγ activation in our previous study (Fang et al., 2015), were evaporated to near dryness under a gentle stream of nitrogen and reconstituted in hexane/DCM (1:1, v/v) to a final volume of 1 mL prior to injection. In Dust I, fractions were collected every 1.5 min, resulting in 30 fractions. After finding most active fractions were in the first 20 min fractions, 1 min fraction was collected for Dust II and III. Fractions were split for toxicity testing and chemical analysis. 25% of each fraction was

evaporated under nitrogen gas and reconstituted in DMSO for PPARγ activity test and the remaining 75% was retained for chemical analysis. Preliminary experiments evaluated semi-preparative reverse-phase HPLC (RP-HPLC, Nucleosil 100-5 C18) for the separation of Dust I (data not shown); however, most PPARγ activity was lost after fractionation, but could be mostly recovered in the insoluble fraction attached to the vial bottom (i.e., A-$F_{hydrophobic}$). Losses were attributed to the high hydrophobicity of the active components, which was not soluble in the initial loading solution of methanol:H_2O (1:1, v/v). Therefore, RP-HPLC fractionation was rejected in favor of NP-HPLC fractionation.

5.2.5 Chemical Identification

Fractions with significant PPARγ activity were subjected to qualitative mass spectrometric analysis by gas chromatography mass spectrometry (Agilent GC 6890N, MS 5975, Newark, DE) operated in full-scan mode (*m*/*z* 50 to 1050) under the electron ionization (EI) mode (GC/EI-MS). The chemical identification was based on our previous study (Fang et al. 2014a) and fully described in Appendix, Chemical Identification. To further investigate how much of the PPARγ activity could be explained by the identified chemicals, a chemical mixture containing the equivalent concentrations of the primary compounds identified during the EDA was also prepared and tested for PPARγ activity.

5.2.6 Chemical Analysis

To figure out the elution profile in the NP-HPLC fractionation, the prepared mixture in each fraction was analyzed using mass spectrometry. Specifically, 2-ethylhexyl-2,3,4,5-tetrabromobenzoate (TBB), bis(2-ethylhexyl)-tetrabromophthalate (TBPH), and

polybrominated diphenyl ethers (PBDEs) were analyzed using a gas chromatograph mass spectrometer (GC-MS, Agilent GC 6890N, MS 5975, Newark, DE) in the negative chemical ionization mode. Organophosphates (e.g., TDCPP, TCPP, TPP, and TCEP) and phthalates (e.g., DEHP) were analyzed with GC/EI-MS. Both instruments used selected ion monitoring (SIM). Halogenated phenols, bisphenols, tetrabrominated benzoic acid (TBBA), and other phthalate metabolites were analyzed using liquid-chromatography coupled with triple-quad mass spectrometry (LC-MS/MS, Agilent 6410B) in the multiple-reaction monitoring (MRM) mode. Most of the SIM and MRM transition was described in our previous study (Fang et al. 2014b) and Table 8. Chromatographic conditions were identical to the above-mentioned Chemical Identification. After identifying FAs as the possible chemical candidates for PPARγ activity in the dust extracts, the concentration of phthalates, several organophosphates, and FAs in 35 dust samples were analyzed in the GC-MS/EI. 31d-PA was used as the internal standard of the all FAs analyzed. The quantifier and qualifiers of FAs and phthalates were listed in Table 8. To keep chemical concentration and PPARγ activity comparable, ~5 μL of the dust extracts in PPARγ dosing stock solution was transferred to ~150 μL ASV insert and extra acetone was added.

5.2.7 Data Analysis and Statistical Analyses

PPARγ activation % was calculated to describe the relative potency/efficacy normalized with the maximal response from rosiglitazone. All statistical analyses were conducted using SigmaPlot 12.0 (Systat Software Inc.), testing hypotheses at $\alpha = 0.05$, and all tests were two-tailed. For the dust extracts and their fractions, a one way *ANOVA*

was conducted and Newman-Keuls *post-hoc* test was used to identify which doses were significantly different from the DMSO control and the procedural control; respectively. To examine the relationship between PPAR◎ activation and chemical concentrations in dust extracts, Pearson and Spearman correlation analyses were conducted on data collected from the original 25 dust extracts (normally distributed) and 10 new dust extracts (non-normally distributed) ; respectively. To identify the possible sources of the FAs in the indoor dust, the contribution (%) of each individual FA to the sum of the FAs in the house dust extracts and several possible sources were calculated and principle component analysis (PCA, SPSS 12.0.1, IBM) was conducted.

5.2.8 Quality Control

For each dosing level, triplicates were run in the 384 well plates. To reduce the variability between batches, similar passages (6^{th} or 7^{th}) of cells were collected for the reporter assay. To ensure the dose-response of each dust extract fraction was comparable, PPARγ reporter assay for all fractions from one dust extract were run at the same time on one plate. A solvent blank was prepared for both fractionation procedures and chemical analysis in the house dust. Due to the large number of fractions, the PPARγ reporter assay with the corresponding blank fraction was only run for the active fraction in each dust extract. All the chemical concentration in the house dust was blank corrected.

5.3 Results

5.3.1 Fractionation of dust extracts and PPARγ activation in the fractions

To first ensure that a majority of the targeted analytes were well separated with our gradient elution profile, we first ran a chemical mixture (see methods) through the HPLC and examined their elution behavior. As expected, $LogK_{ow}$ strongly influenced the fractionation process, but all chemical classes were well separated. Nonpolar chemicals such as PBDEs, TBB, TBPH and phthalates were eluted as early as 3-4 min in the hexane fraction, which was followed by the organophosphates flame retardants (i.e., TPP, TDCPP, TCPP, and TCEP). Halogenated phenolic compounds including 2,4,5-tribromophenyl (2,4,5-TBP), 2,4,6-TBP, monochlorophenol, and 6-hydroxylated-2,2',4,4'-tetra-bromodiphenyl ether (6-OH-BDE47) eluted primarily between 17 and 21 min, which was in the DCM fraction. The polar compounds including metabolites of phthalates, TBBA, and organotins were eluted after 40 min during the 100% methanol flush. The elution of organotins on the NP-HPLC column lasted over 8 mins, suggesting those compounds have a very strong retention on the normal phase column.

Fractionation was then performed on Dust I, II and III and PPARγ activity was tested in each fraction. In our previous study, those three dust extract showed a significant dose-response relationship and the maximal PPARγ activation were ~53%, 25%, and 30% of the maximal response of rosiglitazone; respectively. As shown in Figure 15, a clear dose-response relationship was observed in several specific fractions in all dust extracts after fractionation. No obvious PPARγ activity was observed in the corresponding

blanks (data not shown). For Dust I, the active fractions included those from I-F7 to I-F16, and I-F22. The corresponding RT was 9-24 min and 33 min, respectively, since 1.5 min per fraction was collected in this dust sample. The most active fractions were I-F7 (RT: 9-10.5 min), I-F8 (RT: 10.5-12 min), I-F12 (RT: 16.5-18.0 min) and I-F22 (RT: 31.5-33 min). In the Dust II, significant PPARγ activation was observed in the fractions from II-F11 to II-F18 (i.e., RT: 10-18 mins) and II-F32 (RT: 32 min). The most active fractions were II-F11, II-F12, II-F13, and II-F17. In general, the fraction-dependent PPARγ activity pattern in Dust II was very similar to that observed in I. However, in Dust III, the most active fraction was III-F4 (3-4 min) with the highest activation of 53% at the dosing concentration of 4,200 μg DEQ/mL. Besides that, other active fractions included III-F11, III-F12, III-F14, III-F16 and III-F32, which were very similar to the pattern observed in both Dust I and II.

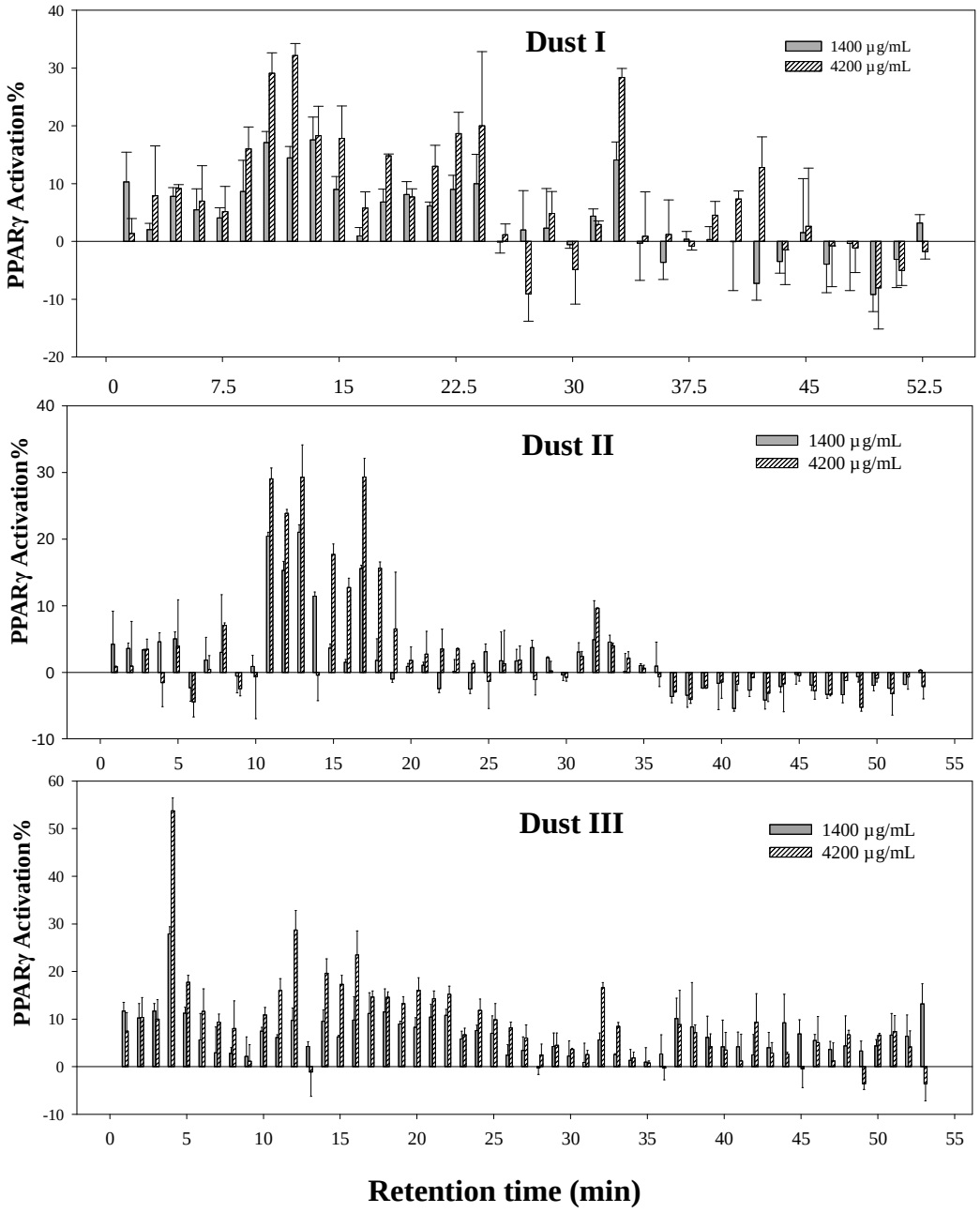

Figure 15: PPARγ activation (%) dosed with NP-HPLC fractions from (a) A3 with a dosing concentration of 467, 1400, and 4200 µg DEQ/mL and 1.5 min per fraction; (b) D3 with 467, 1400, and 4200 µg DEQ/mL and 1.0 min per fraction; (c) D2 with 1400, and 4200 µg DEQ/mL and 1.0 min per fraction. Values represent the average of the triplicates, and error bars represent standard deviation.

5.3.2 Chemical composition of the toxic fractions

The most active fractions from three dust extract after NP-HPLC fractionation and the insoluble fraction I-$F_{hydrophobic}$ from the tentative RP-HPLC fractionation were then analyzed by GC-MS/EI in full scan mode. The total ion chromatographs (TIC) as well as our identification of compounds present in the fractions are presented in Table 9 and Figure S41–43. Figure 16 provides a specific example of the TIC generated from F8 collected in the Dust I. The largest responses in the most active fractions (RT: 10-18 min) from the three dust extracts were identified as FAs and included lauric acid (LA, match factor>90%), myristic acid (MA), stearic acid (SA), oleic acid (OA), and palmitic acid (PA), and the latter four were confirmed with authentic standards. Though some other compounds such as TPP, TDCPP, and tris-(2-butoxyethyl)-phosphate (TBOEP) were also identified in the active fractions (e.g., I-F8 (RT: 10.5-11.5 min), II-F11, and III-F12 in Figure 43), the relative PPARγ activation of these compounds at the measured concentrations in the dust tended to exclude the possibility that they were the active components in the dust extracts. For example, a similar amount of TPP was eluted in II-F10 and II-F11 of Dust II; however, much higher activity was observed in II-F11, suggesting other chemicals other than TPP were responsible for the observed activity. TDCPP and TBOEP did not show much PPARγ activity in the PPARγ reporter assay (Fang et al. 2015). Therefore, those chemicals could be excluded as possible driving compounds. In III-F4 from Dust III, very large amounts of FAs and phthalates, such as benzyl butyl phthalate (BBP) and DEHP, were observed. According to Table 7, the elution of phthalates in this fraction were expected using NP-HPLC. However, no detection of FAs was found in the fractions from Dust I and II fractions with similar RT

(Data not shown). The early elution of FAs in Dust III suggested that high PPARγ activity in this fraction could be caused by poor retention of the chemicals, which might be due to the non-equilibrium of the column when loading the dust extract or the matrix effect. In I-F22 (RT: 32 min) in Dust I and II/III-F32 in Dust II and III, significant PPARγ activity was observed. Bis(2-ethylhexyl) fumarate (BEHF), a typical phthalate replacement, was found in I-F22 of Dust I and confirmed with an authentic standard. However, the PPARγ reporter assay demonstrated that this chemical did not activate PPARγ at 100μM. Another possible compound, azelaic acid (AzA), was identified in II-F32 of Dust II with a match factor of 60% with the NIST library. However, a pure standard would be needed to further confirm this compound and its PPARγ activity. Therefore, the identity of the active components in this fraction remain unidentified after GC/EI-MS analysis. As shown in Figure 41, the TIC of the fraction I-$F_{hydrophobic}$ was very similar to the pattern in the most active fractions including I-F7 and I-F8, suggesting that the active compounds in the dust extract were very hydrophobic.

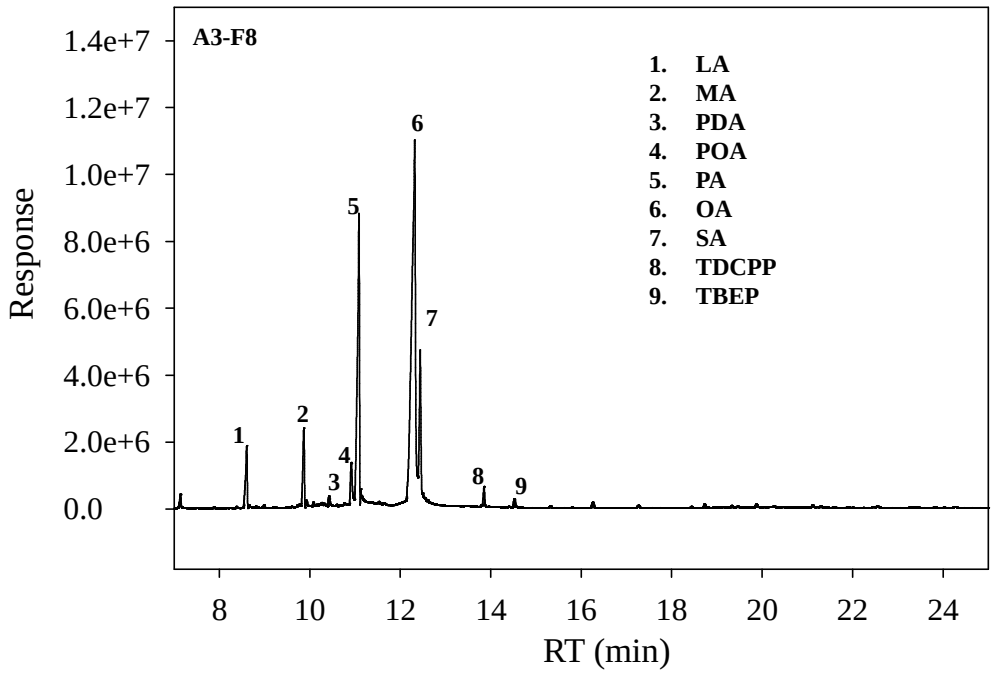

Figure 16: Full scan of F8 in A3 dust extract and the identified chemicals using GC-MS/EI based on authentic standards. See Table 9 for the abbreviation and other information for the chemicals.

5.3.3 PPARγ activity of FAs

To confirm the hypothesis that FAs were the primary contributors of PPARγ in the indoor dust samples, the PPARγ activation of several identified FAs was investigated. As shown in Figure 17 (a), a clear dose-response relationship was observed for OA, SA, PA and MA. However, the PPARγ activities varied greatly between compounds. The unsaturated OA was the most potent in the activation of PPARγ, which began to activate PPARγ at micromolar concentrations and the highest activation was close to 40% of the maximal response of rosiglitazone. The saturated MA began to activate PPARγ at 11μM and the maximal activation (~30%) was less than that of the OA. SA and PA

showed a much weaker PPARγ activation with the maximal activation less than 15% of the rosiglitazone.

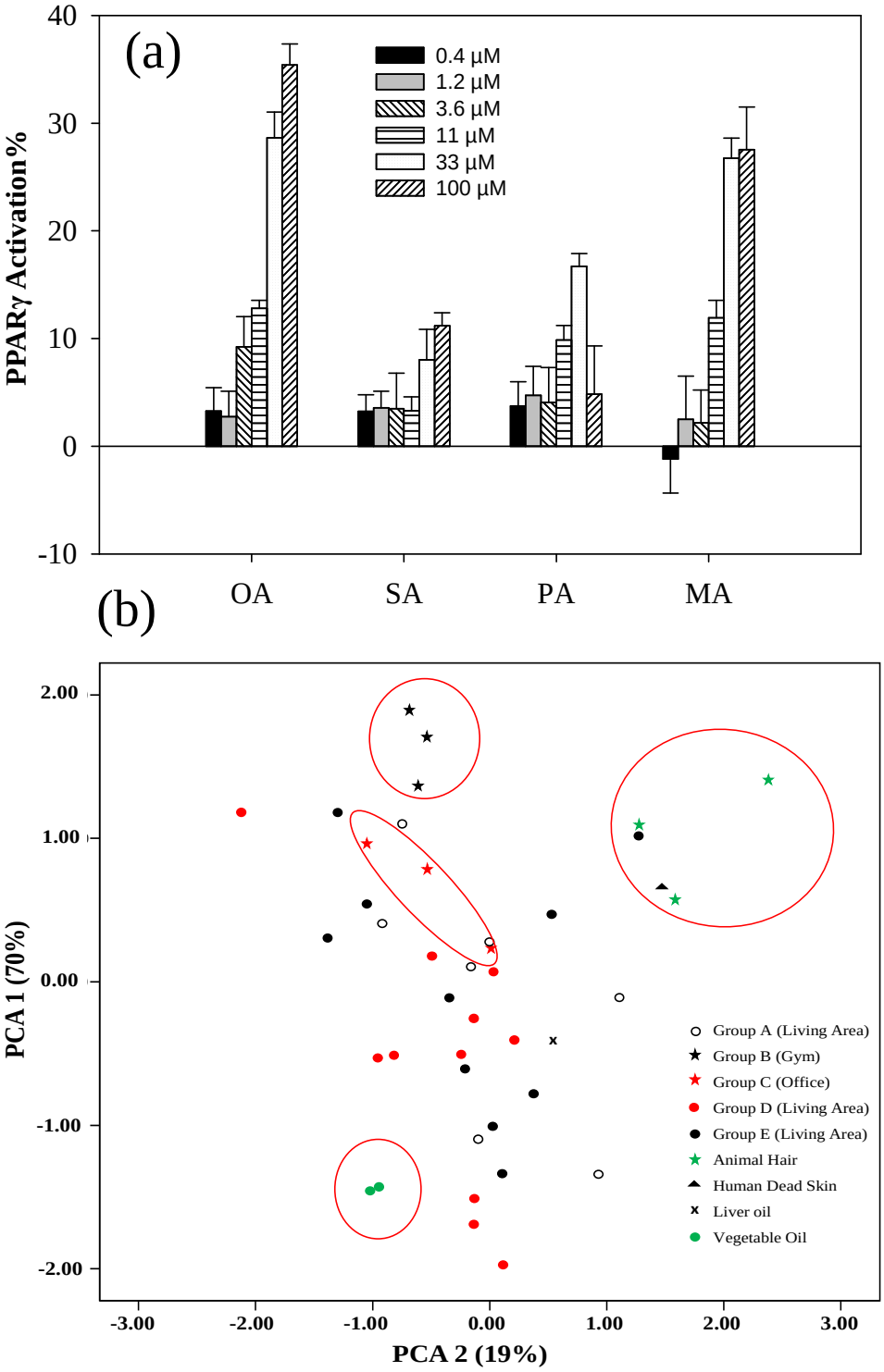

Figure 17: (a): Dose-response relationship of PPARγ activation by four FAs including OA, SA, PA, and MA. Values represent the average of the triplicates, and error bars represent standard deviation; (b): Score plot of the contribution (%) of OA, PA, SA, and MA to the sum of the FAs in 35 house dust extracts and several possible sources using principle component analysis (PCA).

5.3.4 Correlation between PPARγ activity and chemical concentration

After we observed high abundances of FAs, phthalates and several organophosphates in the PPARγ active fractions, we then measured these chemicals in extracts of 25 dust samples. As shown in Table 10, the phthalates and FAs were the most abundant components in the dust extracts. DEHP and diisononyl phthalate (DiNP) were the most abundant phthalates with a median concentration of 113.5 and 118.83 μg/g dust; respectively, which were followed by BBP (median: 16.6 μg/g dust), dibutyl phthalate (DBP, median: 16.06 μg/g dust), and diisobutyl phthalate (DiBP, 8.25 μg/g dust). As for FAs, the median concentrations were 1,104 (range: NA–3,732 μg/g dust), 1,320 (range: 16–4,150 μg/g dust), 324 (range: 7.5–1,781 μg/g dust), and 244 μg/g dust (range: 3.9–832 μg/g dust) for OA, PA, SA, and MA; respectively. The phthalate concentrations measured in these dust extracts are similar to measures reported in previous studies (Butte and Heinzow 2002; Fromme et al. 2004; Nagorka et al. 2005; Rudel et al. 2003). For example, the median concentrations were 13, 29, 480, 80 μg/g dust for BBP, DBP, DEHP, and DINP; respectively based on measurements in 278 dust samples in a German study (Nagorka et al. 2005).

After measuring the concentration of FAs, phthalates and several organophosphates, the correlation between PPARγ activity and chemical analyte concentrations were

analyzed. As shown in Table 12, a positive and significant correlation was observed between the levels of individual FA and PPARγ activation at a dosing level of 200 and 600 DEQ/mL (e.g, r=0.647 and p<0.00002 for OA). However, no significant relationship was observed between PPARγ activity and phthalates and organophosphates. The correlation of each FA level was also very positive and significant with each other (r larger than 0.8 and p<0.0000001), suggesting that many identified FAs might have similar sources. Based on the PPARγ activity and abundance of four FAs in the dust, PA, SA and MA were likely to play less important role than OA in the observed PPARγ activity. Many dust extracts showed clear cyto-toxicity at the highest dose (~1818 DEQ/mL) and the PPARγ activity at the lower dose (Level 5 and 6) was not significantly different from the DMSO control. The correlation analysis between FA levels and PPARγ activity in an additional 10 dust extracts that were not purified using GPC was also investigated, and again a very significant correlation was observed (Figure 44 and Table 13). All these findings suggest that the FAs especially OA in the dust are the primary compounds driving the observed PPARγ activity. To further investigate how much of the PPARγ activity could be explained by the identified FAs, a mock mixture containing the equivalent concentration of four major identified FAs (e.g., OA, PA, SA, and MA) in three dust extract (two were the extracts used NP-HPLC fractionation and one from 10 fresh dust extracts) was prepared and tested for its PPARγ activity. As shown in Figure 46, the mixture could explain ~30-50% of the observed activity in the equivalent dust extract at 606 μg dust/mL. However, when a solution that was three

times the concentration of the mixture was tested the observed activity was very similar or even higher than the activity in the dust extracts.

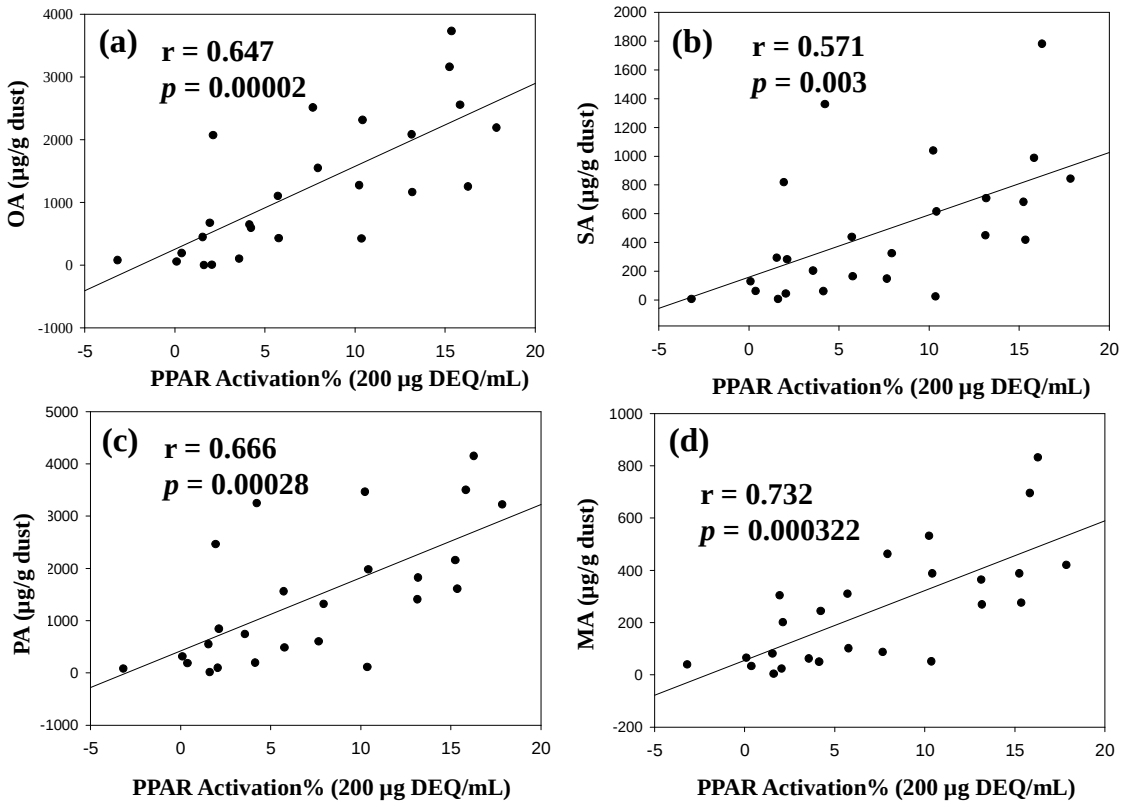

Figure 18: Pearson correlation between the PPARγ activation (%) at the dose of 200 µg DEQ/mL and the concentration of (a) OA, (b) PA, (c) SA, and (d) MA in 25 dust extracts.

5.3.5 Possible sources of FAs in the indoor dust

To the authors' knowledge, there is no available information on the sources and levels of FA in indoor dust. Possible sources could be evaporation during cooking process with oil and deposition into dust, or debris accumulating in dust from animal hair or dead skin cells. To provide more information on possible sources of FAs in

indoor dust, the concentration of four FAs were measured in hair samples collected from a cat, dog and human, in human skin debris, and in cooking oil and fish liver oil. As shown in Table 14, very high level of FAs were detected in all samples and the highest was observed in the human skin debris and oil samples with concentrations as high as 14,868 μg/g sample. To potentially identify the possible sources for FAs in dust, the congener profiles of FAs was compared in different samples and analyzed by PCA (see Figure 45 and Figure 17 (b)). In the cooking oil, the level of OA was more than 50% of the total four FAs, which was followed by the fish liver oil. In the hair samples and skin debris, the contribution of OA was less than 20% and dominated by PA. The OA contribution varied greatly between different dust samples. Overall, OA contribution in the dust Group A, D and E from main living area (Average±SD: 43.1±19.7%, n=28) was significantly higher than that from gym and office sources (Group B and C: 13.6±11.8%, n=6) using the student *t*-test ($p<0.01$). In the PCA score plot (Figure 17 (b)), dust samples from Group B and C were closer to the animal hairs and dead skins, while many of the samples from indoor living area was closer to the vegetable cooking oils.

5.4 Discussion

PPARγ is a master nuclear receptor that regulates lipid metabolism, cell proliferation, and differentiation. In our previous studies, many organic contaminants or their metabolites in indoor dust extracts displayed significant PPARγ activity. In this study, we used an EDA approach to successfully identify FAs as the causal compounds leading to the observed PPARγ activity in the dust extracts.

Some chemicals such as organotins, phthalates and TPP were expected to play an important role in the observed PPARγ activity. Organotins could activate PPARγ at the nanomolar level using the PPARγ reporter assay (Fang et al. 2015) and have been well identified as a moderate PPARγ ligands both *in vitro* and *in vivo* (Grün et al. 2006). However, during the NP-HPLC fractionation, very little activity was observed in the late eluting fractions, suggesting organotins might not be important contributors to the observed PPARγ activity in the indoor extracts since the RT of TBT and TPT ranged from 42 to 50 min. In a previous study, TBT was detected with a median concentration of 22 ng/g dust (range: <2 ng/g to 300 ng/g) and TPT was not detected (Kannan et al. 2010). In a preliminary experiment using spiked dust samples we found that our current extraction method could recover >80% of any organotins present in the dust samples (data not shown). If 1,000 μg DEQ/mL dosing concentration and the maximal concentration of TBT (i.e., 300 ng/g dust) was used in the reporter assay, the calculated TBT concentration was approximately 0.92nM , which was just above the non-observed adverse effect level (NOAEL: 0.50nM) of TBT (Fang et al. 2015). Therefore, the level of the organotins in the indoor dust might not cause much PPARγ activity. Another possible group of chemicals contributing to activity are the phthalates with concentrations in the mg/g range in dust. In our previous study, BBP itself showed significant PPARγ activation at the micromolar level (Fang et al. 2015). In the current study, BBP was measured with a median concentration of 16.1μg/g dust (range: 0.36-181.1μg/g dust). A similar calculation was conducted for BBP and the dosing concentration could reach 0.6μM in the reporter assay if the maximal concentration of

BBP in the dust was used. The NOAEL was 0.13μM for BBP in the PPARγ reporter assay and again this chemical might not be a potent contributor for the observed PPARγ activity. In contrast, the level of FAs such as OA has a median concentration of 1,104μg/g dust with a maximal concentration of 3,732 μg/g dust. Similarly, the maximal calculated OA from dust extract in the reporter assay was 13μM at 1,000μg DEQ/mL, which could lead to a PPARγ activation of approximately 15% in the reporter assay. However, it should be noted that it was very possible that some other unidentified FAs in the indoor dust could also exist due to the low sensitivity in the GC-MS full scan or lack of standards. The observed PPARγ activity could likely be a result of contributions from several of the FAs identified in the mixture. The fact that the mock mixture of four FAs could explain ~30-50% of the observed activity in the dust extracts suggests that some unidentified PPARγ ligands are still present in the dust extracts. Further research is needed to identify these active compounds.

PPARγ is thought to be an adopted orphan nuclear receptor, implying no specific endogenous ligands have been identified. Despite intensive research efforts, it remains to be determined whether PPARγ has a highly specific natural ligand or whether it is activated by the combined concentration of weakly activating ligands. A variety of chemicals have been suggested to be natural PPARγ ligands, including fatty acids and eicosanoids (Desvergne and Wahli 1999), components of oxidized low-density lipoproteins (Nagy et al. 1998), and oxidized alkyl phospholipids including lysophosphatidic acid (McIntyre et al. 2003) and nitrolinoleic acid (Schopfer et al. 2005).

The prostaglandin J2 derivative, 15-deoxy-$\Delta^{12,14}$-PGJ2, does not naturally exist at sufficient concentrations to activate PPARγ in mammalian cells (Bell-Parikh et al. 2003). FAs are major components of biological cell membranes that play important roles in intracellular signaling and as precursors for ligands that bind to nuclear receptors. Six FAs including myristic, palmitic, palmitoleic, stearic, oleic and linoleic acid constituted the majority of the FA mixtures in every tissue sample. Among them, OA and PA identified in this study were the most abundant FAs in human tissue. The mean percentage of OA ranged from 47.3% to 52.0% of the total fatty acids in the adipose tissue depending on anatomical site and age-race group (Kokatnur et al. 1979). According to a previous study, the concentration of free fatty acid in serum can be as high as several hundred micromolar (JW Zhang et al. 2014). Consistent with the PPARγ activity observed for FAs in this study, cells treated with OA displayed PPARγ gene activation in three hepatocytic cell lines (Ricchi et al. 2009). Therefore, it is possible the FAs themselves might be important activators for PPARγ *in vivo*.

To date, no occurrence of FAs in the dust has been reported and the sources of FAs remain unidentified. Though it is not the main focus of the current study, it is still interesting to tentatively identify the potential sources of FAs in the dust. In this study, several possible sources of FAs including hair, dead skin cells and cooking oils were investigated. High levels of FAs were detected in all those samples, especially in the cooking oil and dead skin cells. However, the congener pattern differed greatly between samples. Vegetable oil has a higher level of unsaturated OA than other sources. In the

animal hair samples, saturated PA is the most dominant congener, accounting for more than 50%. This difference could be potentially used to identify the contribution of FAs in the dust extracts. For example, dust samples from Group A, D and E, tended to have a higher level of OA, comparing with Group B and C. The former groups were from the main living room where cooking activity could occur frequently. In contrast, samples of Group B and C were from gymnasium and office, where the primary source should be from human dead skin debris or hair. Also, the level of FAs in dust from Group B (n=3) was the lowest in all samples. Therefore, the cooking activity could be an important source for the elevated level of OAs in the indoor dust. However, it should be noted that very few possible source samples have been analyzed in this study which might increase the uncertainties of the result. Further studies should be conducted to investigate the relationship between the level of FAs in the dust and cooking activities. For example, FA emission during cooking should be measured or house dust could be collected with different distance from kitchen and then investigate the spatial distribution. Also, it should be noted that FAs from house dust ingestion were not expected as the primary source and other pathways such as food intake could be more important sources of human FA exposure.

This study also showed that the natural ligands could out-compete with the synthetic compounds in the environmentally relevant mixtures to activate PPARγ. The co-exposure of natural ligands and environmental contaminants should be considered in future studies, which also match the cutting edge field of exposome and health effect is

the combination of the entire chemical input. The environmentally relevant samples such as house dust which contain both natural ligands and synthetic ligands could be a very important matrix to evaluate the health effect of realistic exposure and relative contribution of the both input. Together with the effect-directed analysis (EDA) approach, house dust could serve as a possible surrogate to estimate the health effect of realistic SVOC indoor exposure and prioritize the chemicals inside. However, it should be noted that this study failed to consider the effect of bioactivation of chemicals. For example, the *in vivo* half-lives of most phthalates were less than 3 hours, suggesting the *in vivo* bioactivation of those chemicals was very effective (Hoppin et al. 2002). The HEK 293H cells used in the reporter assay is not expected to have a significant xenobiotic metabolic activity. The bioactivated phthalates (e.g., MEHP) could be more potent than its parent compound DEHP in activating PPARγ (Fang et al. 2015). Also, the potency of those phthalates metabolites (e.g., MEHP, EC_{20}: 2μM) was more potent than the FAs (e.g., OA, EC_{20}: 20μM) in activating PPARγ. In this study, the levels of phthalates such as DEHP were found to have the same order of magnitude with FAs. Therefore, the bioactivation might change the contribution of both types of ligands and should be investigated in the future.

5.5 Conclusion

This study was a follow-up investigation on the PPARγ binding and activation by organic contaminants and the chemical mixtures in the indoor dust. Using the EDA, FAs in the indoor dust were found to outcompete with other possible PPARγ ligands such as

phthalates, TPP and organotins, and identified as the driving chemicals leading to the observed the PPARγ activities. This result was further confirmed with correlation analysis and PPARγ activity of the identified compounds. The possible source of FAs could be heterogonous, including vaporization and deposition of cooking oil, animal hair and dead skin debris. Overall, this study is the first report of FAs in the house dust and probably working as the primary PPARγ ligands. In the future study, the effect of bioactivation on house dust and the interaction between natural ligands and the environmental contaminants should be investigated in PPARγ signaling.

6. Discussion

To date, very few exogenous chemicals or their metabolites (e.g., organotins and MEHP) have been known to disrupt PPARγ signaling pathway. The obesity epidemic and its possible relationship with chemical exposures that disrupt adipogenesis is a significant global societal concern in both developed and developing countries. Results from research conducted within this thesis provide important information including, but not limited to, identifying several novel PPARγ ligands, estimating potential PPARγ activity from chemical mixtures in environmentally relevant samples (i.e. house dust), and the effect of bioactivation and bioaccessibility in modulating PPARγ activity.

6.1 Families of SVOCs as possible PPARγ ligands

The PPARγ ligand binding potency and activation of several major FRs, plasticizers, phthalates, halogenated phenols and bisphenols, organotins and some of their metabolites were investigated. Most of the compounds tested exhibited dose-dependent binding to PPARγ. In the study, 28 of 35 tested chemicals showed a significant dose-response relationship with different activation potency/efficacy. Overall, the results from Aim 1 has led to the identification of additional exogenous ligands of PPARγ . Most of the previously reported PPARγ partial agonists (e.g., TBBPA, TCBPA, TB-MEHP, TBT, and TPT) were also identified as active in this study using a different bioassay. To the best of our knowledge, many of the compounds tested here, including halogenated phenols, hydroxylated metabolites of PBDEs (i.e., 3OH-BDE47), FM550 components (i.e., TPP and TBBA (the metabolite of TBB)), TBDPD, tri-ITP and TBuP, were shown for the

first time to have the potential to activate PPARγ. Interestingly, the most potent compound in the PPARγ binding assay was 3-OH-BDE47, with an IC_{50} of 0.24 μM, which was similar to the IC50 value for the positive control, rosiglitazone (IC50 = XX), though the PPARγ activation was much weaker. In general, most of the compounds examined showed obvious activation of PPARγ at the micro-molar level, and the activity differed greatly with slight changes in the chemical structure. Organotins compounds were the most potent chemicals, followed by the phthalate metabolites, halogenated BPA (e.g, TBBPA) and several tri-aryl phosphates (e.g., TPP and BPDP). Measured concentrations of TPP and phthalates in house dust can be as high as μg/g to mg/g (Table 1). One recent study also found that TPP could activate PPARγ using a Cos7 reporter assay, stimulate adipogenesis, and suppress osteogenesis in primary mouse bone marrow cultures (Pillai et al. 2014). In that study, Pillai et al (2014) estimated that young children could ingest 120 μg/day TPP from indoor exposure to dust alone. Therefore, those compounds including TPP, phthalates (e.g., BBP), and organotins should be prioritized in the risk assessment of PPARγ disruption by SVOCs due to either their greater potency/efficacy in activating PPARγ or high abundance/ubiquitous detection in environmental samples.

6.2 PPARγ activity in the house dust extract

To our knowledge, very few studies have used environmentally relevant samples in toxicological research, especially when examining PPARγ disruption. In this study, 21 of 24 dust samples tested showed significant binding potency at a concentration of 3 mg

DEQ/mL. In the PPARγ reporter assay, we also observed that 15 of 25 dust extracts showed an activation percentage more than 10% of the maximal activation induced by rosiglitazone. The maximal activation was more than 50% of the rosiglitazone activation for the most potent dust extracts. Furthermore, the correlation between the results from PPARγ reporter assay and those from the ligand binding assay was significant and positive ($r = 0.7$, $p < 0.003$), suggesting the binding potency in the house dust can lead to activation of PPARγ. This is the first study showing that the chemical mixtures present in house dust can potentially activate human PPARγ. Many dust samples began to activate PPARγ at ~100 μg DEQ dust/mL. The USEPA estimates that children ingest between 50–100 mg/dust day (U.S. EPA 2009). Therefore, chemical mixtures present in house dust can activate human PPARγ in cell culture systems at environmentally relevant levels of exposure. Furthermore, this thesis project also demonstrated that house dust could be a very excellent indoor sample to investigate potential health effects caused by exposure to environmentally relevant mixtures. A large number of indoor SVOCs accumulate in house dust due to their high $LogK_{OA}$. And previous studies have shown that dust ingestion is a very important pathway for the uptake of SVOCs, especially for infants and toddlers (Johnson et al. 2010; Stapleton et al. 2012a). To date, several toxicological assays, including aryl hydrocarbon receptor (AhR), estrogen receptor alpha, progesterone receptor, glucocorticoid receptors, and transthyretin binding, have been tested with house dust extracts (Suzuki et al. 2008; Suzuki et al. 2013; Tue et al. 2010). Therefore, house dust could be possible used as the surrogate

environmentally relevant samples to investigate the health effect for indoor SVOC mixture exposure.

6.3 The role of natural PPARγ ligands in the dust

As a follow-up to the PPARγ binding and activation observe by chemical mixtures in the indoor dust extracts, EDA was used to try and identify the compounds leading to the observed PPARγ activity. After fractionation and testing, FAs were identified as the likely chemicals responsible for the observed activity. Further support was also found by examining the correlation between PPARγ activity in the dust extracts with the concentrations of FAs in each sample. The possible sources of FAs could be heterogeneous, including vaporization and deposition of oils (e.g. vegetable, olive, canola, etc) used during cooking, and animal and human hair and skin cells that may accumulate in dust. However, further studies are needed to investigate this in greater detail. Overall, this is the first study to report on the occurrence of FAs in house dust, which may be the primary PPARγ ligands in dust. Another important conclusion from this thesis research is that the natural ligands could probably play more important roles than the synthetic SVOC contaminants in the environmentally relevant mixtures. However, as stated in Chapter 3, it is also possible that biotransformation/metabolism of ingested SVOCs present in indoor dust particles may alter the PPAR activation potential, resulting in greater activity. Overall, the co-exposure of natural ligands and environmental contaminants present in dust should be considered in future studies on potential PPARγ disruption, which is also a fundamental concept of the exposome research field. In real world exposure scenarios, humans can be exposed to both

endogenous and exogenous chemicals and any potential health effects are related to interactions of both chemical classes. To estimate the effect of an exogenous chemical, its competition with endogenous ligands should be considered. In the case of the so called "orphan nuclear reporter" PPARγ, the interaction and relative contributions of both natural ligands and synthetic environmental contaminants in activating PPARγ should be investigated. Furthermore, this study also showed that EDA could be used as an effective approach to identifying the endocrine active compound in a complex mixture.

6.4 The role of bioactivation and bioaccessibility in the risk assessment of PPARγ disruption

To date, very few studies have investigated the role of bioactivation in the risk assessment. In a previous study, metabolically activated nonpolar contaminants in sediment extracts were found to competitively bind to the thyroid hormone transport protein, transthyretin, and increase the binding potency up to 100 times, relative to the non-activated extracts (Montaño et al. 2013). The results in this thesis study also suggest that metabolism may lead to increased binding affinities for PPARγ for many of the compounds tested here. In Aim 1, we found that several of the FR metabolites can be more potent than their parent compounds. For example, BDE-47 and -99, which are the primary components of the banned PentaBDE commercial mixture, did not show strong binding potency to PPARγ. However, their metabolites, OH-BDEs, were found to be potent PPARγ ligands. As for FM550, TBB and TBPH, the two major brominated components, did not show any binding activity, but their metabolites (TBMEHP and TBBA) were moderate ligands of PPARγ. It is also well known that one of the primary

metabolites of DEHP (i.e., MEHP) is also much more potent than its parent compound. In the research here, mixtures present in house dust showed stronger binding potency in the bioactivated samples compared with the raw dust extracts. A 3–16% increase in PPARγ binding potency was observed following bioactivation of the dust using rat and human hepatic S9 fractions. In reality, chemicals in the human body would have a longer contact time with xenobiotic metabolizing systems and it is possible that in vivo metabolism would lead to higher binding activity after bioactivation. Therefore, bioactivation should be considered when evaluating potency of environmental chemicals and potential human health risks.

The bioaccessibility of endocrine active contaminants in house dust should also be considered to fully evaluate potential health impacts. FRs were chosen as the model compounds because of their range in physic-chemical properties and ubiquitous detection in house dust. In Aim 3 of the thesis study, Tenax beads (TA) encapsulated within a stainless steel insert were used as an infinite adsorption sink to estimate the dynamic absorption potential of a suite of FRs commonly detected in indoor dust. This novel in vitro method showed a more comparable result with data collected from in vivo studies, suggesting that an infinite adsorption sink should be incorporated when evaluating the in vitro bioaccessibility of chemicals. OPFRs had the highest estimated bioaccessibility (~80%) compared to brominated FRs (e.g. PBDEs), and values generally decreased with increasing LogKow, with <30% bioaccessibility measured for BDE209. All the primary FAs identified in the house dust have a Log Kow value larger than 7

(estimated using EPI suite), suggesting their bioaccessibility may be less than 40% based on Figure 6. However, TPP (LogKow~4.6), a moderate PPARγ agonist, would have a much higher bioaccessibility in the gastr-intestinal fluid. Therefore, although both TPP and OA have a very similar PPARγ activation potency, their bioaccessibility might change their relative contribution to the overall PPARγ activity in vivo. In addition, the stability of more labile FRs containing ester groups (e.g. OPFRs, TBB, and TBPH) was examined in a mock-digestive fluid matrix and TBB was found to readily hydrolyze to TBBA in the intestinal fluid in the presence of lipases. In previous studies, DEHP was also found to be hydrolyzed by rat lipases in several tissues, and the observed rates of phthalate ester hydrolysis by intestinal enzymes suggest that low amounts of orally ingested DEHP would have the opportunity to be absorbed as the parent compound (Albro 1986; Albro and Thomas 1973). As mentioned, those metabolites (e.g., TBBA and MEHP) are either weak or moderate PPARγ ligands. Therefore, the thesis study demonstrates that the bioactivation, bioaccessibility and breakdown of FRs following exposure should be considered in exposure assessments and its possible modulation on PPARγ activity.

6.5 Data Limitations and Research Needs

The effect of bioactivation on endocrine disruption has not been extensively investigated and further studies are needed. However, one of the potential problems in investigating effects of bioactivation in bioassays using in vitro systems is the low efficiency of biotransformation. In these experiment, only ~5% of the 20 μM DEHP dose

could be bio-transformed to MEHP during the incubation, which was a few hours. It is also possible that some in vitro enzymes such as cytochrome P450 could lose activity within an hour after depleting NADPH. However, the in vivo half-lives of most phthalates are estimated to be less than 3 hours, suggesting that in vivo bioactivation was more effective or keep longer contact time with active enzymes (Hoppin et al. 2002). Therefore, the PPARγ activity of house dust extracts might be more potent after in vivo biotransformation than the raw dust extracts. To date, very few effective bioactivation methods have been developed. In most commercially available reporter assays, cell lines such as HEK293, with low xeno-metabolism potential, are used as the primary cell models. In the future, it might be more effective to try and use other cell lines, such as hepatic cell lines, to increase the metabolic rate of the parent compounds and evaluate the effect of bioactivation. Alternatively, the bioactivation efficiency could be enhanced by increasing incubation time or involving high level of specific enzymes such as esterase during the incubation. It is also possible that exogenous ligands could have stronger binding affinities than natural ligands such as fatty acids if all the phthalates were transformed to their metabolites. The binding affinity of some phthalates metabolites (e.g., MEHP) are more potent than the FAs investigated in this study in activating PPARγ and the highest levels of phthalates such as DEHP were found to have with a comparable level with FAs in the house dust. Therefore, the complete bioactivation of several contaminants (e.g., DEHP) might change the relative contribution of the ligands to the overall activity and should be examined in future studies.

The mixture effect (i.e., additive or synergistic effect) of many weak PPARγ ligands could be studied in the future. In this study, most of the tested compounds began to show significant PPARγ activation at a concentration in the μM level. Therefore, a single compound alone might not have the potential to activate PPARγ *in vivo*. It would be interesting to investigate the effect of co-exposures to multiple weak PPARγ ligands. In Appendix E, I tested the PPAR activity of a mixture containing several identified PPARγ ligands at what was proposed to be a relevant human serum concentration and found that organotins were the primary contributors. However, the concentrations tested were based on human measurements collected from previous studies with different sampling time frames, locations, and sample size. Therefore, the representativeness of those concentrations is questionable. In the example of environmental relevant estrogens (hydroxylated PCBs, benzophenones, parabenes, bisphenol A, and genistein) and pharmaceuticals (atenolol, bezafibrate, carbamazepine, cyclophosphamide, furosemide, hydrochlorothiazide, ibuprofen, lincomycin, ofloxacin, salbutamol, and sulfamethoxazole), significant effects were observed after mixing several weak agonists at the concentration of NOAEL using the recombinant yeast estrogen screen (YES) and human embryonic cells HEK293; respectively (Pomati et al. 2006; Silva et al. 2002). Therefore, further studies investigating effects of mixtures of PPARγ agonists at their respective NOAEL should be investigated. It would be of particular interest to determine if the PPARγ ligands have additive, synergistic or other types of interactions. Also, endogenous ligands (e.g, fatty acids or 15d-PJG2) could also be included to

examine the effect of exogenous ligands on the PPARγ activation by endogenous compounds.

In this thesis research, exhaustive extraction methods were used to extract chemical mixtures in house dust. As shown in Aim 3, the bioaccessibility varied greatly between chemicals and sample matrixes. For example, at least 70% of the BDE209 will still be retained by the dust particles after dust ingestion. Also, the FAs identified using EDA were estimated to have a bioaccessibility less than 40% based on their hydrophobicity (i.e. Log Kow). Therefore, an extraction method that accounts for bioavailabilty/bioaccessibilty would be more practical in estimating the potential health risks of chemicals ingested by house dust, and probably change the contribution to PPARγ activity based solely on relative potency and concentrations in dust. Therefore, the bioaccessibility of the contaminants in environmentally relevant samples prior to bioassay testing should be considered. Several possible methods have been proposed/reviewed in a previous study, including mild solvent extraction, supercritical extraction, and hydroxypropyl-β-cyclodextrin (HPCD) extraction (Yang et al. 2013). The TA method used in this thesis could also be a potential method for estimating the bioavailable fraction.

Lastly, only in vitro PPARγ bioassays were used in this study and the use of additional in vivo models should be considered in future studies. Agonists of PPARγ do not necessarily equate to "Environmental Obesogens", though several contaminants including organotins, TBBPA, and phthalates metabolites have already shown both

PPARγ activation and adipogenesis. In the future, adipogenesis assays (e.g, 3T3-L1) should be conducted using dust samples and compared with the PPARγ activation results to confirm if PPARγ involved mechanisms could lead to lipid accumulation. Furthermore, in vivo models could be considered in future studies. The effect of these SVOCs in in vivo models (e.g., rodent or fish models) could be multi-mechanism of actions and more complex. Therefore, the similarities and differences between in vitro and in vivo models could be bridged. To date, several lines of evidence have suggested that in vitro data could be correlated with in vivo data for PPARγ disruption. For example, TBBPA and TCBPA were first found using in vitro models and then confirmed and classified as obesogen using an in vivo animal model (zebrafish) (Riu et al. 2014). Though rodents including mouse or rats have been used in most obesogen studies, Riu et al (2014) showed that zebra fish larva development could be a possible and effective in vivo model for obesogen research with the advantage of rapid development and high rates of fertilization. TPP was identified as a moderate PPARγ ligand in this thesis research, and TPP is a component of the flame retardant mixture FM 550. Also, pre-and postnatal exposure to FM550 resulted in a 20-30% weight gain in both male and female rats relative to controls at a dose of 1,000 μg/day (Patisaul et al. 2013). Therefore, future research using animal models using investigating environmentally important PPARγ ligands such as TPP should be conducted.

Appendix A: Evaluating the Bioaccessibility of Flame Retardants in House Dust Using an In Vitro Tenax Bead-Assisted Sorptive Physiologically Based Method

A.1 Chemical Analysis

The extraction, cleanup and analysis of FRs in the recovered dust samples and TA were modified from our previously published methods (Fang et al. 2013; H. M. Stapleton et al. 2014). Dust and TA were first extracted with acetone to remove all the water residues, then extracted two times with hexane:acetone (1:1). All extracts were combined. F-BDE 69 was used as an internal standard for tri-nonaBDEs, EH-TBB, and BEH-TEBP, and ^{13}C BDE-209 was used as an internal standard for BDE-209. D-TDCIPP and d-TPHP were used as internal standards for TCEP/TCIPP/TDCIPP and TPHP; respectively. An ENVI-Florisil SPE column (500 mg, 3 mL) was used to clean and purify the dust extracts. The SPE column was first conditioned with 5 mL methanol and rinsed with 3 mL hexane. Then the dust extract (in hexane) was loaded on the SPE using 0.5 mL hexane and 4 mL hexane was used to elute hydrophobic FRs (e.g., PBDEs, EH-TBB, and BEH-TEBP) in fraction one (F1). Subsequently, most OPFRs were eluted in fraction two (F2) using 10 mL ethyl acetate. After evaporation, 13C-CDE-141 and d-TCEP were spiked into each sample to serve as a recovery standard (measure recoveries of internal standards). PBDEs, EH-TBB, and BEH-TEBP were analyzed using gas-chromatography coupled to a mass spectrometry detector (GC-MS, Agilent GC 6890N, MS 5975, Newark, DE) operating in the negative chemical ionization (NCI) mode. OPFRs were analyzed by GC/MS operated in electron ionization (EI) mode. The extraction and analysis of the foam and recovered TA were similar to the dust samples. Due to the high levels of FRs

in the foam, foam/TA bead and digestive extracts were diluted 100 times and 20 times; respectively. Surrogate standards were spiked and no further cleanup was performed. To analyze the FRs in the digestive fluid, 20 mL of the digestive fluid was first treated with 6 M HCl to denature the protein and then liquid-liquid extracted with hexane:ethyl acetate (1:1) three times. The extracts were combined and concentrated to 1.0 mL for chemical analysis. The surrogate standard and recovery standard were identical to the standards described above. The analysis of TBBA was performed by liquid-chromatography mass spectrometry (LC-MS/MS) operating in negative electron-spray ionization (ESI-) as described in our previous study (Roberts et al. 2012).

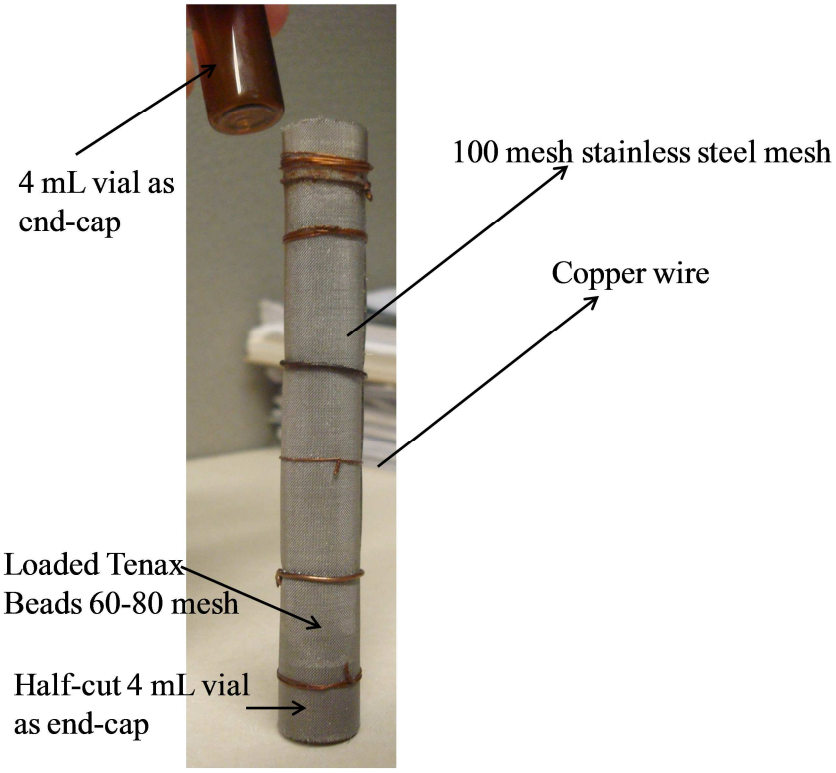

Figure 19: Schematic showing the TA trap that was designed using 100 mesh stainless steel mesh

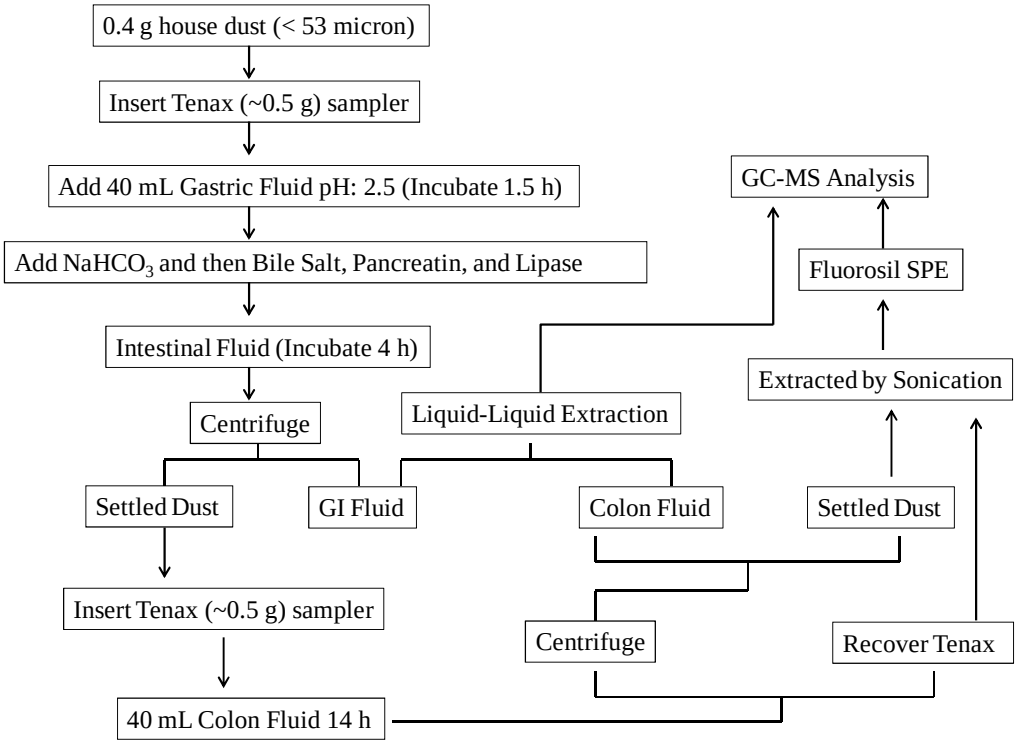

Figure 20: Flow chart displaying the steps involved in the dust sample incubation, cleanup and analysis.

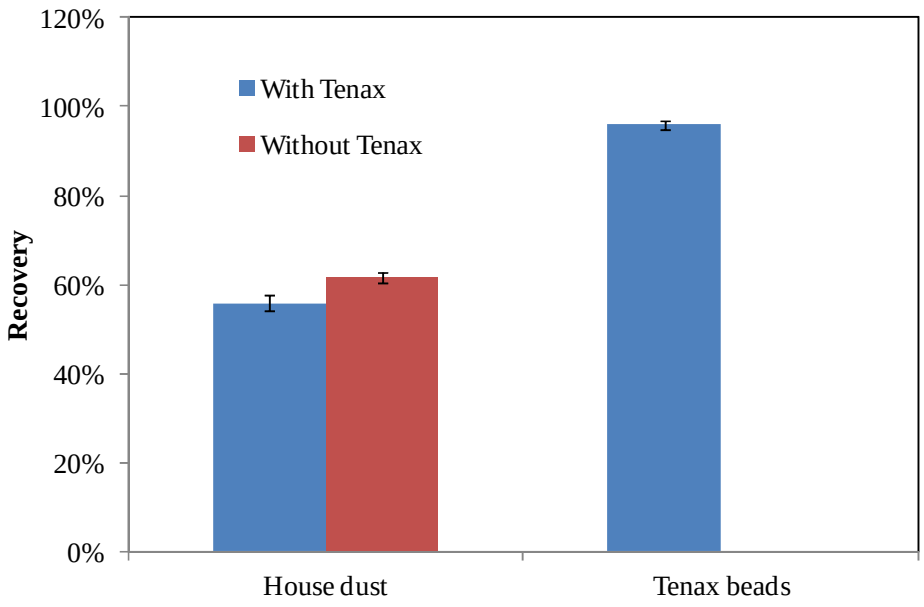

Figure 21: Recovery of TA and SRM2585 (n = 3) relative to the amount added before incubation. The mass of dust recovered without adding TA was run for comparison purposes. Error bar represents the standard deviation of triplicate analyses.

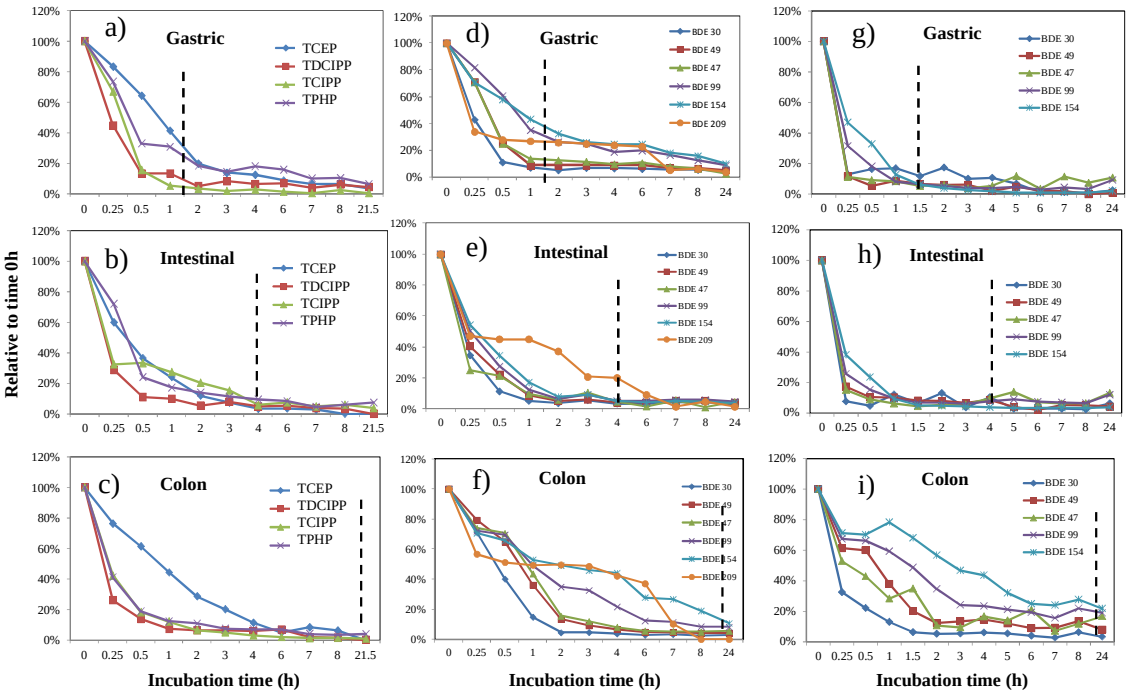

Figure 22: Mass of OPFRs (TCEP, TDCIPP, TCIPP, and TPHP) and PBDEs in spiked gastric, small intestinal, and colon fluid relative to Time 0. Figure a-c): OPFR sorption kinetics in high spike level 2 μg/mL; Figure d-f): PBDE sorption kinetics in high spike level 2 μg/mL; and Figure g-i): PBDE sorption kinetics in low spike level 10 ng/mL. BDE209 and OPFR sorption kinetics in low spike level were not shown due to non-detection at several late time points. Dashed lines indicate the incubation times in stomach (t = 1.5 h), small intestine (t = 4 h), and colon (t ~ 16 h) fluid.

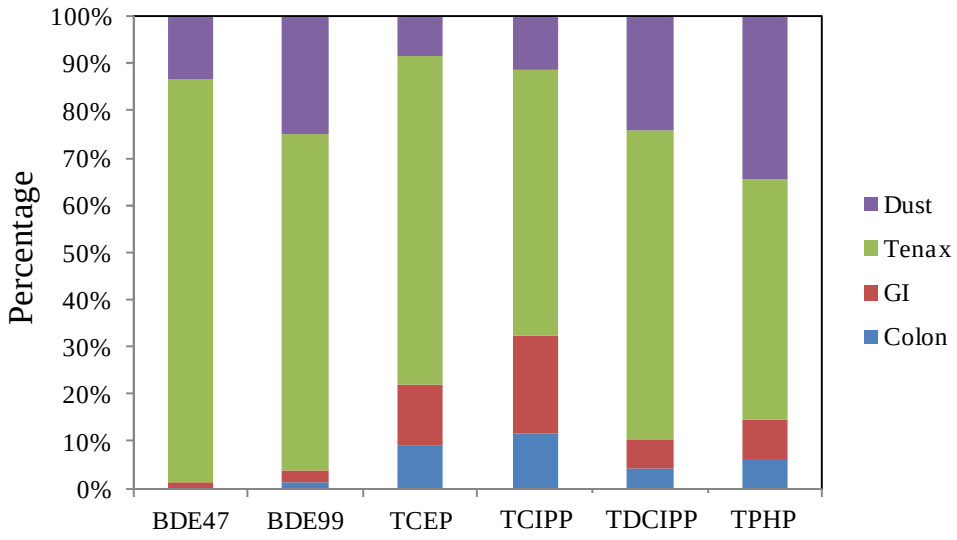

Figure 23: The distribution of BDE-47, BDE-99, and several OPFRs in four compartments including dust, TA, gastric-intestinal fluid and colon fluid after incubation.

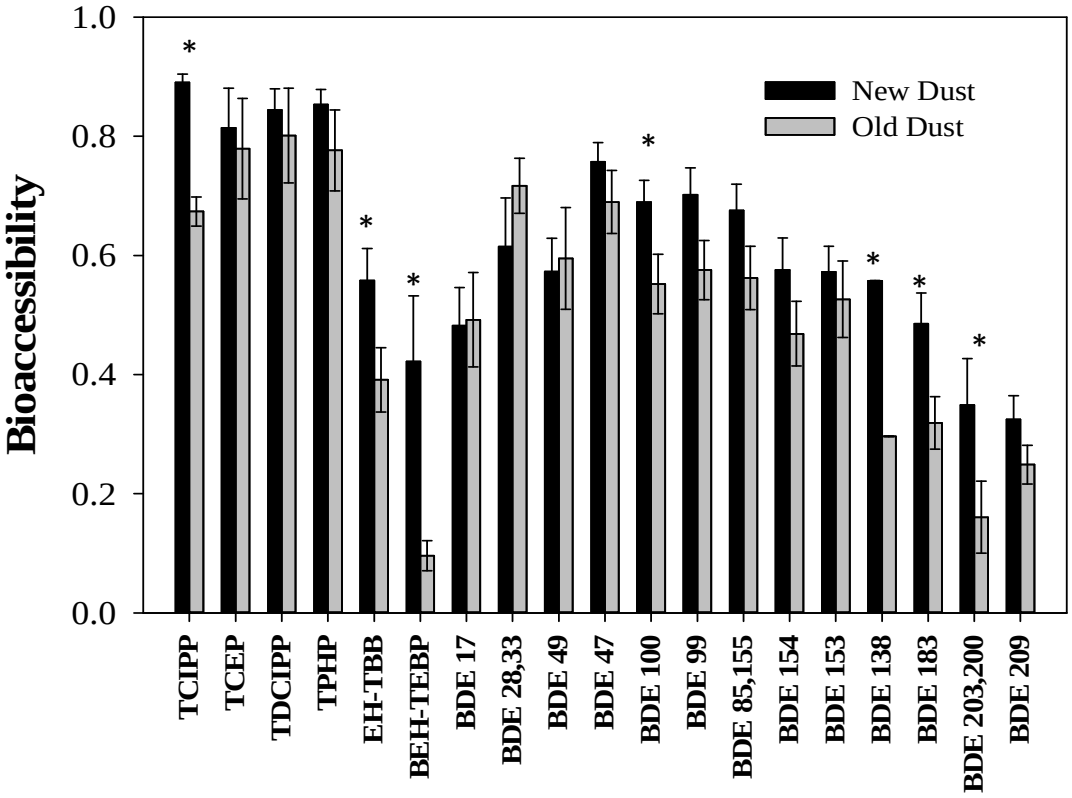

Figure 24: Flame retardant bioaccessibility measures in old dust samples (n=7, collected in 2006) and new dust samples (n=9, collected in 2010). Error bar represents the standard error.

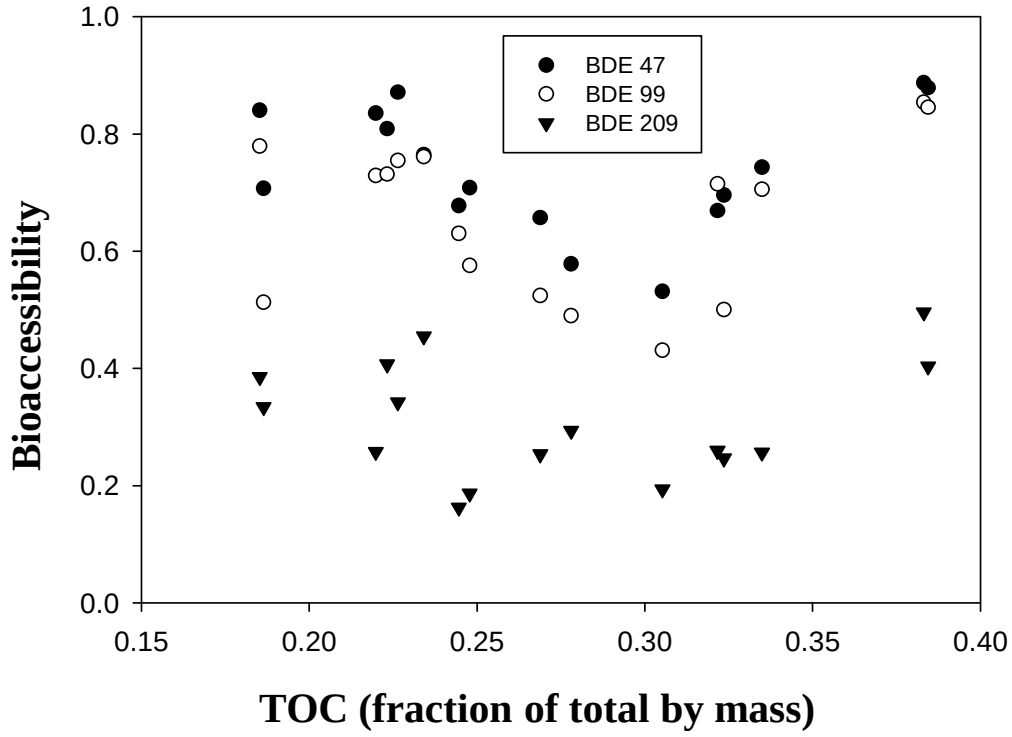

Figure 25: Association between measured bioaccessibility of BDEs and TOC in the various dust samples analyzed in this study (n=17).

Figure 26: Microscopic imaging (60 time magnification) of fragmented foam with particle size a) < 100 µm, b) <250 µm, and c) <500 µm in series.

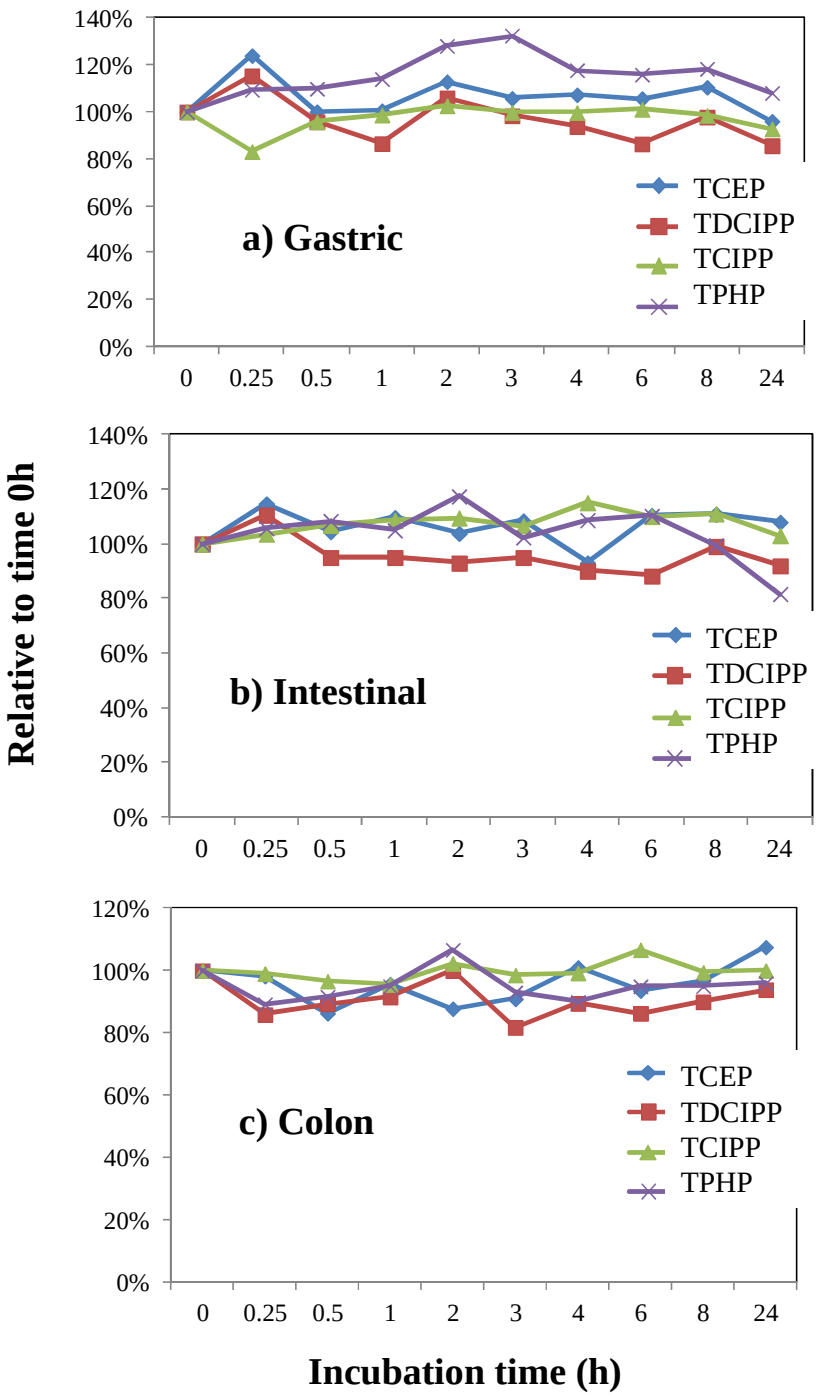

Figure 27: Relative amounts of TCEP, TDCIPP, TCIPP, and TPHP in the gastric, intestinal, and colon fluid during incubation at 37℃.

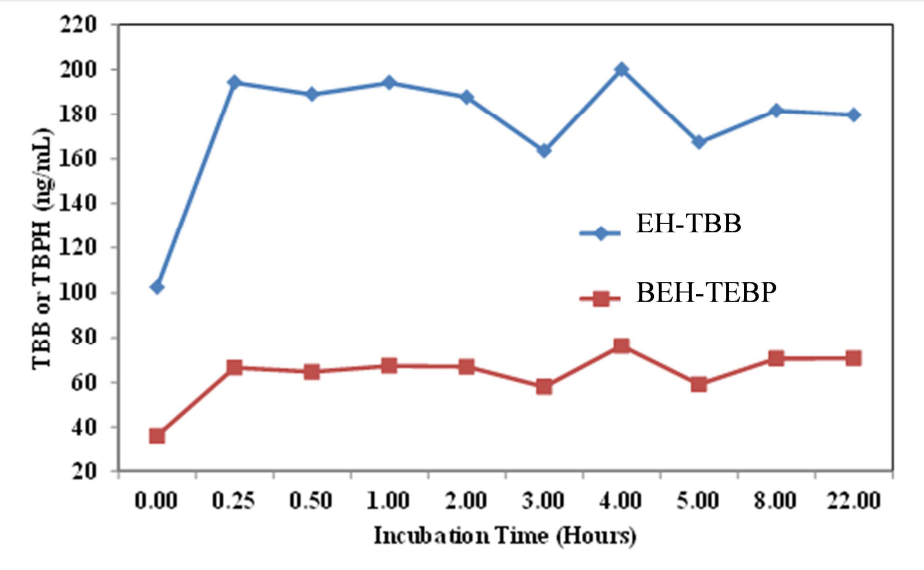

Figure 28: Concentrations (ng/mL) of EH-TBB and BEH-TEBP in intestinal fluid without addition of lipases at 37 ℃.

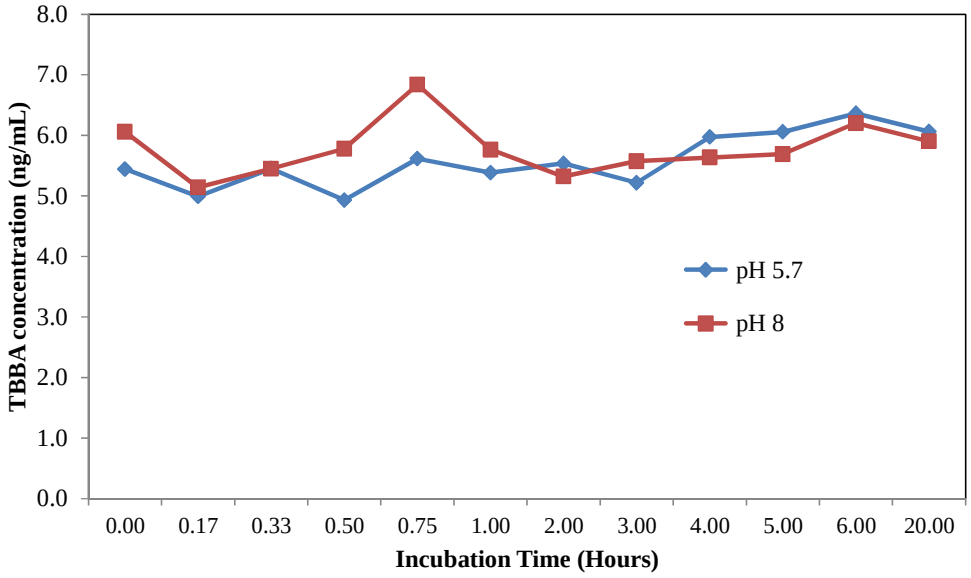

Figure 29: Concentrations of TBBA measured in intestinal fluid with 0.5 g TA added at two different pH values (5.7 and 8) at 37℃.

Table 4: Bioaccessibility measurements for OPFRs, FM550, and PBDEs in house dust samples (< 53 μm, n = 17)

	TCIPP	TCEP	TDCIPP	TPHP	EH-TBB	BEH-TEBP	BDE 17	BDE 28,33	BDE 49	BDE 47	BDE 100	BDE 99	BDE 85,155	BDE 154	BDE 153	BDE 138	BDE 183	BDE 203,200	BDE 209
DS1	91%	84%	83%		43%					68%	62%	63%	62%	58%	46%		44%	26%	16%
DS2	83%	76%	85%	78%	62%	79%		54%	53%	67%	68%	72%	67%	60%	46%		48%	23%	26%
DS3	93%	98%	93%	93%	67%	2%		91%	88%	89%	80%	85%	82%	74%	73%		55%	31%	50%
DS13	87%		64%	84%	67%	56%	37%	52%	59%	76%	72%	76%	72%	70%	65%	56%	59%	46%	45%
DS14	86%	48%	79%	80%	51%	36%	41%	33%	63%	74%	68%	71%	69%	60%	56%		43%	30%	26%
DS15	92%	65%	98%	76%	64%	49%	57%	82%	56%	84%	76%	78%	78%	34%	71%		66%	42%	39%
DS16	94%	88%	88%	91%	77%	60%	59%	36%	56%	88%	84%	85%	80%	78%	68%		66%	76%	40%
DS5	90%	96%	79%	92%	36%	14%		65%	44%	66%	55%	52%	51%	44%	42%		26%		25%
DS6	86%	96%	92%	88%	35%	0%		79%	39%	70%	54%	50%	46%	40%	49%		30%	6%	25%
DS7					34%	3%	43%	61%	56%	71%	51%	58%	55%	45%	44%		28%	8%	19%
DS8	73%	79%			61%		39%	85%	82%	87%	74%	75%	79%	70%	68%		52%	47%	34%
DS9			93%	95%	38%	6%	69%	81%	69%	71%	53%	51%	51%	41%	40%	30%	31%	12%	33%
DS10	69%	89%	85%	87%	32%	11%		63%	40%	58%	43%	49%	46%	35%	38%		23%	3%	29%
DS11	60%	72%	80%	77%	27%	10%		65%	25%	53%	41%	43%	43%	32%	79%		19%	17%	19%
DS12	70%	96%	90%	68%	42%	18%	46%	85%	81%	84%	68%	73%	69%	59%	55%		37%	20%	26%
DS17	65%	53%	53%	61%				62%	64%	60%	55%	54%	51%	46%	45%			15%	13%
DS4	92%	99%	89%	94%	35%	4%		91%	85%	87%	71%	73%	74%	59%	57%		46%	37%	28%

DS1, DS2, DS3, DS13, DS14, DS15, DS16, DS5, and DS6 were collected in 2010. DS7, DS8, DS9, DS10, DS11, DS12, and DS17 were collected in 2006. DS4 was collected in 2008.

Appendix B: Characterizing the Peroxisome Proliferator–Activated Receptor (PPARγ) Ligand Binding Potential of Several Major Flame Retardants, Their Metabolites, and Chemical Mixtures in House Dust

B.1 PPARγ Competitive Binding Assay

PPARγ Competitive Binding Assay. Fluorescence polarization (FP) assays allow ligand binding to be quantified in a homogeneous format without perturbing equilibrium by physical separation of bound vs. free ligand, which is advantageous for the measurement of low-affinity interactions (Rossi and Taylor 2011). In this study, a commercially available high-throughput ligand binding assay (PolarScreen™ PPARγ-competitor assay kit, Invitrogen) was used to investigate the binding potency of tested compounds to PPARγ LBD. The kit uses the human-derived recombinant PPARγ-LBD tagged with a N-terminal GST-tag and a selective fluorescent PPARγ ligand (PPARγ Green) in a 384-well plate (Corning Thermowell GOLD 3756). The test compounds were dissolved in DMSO and dosed into each well with a final volume of 40 μL containing 38 nM PPARγ LBD and 1.25 nM PPAR-Green as recommended by the protocol. We used 3% DMSO in the final incubation mixture to reduce potential effects on polarization by the solvent. The well plate was mixed and incubated for 3 hours at room temperature to reach equilibrium. A SpectraMax M5 plate reader was used in polarization mode with 485 nm excitation and 535 nm emission wavelenth. To measure ligand binding, we quantified polarization (mP) of the bound protein using the following equation:

$$mP = 10^{3*}(I_p - I_s)/(I_p + I_s) \quad [1]$$

where I_P and I_s are the fluorescence intensity of emissions that are parallel (P) and perpendicular (S) to the excitation light; respectively (Rossi and Taylor 2011).

B.2 Quality Assurance/Quality Control

For each dose level of tested compounds, triplicate samples were prepared and each well was read five times in the plate reader. DMSO and rosiglitazone were run alongside each batch as a control and positive control, respectively. For the dust samples, a procedural blank was prepared and preceded alongside the dust extracts to examine the background contamination. Since variability of FP was observed across the batches, normalization to DMSO control was conducted when comparing between batches. The potent ligands such as 3-OH-BDEs were tested three times at different days with different well plates.

B.3 Operation of Gel Permeation Chromatography

The flow rate was set to 10 mL/min and DCM was used as the mobile phase. To test the elution profile, several compounds ranging from small MW halogenated phenols to large MW TBPH were loaded onto GPC and fractions were collected at 0–10 min, and then 2 min for each fraction until 30 mins. As shown in Appendix Table 5, most of the chemicals were eluted after 14 mins except TBPH. To recover the highest amount from the mixture, a fraction from 12–28 min was collected, concentrated, and solvent exchanged into DMSO.

B.4 Appendix, Bioactivation of Dust Samples

The incubation method was modified based on previous studies (Montaño et al. 2012) and the flow chart was shown in Figure 32. To increase the amount of the metabolites, incubation was up-scaled and performed in a borosilicate glass tube in 3 mL phosphate buffer (PB, 100 mM, pH 7.4), S9 fraction (1 mg protein/mL), and dust extract in ~30 μL DMSO (~33 mg dust/mL PB). 10 mM DTT and 6 mM magnesium chloride were added. After 5 minutes pre-incubation in a shaking water bath at 37℃, the reaction was initiated with the addition of 50 μL of 60 mM NADPH in PB. Additional 50 μL of 60 mM NADPH in PB were added after 60 mins. Metabolism was stopped after 120 minutes by denaturation of microsomal protein with 150 μL of ice-cold 6M HCl. An additional sample for each dust extract was incubated with inactive S9 by 150 μL of ice-cold 6M HCl before incubation and run alongside as the comparison control.

The challenges in the bioactivation of dust samples for the PPARγ binding assay includes the low metabolic rate, interference from coextracts in S9 fraction, and FB of dust (Montaño et al. 2013). In our preliminary study, we found that S9 extract could interfere with the PPARγ polarization assay [see Figure 31 (b), (c), (d), and Figure 38], which might be caused by the lipids which can work as natural ligands for PPARγ. Therefore, further cleanup was needed to remove the coextracts that interfere with PPARγ binding. In this study, the extraction and cleanup method for the metabolites was modified according to a recently published low-fat method for metabolite extraction, including dextran assisted extraction and lipid removal agent (LRA) cleanup (Montaño

et al. 2012). Briefly, the fat was flocculated with 50 μL of 10% dextran with 150 μL of 6 M HCl previously added to facilitate the flocculation. Metabolites were extracted with 2 × 2 mL ethyl acetate and 1× 2 mL hexane : methyl tert-butyl ether (1:1, v/v). TBBA, TBBPA and MEHP were tested for the recovery of dextran and LRA cleanup. Good recovery (> 80%) was observed in the dextran assisted extraction and no elution of any compound in the LRA. Therefore, only dextran extraction was used in the study.

The low metabolic rate does not generate sufficient metabolites to activate the PPARγ binding and further concentration of the metabolites was needed. However, the dust matrix will be concentrated and cause fairly high fluorescence background to interfere with the PPARγ binding. Thus, further cleanup of the dust matrix was still needed. In our previous studies, we found that the phenolic extraction could retain most of the dust matrix in the organic solvent. Furthermore, most of the known PPARγ agonists or antagonists are the chemicals with polar groups such as –OH, –COOH, and $–NH_2$. If we hypothesize that charged chemicals including phenolic or carboxylic metabolites were the major metabolites, it would be possible to reduce the dust matrix without losing most of the metabolites as a tradeoff. In this study, the extracts from dextran assisted liquid-liquid extraction was blown down to near dryness under nitrogen gas and the sample was reconstituted in 1 mL DCM, which was then extracted with 3×1 mL deionized water with a pH of ~13. The pool of the 3 mL water was then acidified with 6 M HCl to pH < 3 and extracted with 2 × 2 mL ethyl acetate and 1 × 2 mL hexane : methyl tert-butyl ether (1:1, v/v). The final extracts were dried and reconstituted with 200 μL

DMSO. As shown in Figure 31 (b), the phenolic extraction can reduce the matrix background of the dust extracts to the level which was only slightly above the DMSO control and would not greatly interfere with the binding assay. The recoveries of tested compounds such as TBBPA, MEHP and TBBA were > 85% using the above-mentioned method. Therefore, the combination of dextran-assisted extraction and phenolic extraction make the PPARγ binding assay feasible for the bioactivated dust extracts.

B.5 Performance of the Bioactivation of Dust

The challenges in the bioactivation of dust samples for the PPARγ binding assay includes the low metabolic rate, interference from coextracts in S9 fraction, and FB of dust. As shown in Figure 38, the natural ligands such as fatty acid in the S9 fraction can competitively inhibit ~20% of the binding between PPARγ-LBD and PPARγ Green at a concentration of 250 μg protein/mL. Dextran was used to selectively remove the lipid during extraction (Montaño et al. 2012). The result showed the dextran assisted extraction could partially remove the interference from the coextracts, which was close to 90% of the DMSO control. The application of incubation with inactive S9 running alongside as control could correct this interference. Phenolic extraction could further reduce the FP background by approximately five times than that of the raw extract, leaving the FP of dust with a concentration of 6 mg DEQ/mL close to DMSO control (see Appendix Figure 31 (b)). As shown in Appendix Figure 33, MEHP could be formed by the incubation of dust with S9 fraction and the formation rate was approximately 70 pmol/mg protein/min, which was slightly higher than that of 25 μM DEHP pure

chemical. However, the formation rate was decreased when the dosing amount of dust was 100 mg/mL, which might due to the decrease of enzyme activity caused by the impurities in dust extracts. Therefore, we used ~33 mg DEQ/mL throughout the incubation experiment in this study to maintain a high metabolic rate.

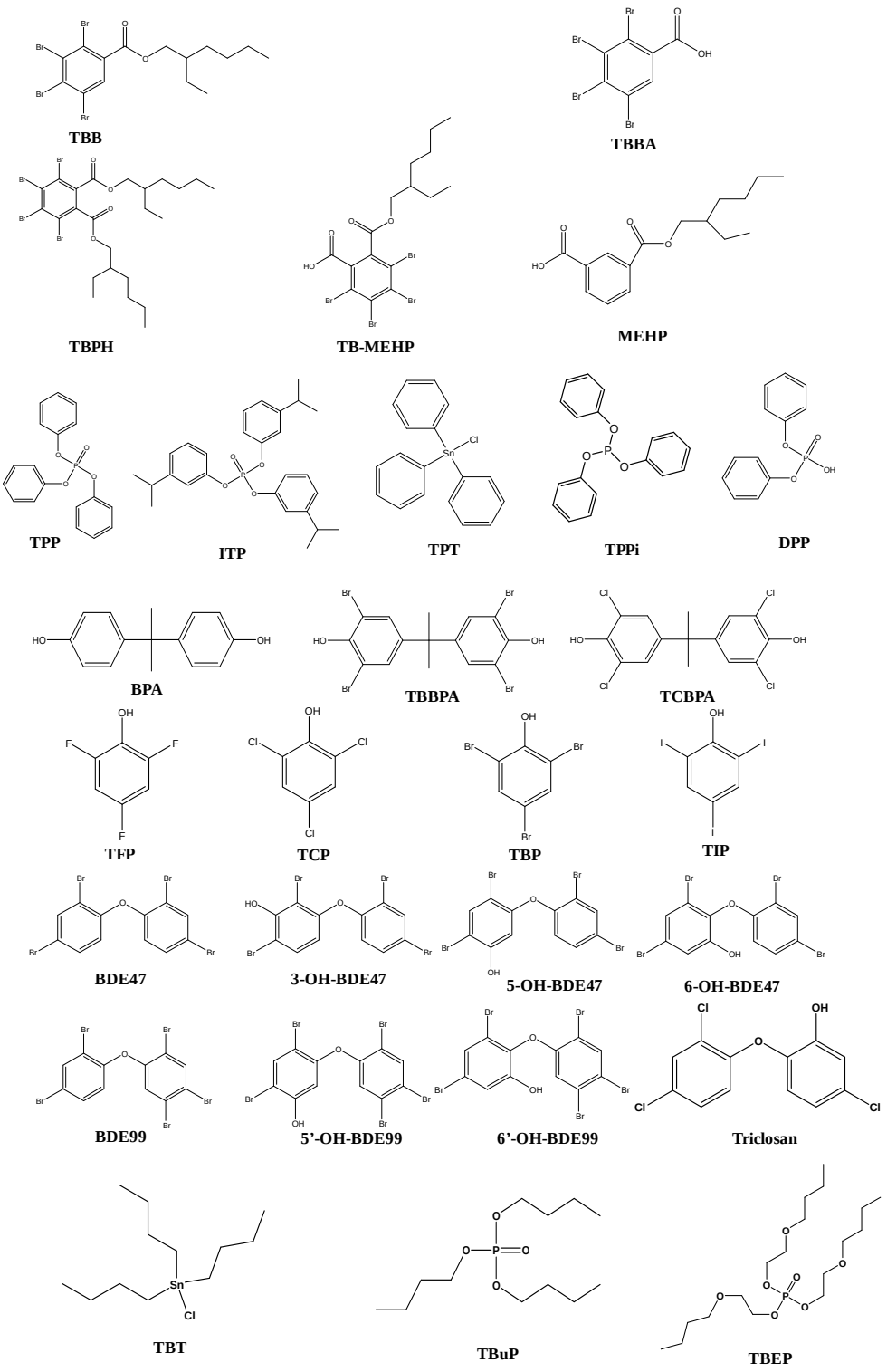

Figure 30: Structures of the flame retardants and their major metabolites tested in this study.

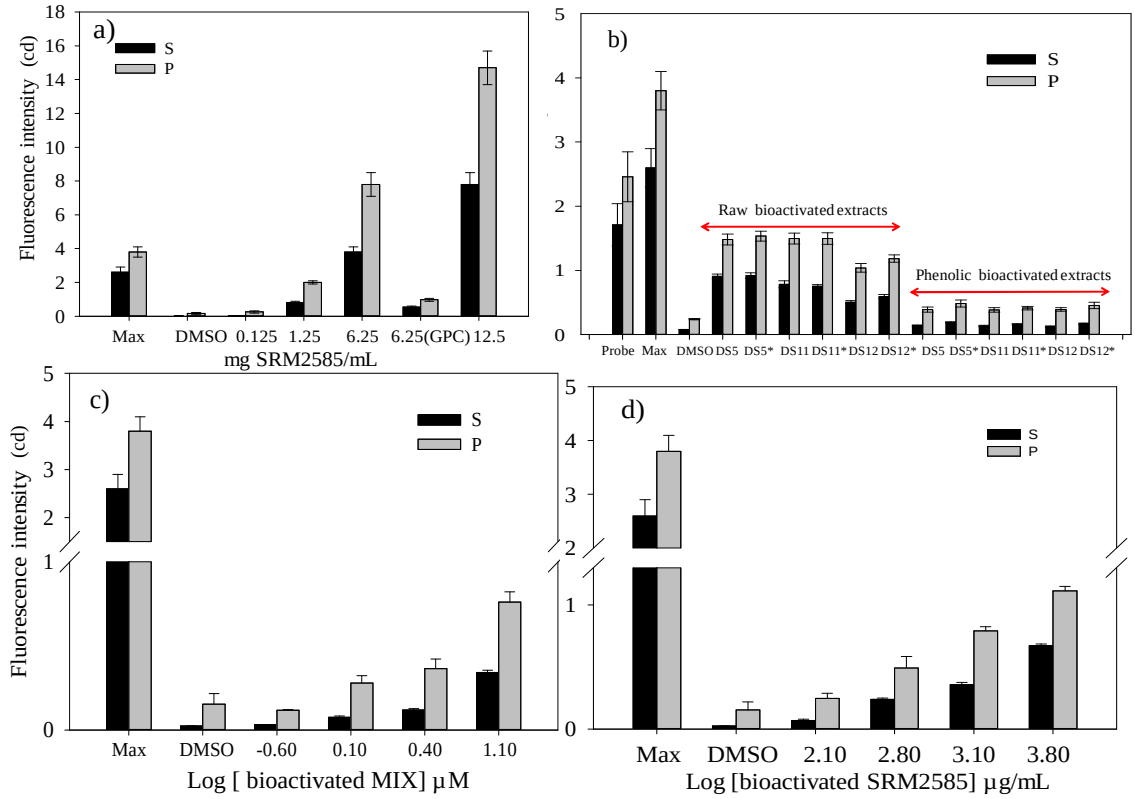

Figure 31: The fluorescence interference from dust matrix and rat liver S9 fraction coextracts before and after cleanup treatments. In details, the figures show fluorescence intensity (cd) of emission parallel (P) to the excitation plane, and fluorescence intensity perpendicular (S) to the excitation plane of: (a) SRM 2585 prior to and post GPC treatment; (b) raw bioactivated dust extracts (6 mg DEQ/mL) and phenolic fraction; (c) bioactivated MIX; and (d) bioactivated SRM2585 with different concentrations. The assay was conducted by dosing dust extract to the buffer solution without PPARγ-LBD and PPAR-Green. DMSO represents the control without PPARγ-LBD and PPAR-Green. Max represents the DMSO with PPARγ-LBD and PPAR-Green. Probe represents PPAR-Green only. The labels with "*" in b) represent dust incubated with active S9 fraction. Those values represent average of the triplicates and error bar represents standard deviation.

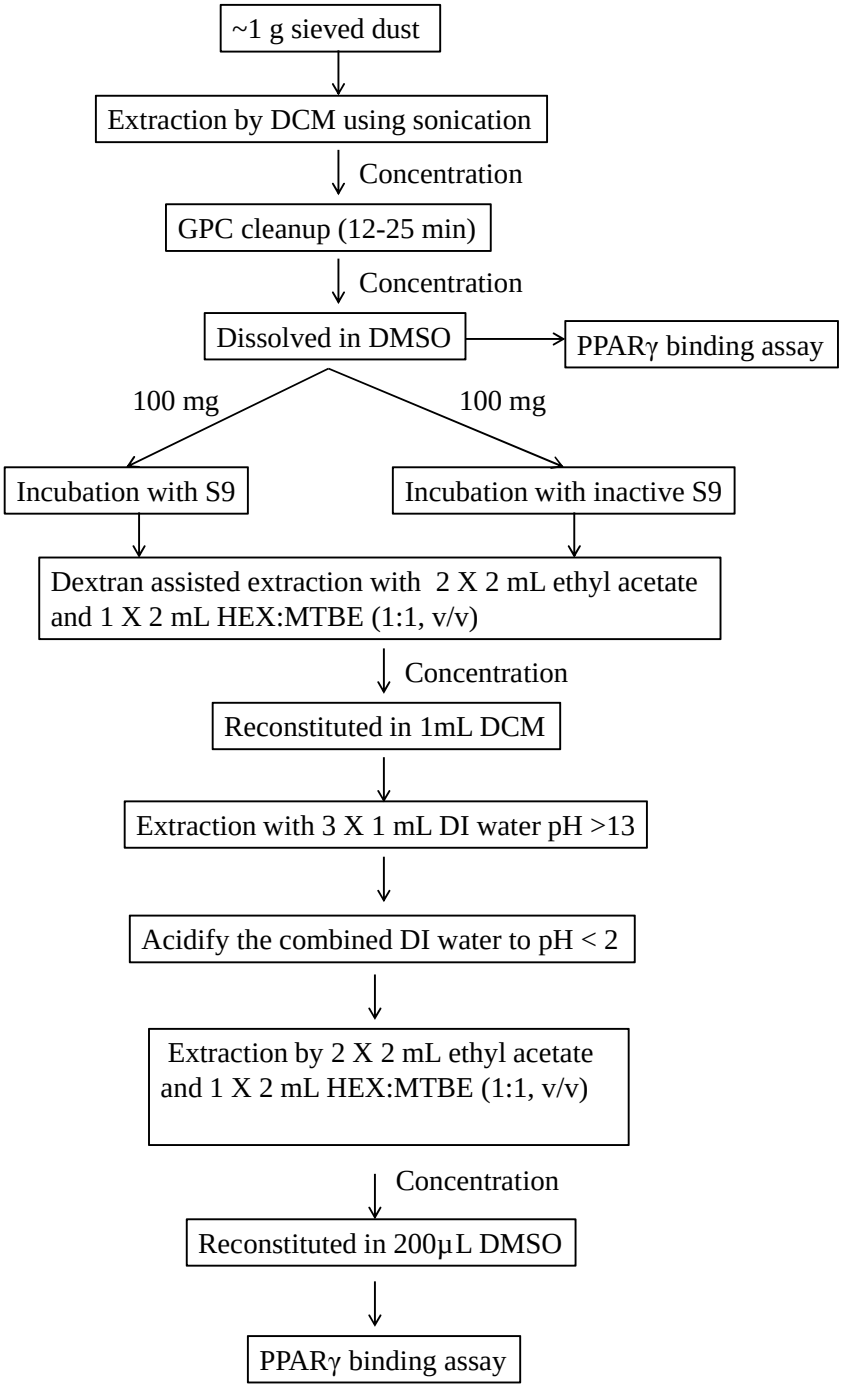

Figure 32: Flow chart of incubation, extraction, and cleanup steps for dust bioactivation experiments using rat liver S9 fraction.

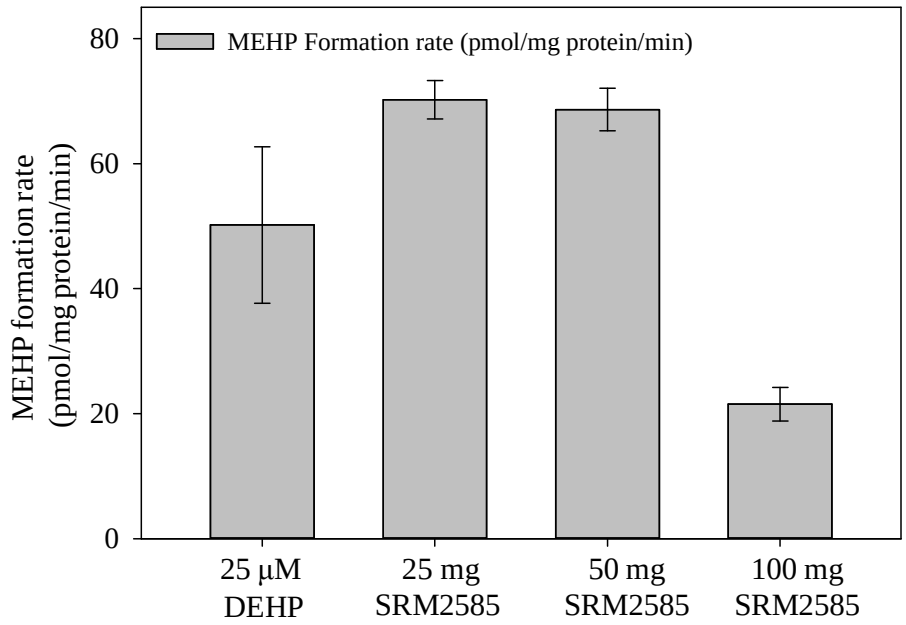

Figure 33: MEHP formation rate in incubations with either pure DEHP (25µM) or increasing concentrations of an extract of indoor dust SRM 2585. Values represent average of the triplicates and error bar represents standard deviation.

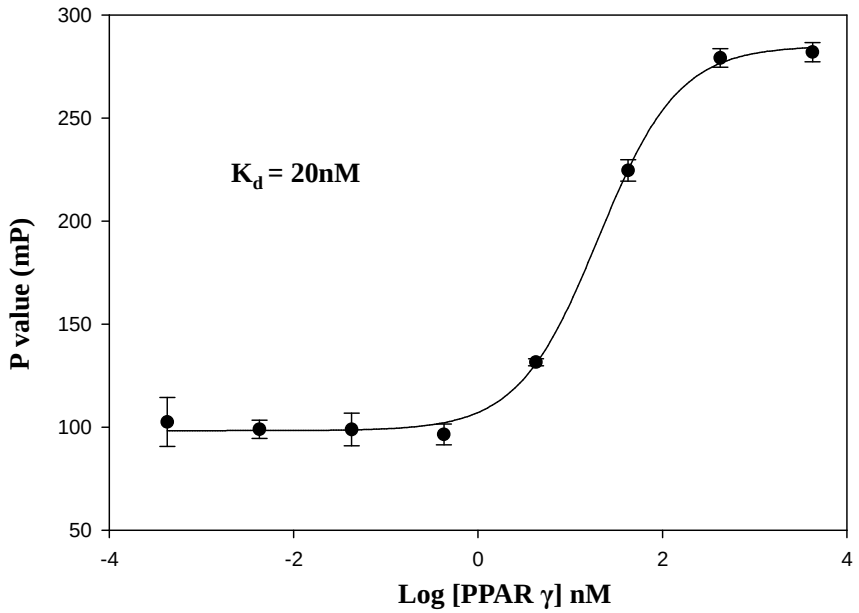

Figure 34: Fluorescence polarization value (mP) of 1.25 nM PPAR-Green as a function of added PPARγ LBD concentration. Values represent average of the triplicates and error bar represents standard deviation.

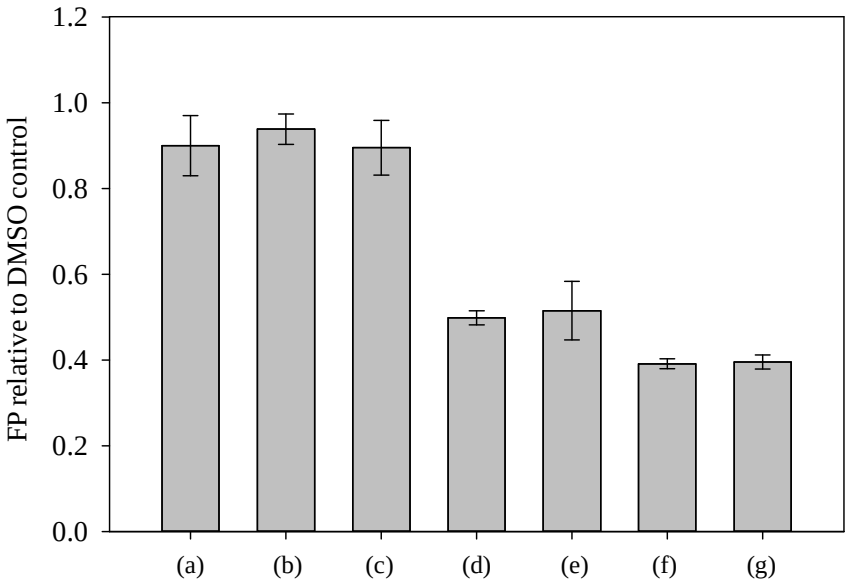

Figure 35: Competitive PPARγ binding potency of (a). 1.25 mg SRM2585 (cleaned by GPC)/mL; (b). 0.125 mg SRM2585/mL; (c) 12.5 mg SRM2585/mL spiked with 12.5 μM Rosi.; (d) 1.25 mg SRM2585/mL spiked with 12.5 μM Rosi.; (e) 0.125 mg SRM2585/mL spiked with 12.5 μM Rosi.; (f) 0.0125 mg SRM2585/mL spiked with 12.5 μM Rosi.; and (g) 12.5 μM Rosi. relative to the DMSO control. Values represent average of the triplicates and error bar represents standard deviation.

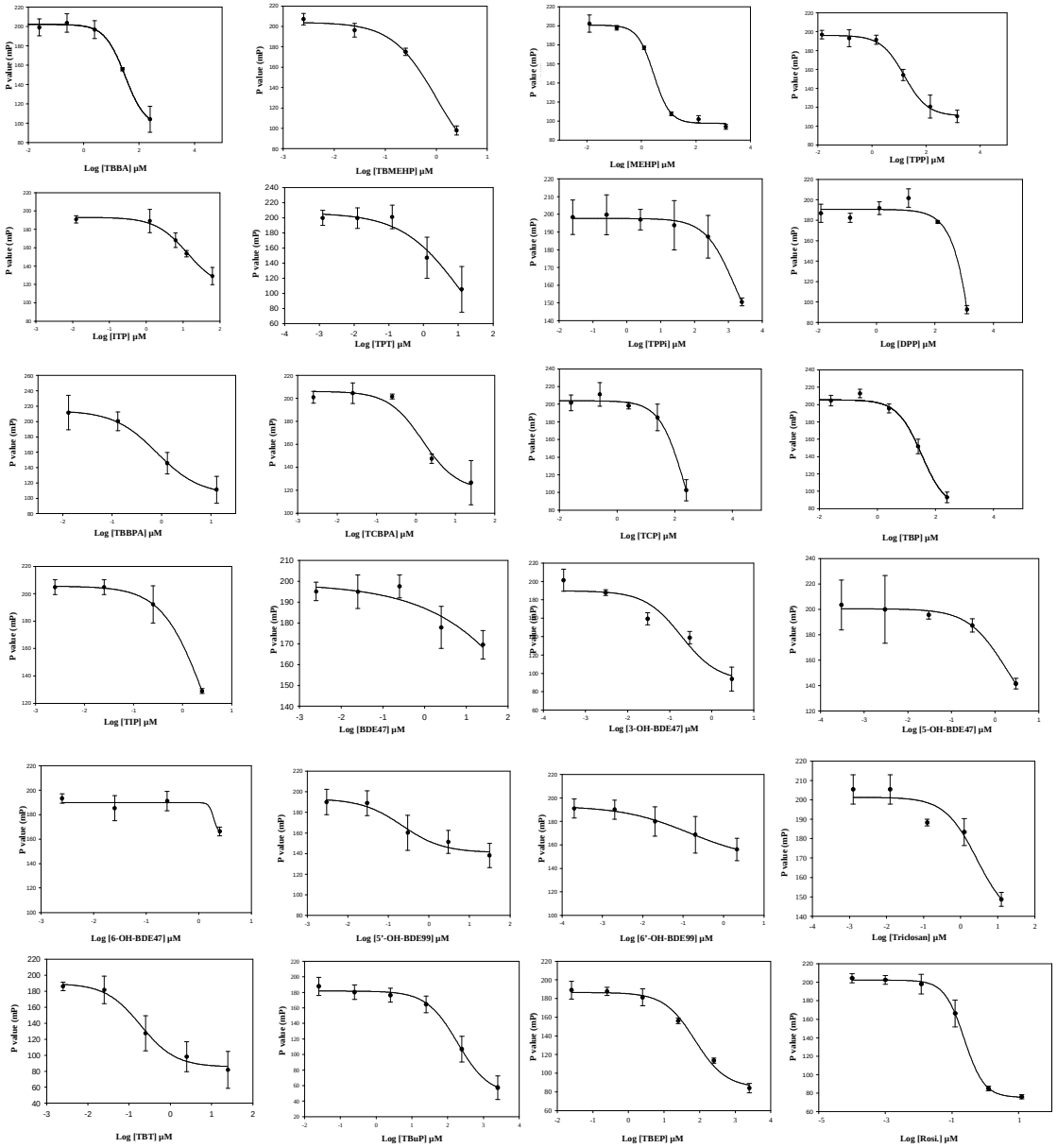

Figure 36: Dose response curve of tested flame retardants and their major metabolites. All assays were done with triplicates in 40µL of 38 nM PPARγ LBD and 1.25 nM PPAR-Green. Values represent average of the triplicates and error bar represents standard deviation.

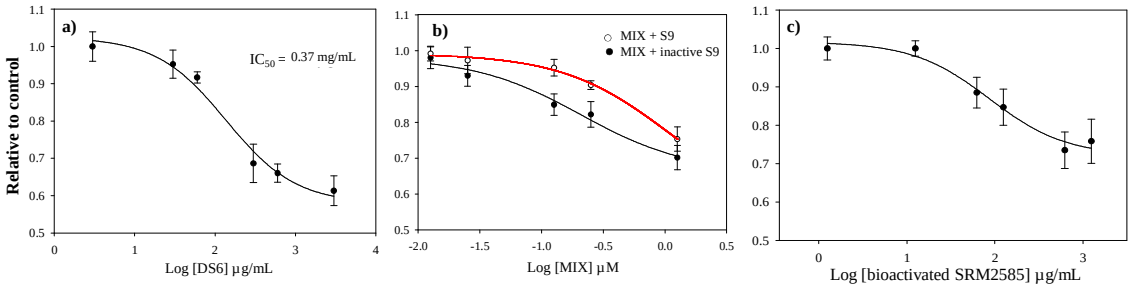

Figure 37: Dose response curve of PPARγ ligand binding using a) an indoor dust sample (DS6); b) MIX incubated with active and inactive S9 fraction; c) bioactivated SRM2585. MIX includes 5 µM FM550, ITP, BDE47, BDE99, and DEHP. Values represent average of the triplicates and error bar represents standard deviation.

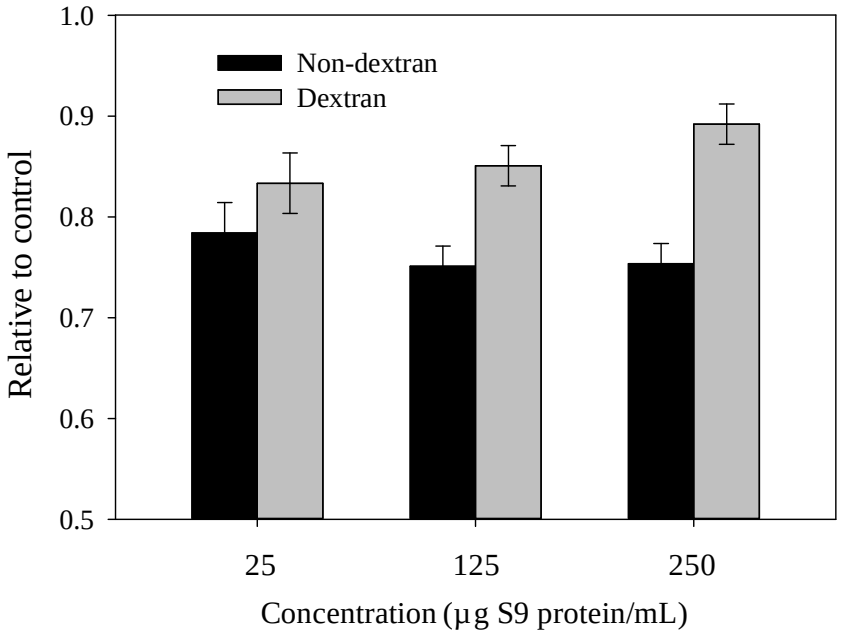

Figure 38: Competitive PPARγ binding potency of the raw coextracts and dextran assisted extracts from S9 fraction relative to the DMSO control. Values represent average of the triplicates and error bar represents standard deviation.

Table 5: Chemical analysis of related compounds in this study

Analytes	I.S.	MRM/SIM	Fragmentor	Collision energy	Ionization
TBPH	F-BDE69	463			GC/ECNI-MS
13C BPA		239.1-223.1	120	5	ESI negative
		239.1-75	120	35	
BPA	13C BPA	227.1-212.1	120	15	ESI negative
		227.1-133	120	25	
TBBPA	13C TBBPA	543-447.8	160	45	ESI negative
		543-445.8	160	35	
13C TBBPA		555-459.8	160	35	ESI negative
13C TRICLOSAN		301-35.1	80	10	ESI negative
Triclosan	13C TRICLOSAN	289-35.1	80	10	ESI negative
		287-35.1	80	10	
2,4,6-TBP	13C TBBPA	330.8-79	120	40	ESI negative
		328.8-79	120	40	
2,4-dichlorophenol	13C TBBPA	161-125.1	80	10	ESI negative
		161-34.9	80	18	
4-monochlorophenol	13C TBBPA	127-34.9	80	15	ESI negative
DEHP	TIBA	391.4-149.1	80	24	ESI negative

MEHP	TIBA	277-134	120	8	ESI negative
		277-127	120	8	
TBBA	TIBA	436.6-392.6	75	5	ESI negative
		436.6-79	75	25	
TIBA		498.7-454.8	75	5	ESI negative
		498.7-127	75	15	

Table 6: Elution profile of several pure compounds in GPC.

Compounds/Time (min)	0-12	12-14	14-16	16-18	18-20	20-22	22-24	24-26	26-28
TBPH		73%	20%	7%					
BPA				77%	13%	5%	5%		
TBBPA			63%	34%	3%				
Tricolsan				91%	9%				
2,4,6-TBP					62%	33%	5%		
2,4-dichlorophenol					76%	24%			
4-monochlorophenol				11%	52%	19%	11%		
Triphenyltin Chloride				11%	12%	15%	16%	23%	24%
Tributyltin Chloride				26%	27%	20%	11%	9%	6%
Matrix	+++*	+++	++	+					

***represents the darkness of the color observed in the fractions.**

Appendix C: Activation of Human Peroxisome Proliferator-Activated Nuclear Receptors (PPARγ) by Semi-Volatile Compounds (SVOCs) and Chemical Mixtures in Indoor Dust

C.1 Tested Compounds

BDE-47, their metabolites (i.e., 3-OH-BDE-47 and 6-OH-BDE-47), benzyl butyl phthalate (BBP), and TBBPA (98%) were purchased from AccuStandard (New Haven, CT). 2,4,6-tribromophenol (2,4,6-TBP, 99%), 2,4,6-triiodophenol (2,4,6-TIP, 97%), TPP (99%), rosiglitazone (98%), triclosan (> 97%), tris (4, tert-butyl-phenyl) phosphate (TBPP), TBT (96%), DEHP (99.7%), TBEP (94%), bis(2-ethylhexyl) fumarate (BEHF), dibutyl phathalate (DBP, 99%), resazurin and triphenyl phosphite (TPPi, 97%) were purchased from Sigma-Aldrich (St Louis, MO). TPT (95%) was purchased from ACROS Organics (NJ, USA). TCBPA (98%) was purchased from TCI America (Portland, OR). Di-iso butyl phathalate (DiBP, 99.5%) and diisononyl phthalate (DiNP) was purchased from CHEM SERVICE (West Chester, PA). MEHP (98%) was purchased from Wako Pure Chemical Industrials, Ltd (Osaka, Japan). 15d-PJG2 (≥97%) was purchased from Santa Cruz Biotechnology Inc. (Dallas, Texas). The metabolic product TBBA (estimated > 98% purity by H1-NMR) was synthesized by the Duke Small Molecule Synthesis Facility. TBMEHP was a gift from Dr. Kim Boekelhide's group at Brown University. A commercial standard of FM 550 was supplied by Great Lakes Chemical (West Lafayette, IN), a company owned by Chemtura (Philadelphia, PA). Isopropylated triphenyl phosphate (ITP) commercial mixture were purchased from one manufacturer in China and

supplied from US EPA; respectively. Tert-butylphenyl diphenyl phosphate (BPDP) commercial mixture was supplied by National Toxicology Program (NTP, National Institute of Environmental Health Sciences). ITP isomers (mono-, di-, and tri-ITP) were purified from FM550 and enriched to ≥ 90% purity as described in a previous study (McGee et al. 2013). All solvents and other materials were of HPLC grade. All the cell culture reagents were from Life Technology Inc. (Grand Island, NY).

C.2 PPARγ Reporter Assay and Cell Viability Assay.

A commercially available reporter gene assay (GeneBLAzer PPARγ non-DA Assay, Invitrogen) was used to investigate the PPARγ activation of groups of possible PPARγ ligands and house dust extracts. The details of the assay were fully described in the Appendix, PPARγ reporter assay. Briefly, PPARγ-UAS-bla 293H cell line contains a PPARγ ligand-binding domain/GAL4 DNA-binding domain chimera stably integrated into a parental cell line previously engineered with a β-lactamase reporter gene under control of an upstream-activating sequence-response element. As a result, HEK 293H cells stably expressing a GAL4-PPARγ-LBD fusion protein and a UAS-beta-lactamase reporter gene were used to evaluate agonism of PPARγ. The cell culture was performed in flasks coated with 1X Matrigel™ matrix and incubated in a humidified 37°C/5% CO2 incubator with Dulbecco's Modified Eagle Medium (DMEM with GlutaMAX™) and 10% dialyzed fetal bovine serum (FBS). After reaching ~90% confluence, the cells were seeded with trypsin/EDTA (0.25%). PPARγ-UAS-bla 293H cells were immediately plated in black-walled clear bottom and poly-d-lysine-coated 384-well plates at a density of 30,000 cells per well in assay medium (phenol red-free DMEM with 0.1% charcoal-

stripped FBS). Cells were then treated with serial dilutions of chemicals or dust extracts and incubated for 16 hours with a final DMSO concentration of 0.1%. Following incubation, LiveBLAzerTM-FRET B/G loading solution containing the substrate was added to the cells, and was incubated at room temperature for 2 h. Fluorescence intensity at 460 and 530 nm emission following excitation at 406 nm was measured using a FLUOstar OPTIMA plate reader (BMG, LABTECH Inc.). To find the optimal concentration range, most of chemicals were prepared in stock with a concentration of approximately 100 mM (i.e.,~100 μM in the dosing medium) and 10 time dilution was used. If any activity was observed in the preliminary test, the highest concentration without any significant cytotoxicity was used as the initial dosing concentration and then a focused dose with 3 time series of dilution was used for both chemical and dust extract tested. For the house dust, the dosing concentration ranged from approximately 2000 μg DEQ dust/mL to several μg DEQ dust/mL with a total of 6 dilution series for most dust samples. Rosiglitazone (1 μM, n=12) was used as the positive control to achieve the maximal PPARγ activation response. DMSO (n=12) was also run as the control in each plate and 24 cell free wells were also run as the negative control in each plate.

Amalar blue assay which was prepared from resazurin was used for the cell variability test (O'Brien et al. 2000). A separate 384 well plate were prepared alongside without adding the substrate after incubation with chemicals or dust extracts. Resazurin with a concentration of 12.5 mg/L was prepared in phosphate saline buffer and was

added in cell culture medium with a volume of 10%. After incubating in the humidified 37°C/5% CO2 incubator for four hours, a FLUOstar OPTIMA (BMG, LABTECH Inc.) plate reader was used to measure fluorescence at wavelengths of 530 nm excitation and 590 nm emission. After each experiment, the cell morphological changes were also observed under the microscope to confirm with the cell viability assay.

C.3 Statistical Analyses and Quality Control

All statistical analyses were conducted using SigmaPlot 12.0 (Systat Software Inc.), testing hypotheses at $\alpha = 0.05$, and all tests were two-tailed. For the chemicals and house dust tested, a one way *ANOVA* was conducted and Newman-Keuls *post-hoc* test was used to identify which doses were significantly different from the DMSO control and the procedural control; respectively. For most tested compounds, only partial dose-response curve was observed. To compare the potency between different dosing chemicals, dose−response curves for these compounds were depicted as sigmoidal plots (three parameter Hill function by setting Hill slope coefficient=1 *a priori*) by using GraphPad Prism (version 6): Y=Bottom + (Top-Bottom)/(1+10^((LogEC50-X))), where Y is the measured PPARγ activity %; X is the compound concentration; Bottom is the PPARγ activity of the DMSO vehicle-only control (i.e., 0%); Top is the PPARγ activity due to the maximal concentration of rosiglitazone (i.e., 100%). EC_{15} and EC_{20} were extrapolated from the curve using GraphPad Prism. To establish the relationship between PPARγ binding potency and activation, Pearson correlation analysis was used to compare the PPARγ ligand binding potency and PPARγ activation of the 24 house dust extracts. The

PPARγ binding potency (%) in the competitor assay was calculated using the following equation:

Binding potency (%) = (1–polarization value of compounds/DMSO control)*100 [1].

DMSO control is the polarization value of PPARγ ligand-binding domain (LBD) and florescence probe without any competitor (Fang et al. 2015). In this study, fluorescence polarization value of 3 mg DEQ/mL of 24 house dust extracts was used. Approximately 200 μg DEQ/mL was chosen for the PPARγ activation assay, since the activity at this concentration was observed without any obvious cytotoxicity for most dust samples. Four dust extracts showed negative PPARγ activity (i.e, three samples in Group B and one sample in Group A) were excluded in the analysis.

For each dosing level, triplicates were run in the 384 well plates. To reduce the variability between batches, similar passages (6^{th} or 7^{th}) of cells were collected for the reporter assay. To ensure the dose-response of all the dosed chemicals or dust extract was comparable, all the possible PPARγ agonists were rerun at the same time after the first-round screening. To evaluate the fluorescence interference from house dust extract matrix, cell free wells dosed with house dust extracts were prepared and no significant difference was observed with DMSO cell free controls, suggesting negligible effect from dust matrix within the dosing levels in this study.

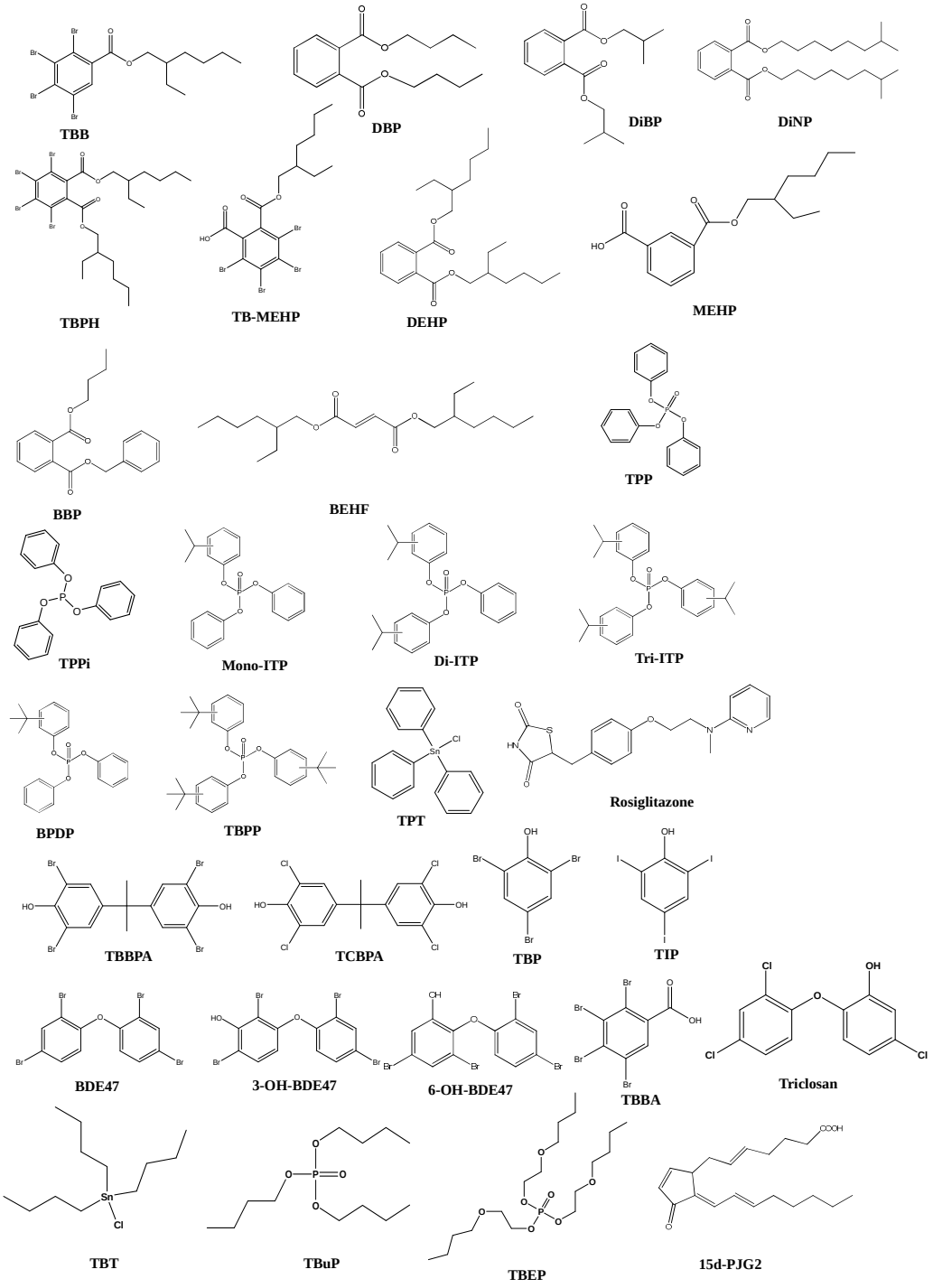

Figure 39: Structures of the chemicals tested in this study.

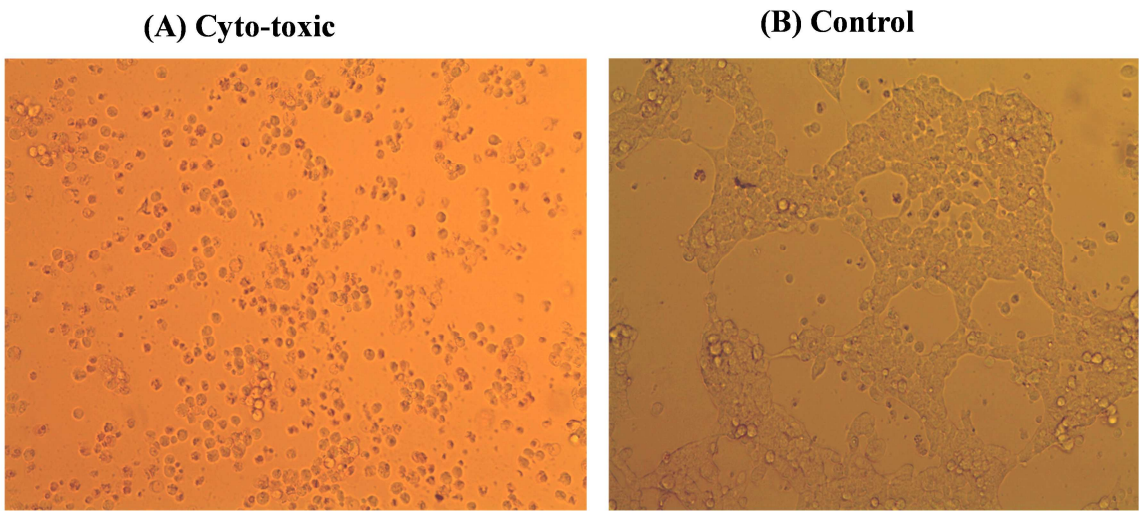

Figure 40: Light microscopy (20X magnification) of HEK293 cells (A) exposed to toxic levels of tested compounds and (B) untreated. Pictures were taken in 384-well plates 24 h after dosing.

Appendix D: Effect-Directed Analysis of Human Peroxisome Proliferator-Activated Nuclear Receptors (PPARγ) ligands in Indoor Dust

D.1 Chemical Identification

Fractions with significant PPARγ activity were subjected to qualitative mass spectrometric analysis by gas chromatography mass spectrometry (Agilent GC 6890N, MS 5975, Newark, DE) operated in full-scan mode (*m*/*z* 50 to 1050) under the electron ionization (EI) mode (GC/EI-MS). The chemical identification was based on our previous study (Fang et al. 2014a) and fully described in Appendix, Chemical Identification. A 0.25 mm (i.d.) × 15 m fused silica capillary column coated with 5% phenyl methylpolysiloxane (0.25 μm film thickness) was used for separation of the analytes. Splitless injections were performed with a PTV inlet maintained at 250°C and 10 psi. The nitrogen flow rate was 1.3 mL min^{-1} and the oven temperature program was as follows: after holding at 40°C for 0.6 min, the temperature was increased at 10°C/min until reaching 280°C, at which point isothermal conditions were maintained for 14 min before returning to initial conditions. The transfer line temperature was maintained at 280°C, and the ion source was held at 230°C. Structural elucidation was performed using MS-Chemstation software (version E.02.01.1177) from Agilent (Palo Alto, CA 94306 United States) equipped with the NIST mass spectral library (version 2005) and NIST Mass Spectral Search Program (Version 2.0d). The mass spectrum of each non-targeted component was extracted and its peaks assigned identities by the automated mass spectral deconvolution and identification system (AMDIS) and the NIST-05-library. Peaks with a signal-to-noise ratio (S/N) above 20 were library searched and assigned

structures based on the presence of a corresponding mass signature with a match factor of at least 60 (out of 100). For several tentatively identified chemicals, further confirmation was achieved by comparing retention times (RT) and mass spectral to those of authentic standards.

Table 7: Elution profile of prepared standard mixtures in the NP-HPLC

	4	5	6	7	8	9	10	11	12	13	14	15	16	17	18	19	20	21	22	23	24	25	26
DEHP																							
TBB																							
TBPH																							
PBDEs																							
TPP																							
TCPP																							
TCEP																							
Triclosan																							
2,4,6-TBP																							
2,4,5-TBP																							
TBBPA																							
6-OH-BDE47																							
Monochlorophenyl																							
BPA																							
TBMEHP																							
TBBA																							
MEHP																							
TPT chloride																							
TBT chloride																							
RT (min)																							

Table 7 (Continued)

	30	31	32	33	34	35	36	37	38	39	40	41	42	43	44	45	46	47	48	49	50
DEHP																					
TBB																					
TBPH																					
PBDEs																					
TPP																					
TCPP																					
TCEP																					
Triclosan																					
2,4,6-TBP																					
2,4,5-TBP																					
TBBPA																					
6-OH-BDE47																					
Monochlorophenyl																					
BPA																					
TBMEHP																					
TBBA																					
MEHP																					
TPT chloride																					
TBT chloride																					
RT (min)																					

Table 8: Quantifier and qualifiers of several FAs, phthalates, and organophosphates analyzed using GC/EI-MS.

	Compounds	Quantifier	Qualifier 1	Qualifier 2	RT (min)
Fatty Acid	OA	264	284		12.3
	PA	256	213	129	11.0
	31D-PA	287	237	141	10.8
	SA	284	241	129	12.4
	MA	228	185	129	9.9
Phthalates	DMP	163	77	194	7.8
	DEP	149	177	222	8.8
	dDEP	153	181	226	
	DBP	149	205	223	11.0
	d-DBP	153	209	227	
	DiBP	149	205	223	10.5
	BBP	149	91	206	14.1
	d-BBP	153	210	91	
	DEHP	149	167	279	16.3
	dDEHP	153	171	283	16.3
	DiNP	293	149	127	19.5
Organophosphates	TBP	99	155	211	9.1
	d-TBP	103	167	231	
	TPP	325	326		14.8
	d-TPP	341	340		

Table 9: Compounds identified in PPARγ active fractions from dust extracts, D2, D3 and A3 (confirmed with standards or with a match factor more than 50%)

Numbers	Compound identified	Abbreviation	CAS number	Identified by	Match Factor
1	Arachidic acid	AA	506-30-9	SM	70%
2	Azelaic acid	AzA	123-99-9	SM	60%
3	Behenic acid	BA	112-85-6	SM	90%
4	Benzyl butyl phthalate	BBP	85-68-7	AS	
5	Bis(2-ethylhexyl) fumarate	BEHF	141-02-6	AS	
6	Bis(2-ethylhexyl) phthalate	DEHP	117-81-7	AS	
7	Dibutyl phthalate	DBP	84-74-2	AS	
8	Diethyl phthalate	DEP	84-66-2	AS	
9	Diisononyl phthalate	DiNP	28553-12-0	AS	
10	Docosahexaenoic acid	DHA	6217-54-5	SM	74%
11	Hexadecanamide	HDM	629-54-9	SM	60%
12	Lauric acid	LA	143-07-7	SM	90%
13	Myristic acid	MA	544-63-8	AS	
14	Octadecanamide	ODM	124-26-5	SM	61%
15	Oleamide	OM	301-02-0	SM	50%
16	Oleic Acid	OA	112-80-1	AS	
17	Palmitoleic acid	POA	373-49-9	SM	90%
18	Palmitic acid	PA	57-10-3	AS	
19	Pentadecanoic acid	PDA	1002-84-2	SM	90%
20	Piperine	PP	94-62-2	SM	91%
21	Stearic acid	SA	57-11-4	AS	
22	Triphenyl phosphate	TPP	115-86-6	AS	
23	Tris(1,3-dichloro-2-propyl)phosphate	TDCPP	13674-87-8	AS	
24	Tris-(2-butoxyethyl)-phosphate	TBEP	78-51-3	AS	

AS=authentic standard; SM=spectral match (these compounds were identified by match to spectra in the National Institute of Standards and Technology's 2005 spectral library with a match factor > 50%).

Table 10: Concentration (μg/g dust) of several organophosphates, phthalates and FAs in the 25 house dust extracts cleaned by GPC.

Sample ID	Concentration (μg/g dust)												
	TBP	DiBP	DBP	BBP	TPP	DEHP	DiNP	DEP	DMP	OA	PA	SA	MA
A-1	0.43	12.06	15.55	11.20	1.17	250.26	127.55	1.55	0.34	1549.97	1320.50	324.66	462.53
A-2	0.59	4.49	11.72	9.21	0.71	72.26	107.47	2.21	0.14	3731.56	1610.53	419.71	275.61
A-3	0.29	0.23	1.98	0.36	0.11	1.98	0.00	1.48	NA	425.46	113.68	25.32	51.42
A-4	0.34	7.20	16.52	54.27	2.03	338.46	105.65	3.60	0.43	1253.57	4150.54	1780.95	832.17
A-5	0.79	24.68	17.71	68.74	1.10	284.31	202.13	4.37	NA	2554.66	3501.86	988.83	695.86
A-6	0.68	12.53	31.93	31.82	2.45	103.50	87.69	10.94	0.43	1164.23	1824.89	708.66	269.07
A-7	0.40	17.05	7.61	7.86	0.42	115.68	59.60	1.24	NA	429.27	485.66	164.88	101.23
B-1	0.48	10.33	275.95	17.36	2.04	2029.78	129.41	18.33	NA	0.00	15.91	7.70	3.89
B-2	0.45	38.51	236.15	33.60	6.78	1236.48	238.10	14.45	0.34	55.74	316.40	129.60	65.63
B-3	0.81	9.28	284.41	149.22	60.67	657.94	81.04	20.54	0.22	6.34	98.18	44.88	23.87
C-1	0.64	38.39	154.91	11.51	1.23	100.94	129.57	16.65	NA	1103.75	1560.99	439.08	310.01
C-2	1.02	20.66	136.16	181.11	0.47	324.32	172.33	9.80	NA	1274.46	3466.45	1038.95	531.43
C-3	0.65	7.15	124.92	16.19	0.86	116.37	67.63	17.82	NA	674.34	2463.82	819.62	304.23
D-1	0.46	8.25	14.88	5.87	1.13	113.00	131.82	4.05	NA	2192.43	3224.51	844.10	420.35
D-2	0.00	8.93	28.84	15.43	1.26	88.83	134.54	6.46	NA	2313.52	1981.21	616.44	387.80
D-3	4.73	11.69	28.51	94.57	0.48	139.49	125.35	46.71	NA	3160.36	2157.56	682.31	387.97
D-4	NA	4.05	13.36	6.07	0.19	191.71	117.36	11.24	0.19	2513.01	604.20	149.25	87.00
D-5	NA	3.71	27.58	16.06	1.01	113.50	121.10	2.01	NA	2085.21	1408.77	449.81	364.05
D-6	0.28	25.22	10.44	9.27	0.40	106.48	74.50	2.35	NA	595.36	3248.12	1361.14	244.08
E-1	1.39	3.02	20.28	18.52	0.78	99.46	148.84	3.03	0.74	648.35	195.55	61.85	49.68
E-2	1.00	5.82	15.43	13.15	1.00	112.64	118.83	4.87	NA	448.43	551.28	294.55	81.39
E-3	1.39	2.07	15.42	7.20	0.43	63.71	34.14	2.56	NA	191.86	187.30	62.59	33.09
E-4	3.94	3.77	15.77	58.92	1.42	217.27	146.52	3.35	NA	2071.82	843.07	283.19	200.86
E-5	0.25	0.78	4.65	66.35	0.23	20.34	19.00	0.87	0.00	103.39	742.51	204.37	61.97
SRM2585	0.94	0.48	3.75	2.72	0.10	3.49	0.00	3.86	1.60	78.66	82.69	7.55	39.64
Median	0.64	8.25	16.52	16.06	1.00	113.50	118.83	4.05	0.34	1103.75	1320.50	324.66	244.08
Max	4.73	38.51	284.41	181.11	60.67	2029.78	238.10	46.71	1.60	3731.56	4150.54	1780.95	832.17
Min	0.00	0.23	1.98	0.36	0.10	1.98	0.00	0.87	0.00	0.00	15.91	7.55	3.89

Table 11: Concentration (μg/g dust) of several organophosphates, phthalates and FAs in the 10 raw house dust extracts.

Sample ID	Concentration (μg/g dust)											
	TBP	DiBP	DBP	BBP	TPP	DEHP	DiNP	DEP	OA	PA	SA	MA
A-8	0.42	6.71	4.71	5.51	0.24	170.15	483.61	3.70	1807.49	1352.46	451.64	107.98
A-9	0.48	7.05	11.57	115.51	0.52	226.65	183.47	3.88	7075.05	6485.11	1402.41	341.56
A-10	NA	7.15	5.79	13.34	0.95	89.28	61.14	7.95	874.26	161.37	19.92	25.60
A-11	0.78	60.04	6.63	8.61	0.61	206.50	110.85	8.25	571.14	181.51	38.19	22.78
A-12	NA	10.55	12.24	30.05	1.83	198.16	150.09	41.54	957.67	1207.73	297.76	220.81
E-6	2.93	4.29	9.08	6.73	1.46	315.88	85.53	6.30	512.47	1131.41	341.57	110.52
E-7	1.42	3.14	20.83	126.58	0.49	83.75	205.45	4.95	1404.40	1158.66	185.69	118.82
E-8	0.59	4.17	7.07	21.66	0.22	205.25	39.65	2.61	271.54	881.73	35.74	91.63
E-9	NA	2.76	8.23	41.36	0.87	41.87	48.78	7.26	1039.08	612.23	115.21	130.92
E-10	NA	1.37	10.33	5.65	0.42	29.47	28.38	5.80	146.94	435.70	107.81	136.07
Median	0.68	5.50	8.65	17.50	0.56	184.15	98.19	6.05	915.97	1006.57	150.45	114.67
Max	2.93	60.04	20.83	126.58	1.83	315.88	483.61	41.54	7075.05	6485.11	1402.41	341.56
Min	NA	1.37	4.71	5.51	0.22	29.47	28.38	2.61	146.94	161.37	19.92	22.78

Table 12: Pearson Correlation Analysis between the concentration of several organophosphates, phthalates and FAs with PPARγ activation potency in 25 dust extracts at 6 different doses (Dose 1: 8 μg DEQ/mL; Dose 2: 25 μg DEQ/mL; Dose 3: 74 μg DEQ/mL; Dose 4: 222 μg DEQ/mL; Dose 2: 667 μg DEQ/mL; Dose 6: 2000 μg DEQ/mL). All the correlation with p < 0.05 was marked in red.

		Dose 5	Dose 4	Dose 3	Dose 2	Dose 1	TBP	DiBP	DBP	BBP	TPP	DEHP	DiNP	DEP	DMP	OA	PA	SA	MA
Dose 6	Cor. Coe.	0.421	0.14	-0.284	-0.127	-0.0574	-0.403	-0.318	-0.537	-0.0811	-0.446	-0.484	-0.47	-0.467	-0.322	-0.272	-0.355	-0.364	-0.339
	p value	0.347	0.765	0.538	0.786	0.903	0.371	0.488	0.213	0.863	0.316	0.271	0.287	0.291	0.481	0.555	0.435	0.422	0.457
	# Sample	7	7	7	7	7	7	7	7	7	7	7	7	7	7	7	7	7	7
Dose 5	Cor. Coe.		0.698	0.176	-0.273	-0.107	-0.0822	0.114	-0.131	-0.0628	0.108	-0.0482	0.262	0.268	-0.518	0.647	0.247	0.158	0.334
	p value		0.0006	0.459	0.244	0.654	0.73	0.632	0.583	0.793	0.651	0.84	0.264	0.254	0.0193	0.002	0.294	0.506	0.15
	# Sample		20	20	20	20	20	20	20	20	20	20	20	20	20	20	20	20	20
Dose 4	Cor. Coe.			0.587	0.214	0.0759	-0.0178	0.0011	-0.354	0.113	-0.192	-0.262	0.252	0.0436	-0.293	0.743	0.666	0.571	0.732
	p value			0.0021	0.304	0.718	0.933	0.996	0.0824	0.589	0.358	0.206	0.225	0.836	0.155	2E-05	0.0003	0.00286	0.0000322
	# Sample			25	25	25	25	25	25	25	25	25	25	25	25	25	25	25	25
Dose 3	Cor. Coe.				0.614	0.469	-0.137	-0.188	-0.457	-0.0413	-0.175	-0.271	-0.0339	-0.305	-0.0176	0.5	0.278	0.257	0.279
	p value				0.0011	0.0179	0.514	0.368	0.0216	0.844	0.404	0.19	0.872	0.139	0.934	0.0109	0.178	0.214	0.177
	# Sample				25	25	25	25	25	25	25	25	25	25	25	25	25	25	25
Dose 2	Cor. Coe.					0.77	-0.0692	-0.35	-0.568	-0.13	-0.289	-0.312	-0.138	-0.508	-0.037	0.118	-0.0297	-0.0307	-0.0298
	p value					7E-06	0.742	0.086	0.0031	0.534	0.161	0.129	0.509	0.0096	0.861	0.574	0.888	0.884	0.887
	# Sample					25	25	25	25	25	25	25	25	25	25	25	25	25	25
Dose 1	Cor. Coe.						0.071	-0.339	-0.351	-0.126	-0.0237	-0.156	-0.0436	-0.213	0.0785	0.0793	-0.273	-0.238	-0.242
	p value						0.736	0.0971	0.0858	0.547	0.91	0.456	0.836	0.308	0.709	0.706	0.187	0.252	0.244
	# Sample						25	25	25	25	25	25	25	25	25	25	25	25	25
TBP	Cor. Coe.							-0.0906	-0.0872	0.335	-0.0224	-0.0811	0.139	0.538	-0.0379	0.277	-0.0273	-0.0415	0.00721
	p value							0.667	0.679	0.102	0.915	0.7	0.509	0.0056	0.857	0.181	0.897	0.844	0.973
	# Sample							25	25	25	25	25	25	25	25	25	25	25	25
DiBP	Cor. Coe.								0.44	0.153	0.0221	0.295	0.57	0.243	-0.191	-0.0597	0.287	0.262	0.233
	p value								0.0279	0.465	0.917	0.152	0.003	0.241	0.36	0.777	0.164	0.206	0.263
	# Sample								25	25	25	25	25	25	25	25	25	25	25
DBP	Cor. Coe.									0.39	0.584	0.785	0.324	0.475	-0.097	-0.392	-0.204	-0.198	-0.223
	p value									0.0536	0.0022	3E-06	0.114	0.0164	0.645	0.0528	0.329	0.342	0.284
	# Sample									25	25	25	25	25	25	25	25	25	25
BBP	Cor. Coe.										0.508	0.14	0.264	0.387	-0.139	0.0274	0.268	0.23	0.264
	p value										0.0095	0.504	0.203	0.0557	0.507	0.897	0.196	0.269	0.202
	# Sample										25	25	25	25	25	25	25	25	25
TPP	Cor. Coe.											0.243	-0.0287	0.263	0.0334	-0.252	-0.224	-0.194	-0.211
	p value											0.243	0.891	0.204	0.874	0.223	0.282	0.353	0.31
	# Sample											25	25	25	25	25	25	25	25
DEHP	Cor. Coe.												0.402	0.303	-0.067	-0.306	-0.225	-0.19	-0.192
	p value												0.0463	0.141	0.75	0.136	0.28	0.362	0.358
	# Sample												25	25	25	25	25	25	25
DiNP	Cor. Coe.													0.209	-0.209	0.378	0.304	0.222	0.395
	p value													0.315	0.317	0.0623	0.139	0.285	0.0505
	# Sample													25	25	25	25	25	25
DEP	Cor. Coe.														-0.126	0.148	0.0284	0.00961	0.00088
	p value														0.548	0.479	0.893	0.964	0.997
	# Sample														25	25	25	25	25
DMP	Cor. Coe.															-0.244	-0.244	-0.188	-0.162
	p value															0.24	0.239	0.367	0.44
	# Sample															25	25	25	25
OA	Cor. Coe.																0.458	0.323	0.546
	p value																0.0212	0.115	0.00476
	# Sample																25	25	25
PA	Cor. Coe.																	0.961	0.896
	p value																	2.63E-14	1.49E-09
	# Sample																	25	25
SA	Cor. Coe.																		0.841
	p value																		1.42E-07
	# Sample																		25

Table 13: Spearman Correlation Analysis between the concentration of several organophosphates, phthalates and fatty acids with PPARγ activation potency in 10 raw dust extracts at 3 different doses (Dose 1: 222 μg DEQ/mL; Dose 2: 667 μg DEQ/mL; Dose 3: 2000 μg DEQ/mL). All the correlation with $p < 0.05$ was marked in red.

		Dose 2	Dose 1	TBP	DiBP	DBP	BBP	TPP	DEHP	DiNP	DEP	OA	PA	SA	MA
Dose 3	Cor. Coe.	--	0	0	0	0	0	0	0	0	0	0	0	0	0
	p value	--	--	--	--	--	--	--	--	--	--	--	--	--	--
	# Sample	0	1	1	1	1	1	1	1	1	1	1	1	1	1
Dose 2	Cor. Coe.		0.873	0.0793	-0.00131	0.297	0.585	0.0407	0.334	0.148	-0.132	0.896	0.873	0.88	0.778
	p value		0.00463	0.852	0.998	0.475	0.128	0.924	0.419	0.726	0.755	0.00261	0.0046	0.00395	0.0229
	# Sample		8	8	8	8	8	8	8	8	8	8	8	8	8
Dose 1	Cor. Coe.			0.0248	-0.15	0.267	0.591	-0.168	0.288	0.498	-0.0783	0.922	0.934	0.966	0.831
	p value			0.946	0.68	0.455	0.072	0.643	0.419	0.143	0.83	0.000149	0.0000752	0.00000581	0.00288
	# Sample			10	10	10	10	10	10	10	10	10	10	10	10
TBP	Cor. Coe.				0.0104	0.23	0.0749	0.178	0.606	0.0158	-0.285	-0.0839	0.0185	0.0553	-0.131
	p value				0.977	0.522	0.837	0.623	0.0631	0.965	0.425	0.818	0.96	0.879	0.719
	# Sample				10	10	10	10	10	10	10	10	10	10	10
DiBP	Cor. Coe.					-0.249	-0.222	-0.0209	0.254	-0.0194	0.0742	-0.105	-0.178	-0.168	-0.356
	p value					0.488	0.537	0.954	0.478	0.958	0.839	0.773	0.624	0.643	0.313
	# Sample					10	10	10	10	10	10	10	10	10	10
DBP	Cor. Coe.						0.786	0.1	-0.174	-0.0211	0.166	0.182	0.223	0.159	0.378
	p value						0.007	0.783	0.63	0.954	0.646	0.615	0.535	0.66	0.282
	# Sample						10	10	10	10	10	10	10	10	10
BBP	Cor. Coe.							-0.165	-0.0965	0.132	-0.107	0.663	0.641	0.551	0.58
	p value							0.649	0.791	0.715	0.768	0.0368	0.0458	0.0989	0.0786
	# Sample							10	10	10	10	10	10	10	10
TPP	Cor. Coe.								0.308	-0.252	0.773	-0.172	-0.122	-0.0597	0.138
	p value								0.387	0.482	0.0088	0.635	0.737	0.87	0.704
	# Sample								10	10	10	10	10	10	10
DEHP	Cor. Coe.									0.163	0.117	0.227	0.347	0.387	0.194
	p value									0.653	0.747	0.528	0.325	0.269	0.591
	# Sample									10	10	10	10	10	10
DiNP	Cor. Coe.										-0.0406	0.316	0.251	0.366	0.153
	p value										0.911	0.375	0.485	0.298	0.674
	# Sample										10	10	10	10	10
DEP	Cor. Coe.											-0.144	-0.106	-0.0713	0.259
	p value											0.691	0.771	0.845	0.469
	# Sample											10	10	10	10
OA	Cor. Coe.												0.971	0.957	0.791
	p value												0.00000287	0.000014	0.00643
	# Sample												10	10	10
PA	Cor. Coe.													0.979	0.865
	p value													0.000000854	0.00123
	# Sample													10	10
SA	Cor. Coe.														0.855
	p value														0.00161
	# Sample														10

Table 14: Concentration (μg/g dust) of four FAs in cat hair, dog hair, human hair, human skin debris, fish liver oil, and two vegetable oil.

Sample	Concentration (μg/g)				
	OA	PA	SA	MA	Total
Cat Hair	41.3	108.6	35.8	40.6	226.2
Dog Hair	25.3	86.5	29.9	44.8	186.5
Human Hair	331.8	889.1	49.3	191.1	1461.3
Human Skin Debris	3061.1	9368.1	548.9	1890.0	14868.1
Fish Liver oil	1533.5	1445.4	172.0	257.9	3408.8
Vegetable oil1	3544.9	1174.2	441.2	26.1	5186.3
Vegetable oil2	3262.0	998.0	425.7	20.5	4706.2

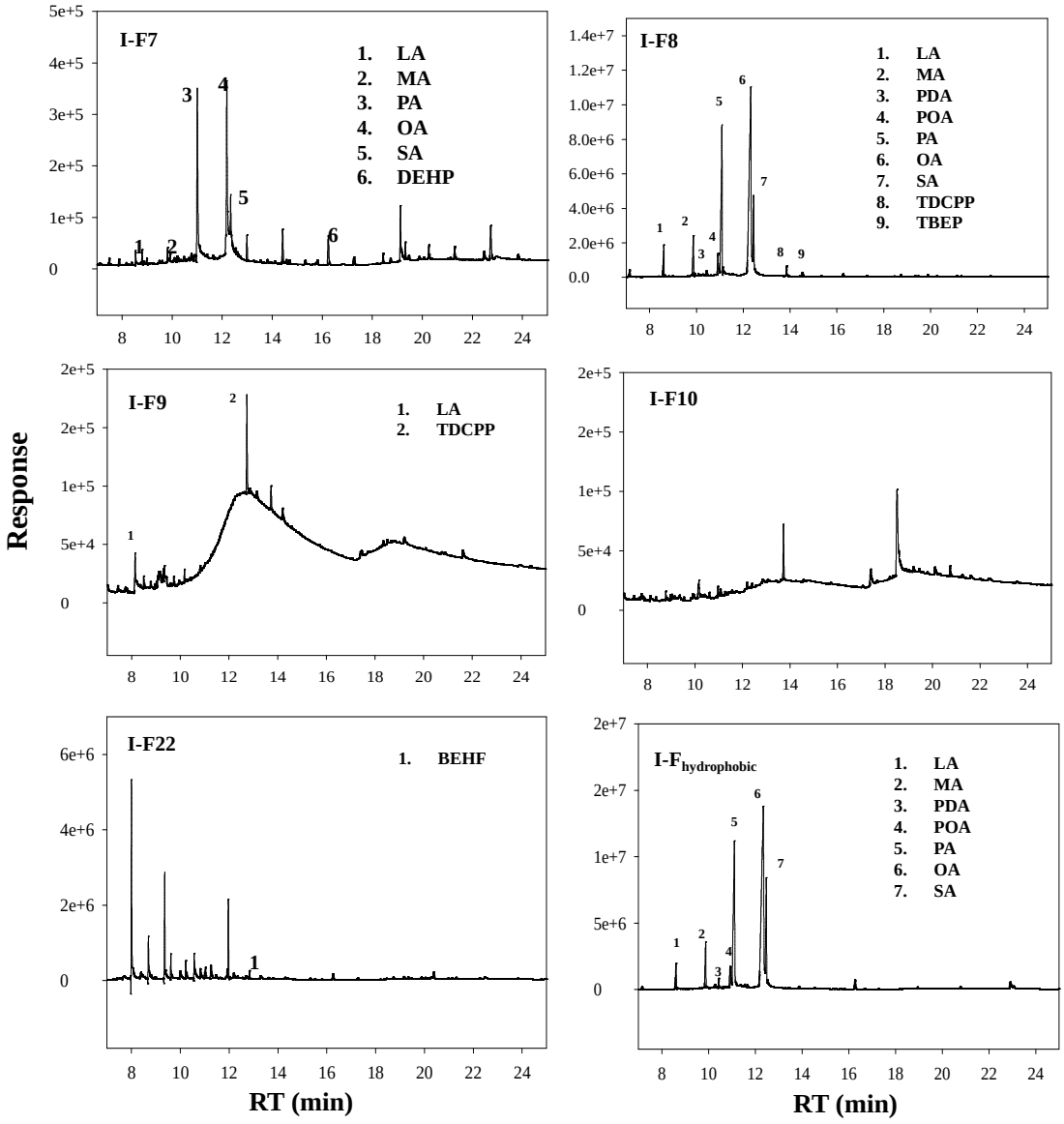

Figure 41: Full scan of PPARγ active fractions (F7, F8, F9, F10, and F22, 1.5 min/fraction; I-F$_{hydrophobic}$ is the insoluble fraction attached to the vial bottom in methanol:H_2O (1:1, V/V)) and the identified chemicals in Dust I using GC-MS/EI based on authentic standards or spectral match. See Table 1 for the abbreviation and other information for the chemicals.

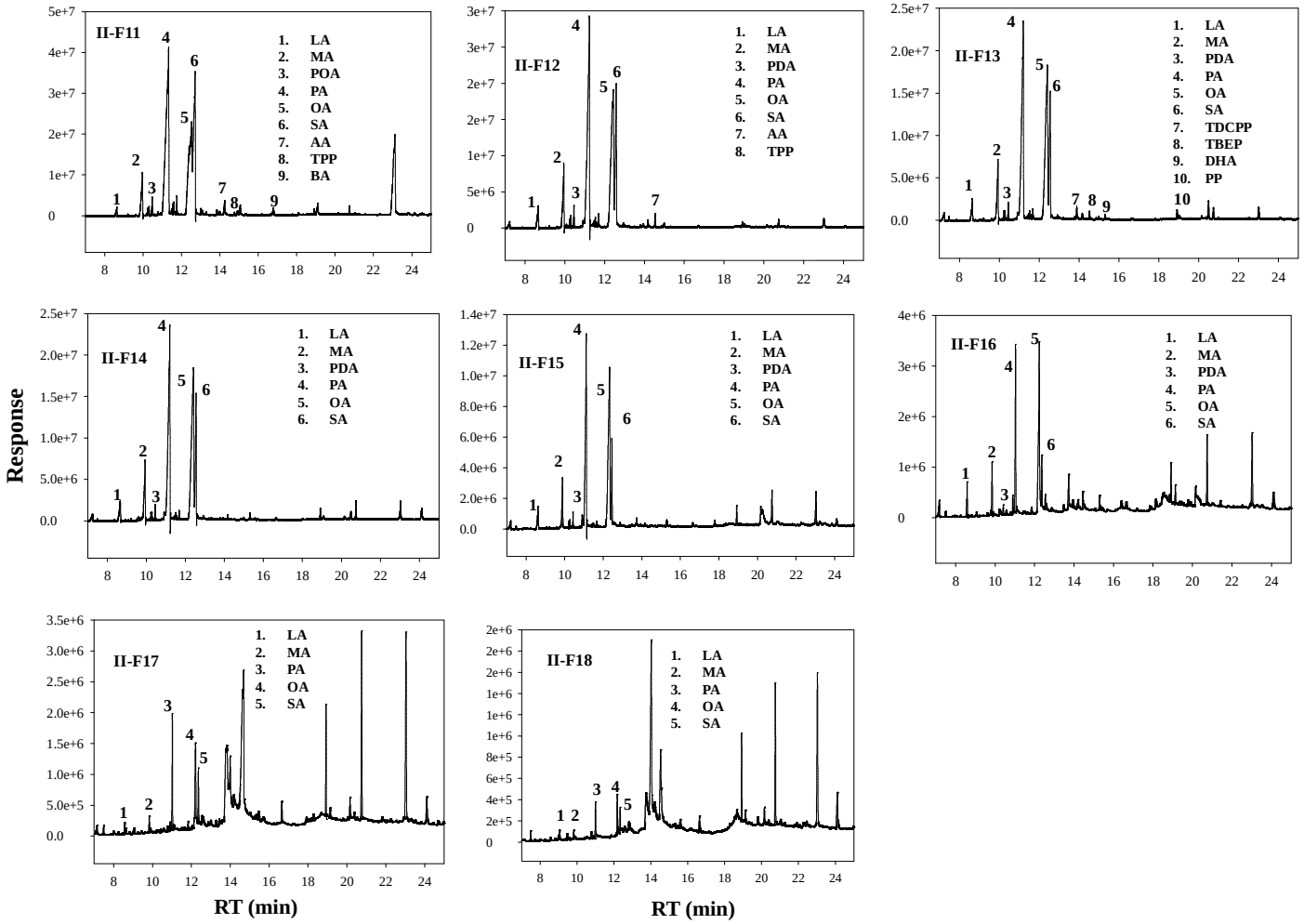

Figure 42: Full scan of PPARγ active fraction and the identified chemicals in Dust II extract using GC-MS/EI based on authentic standards or spectral match. See Table 9 for the abbreviation and other information for the chemicals.

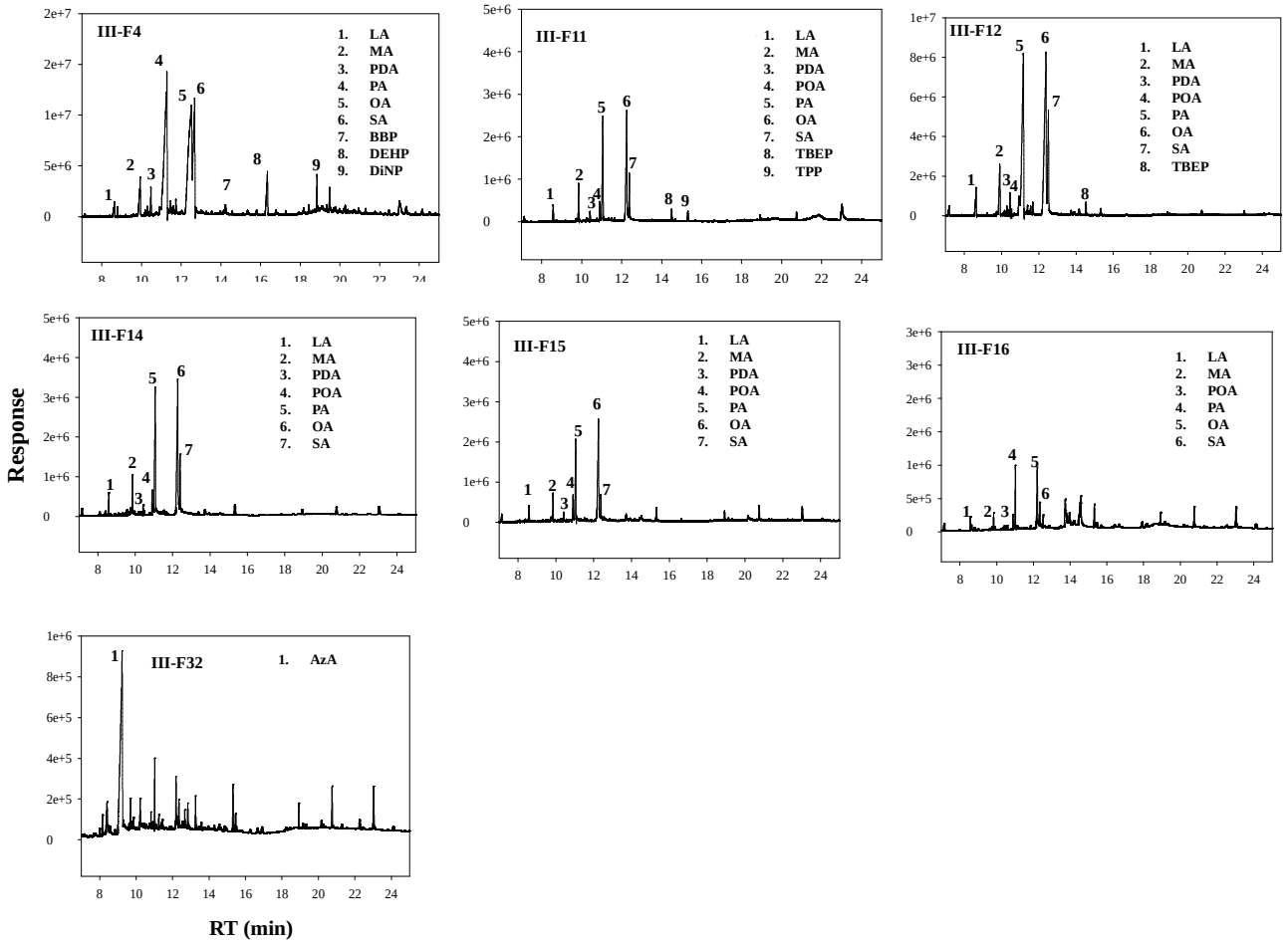

Figure 43: Full scan of PPARγ active fraction (F4, F11, F12, F14, F15, F16, and F32) and the identified chemicals in Dust III using GC-MS/EI based on authentic standards or spectral match. See Table 1 for the abbreviation and other information for the chemicals.

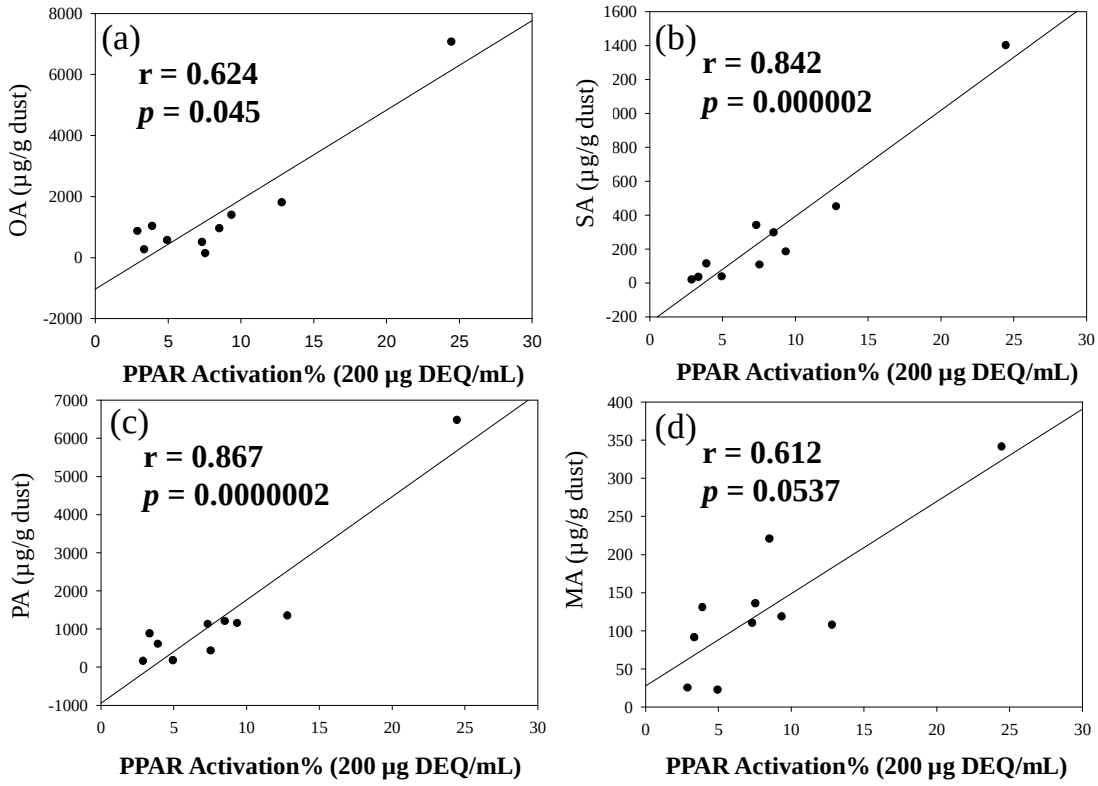

Figure 44: Spearman correlation between the PPARγ activation (%) at the dose of 200 µg DEQ/mL and the concentration of (a) OA, (b) PA, (c) SA, and (d) MA in 10 raw dust extracts.

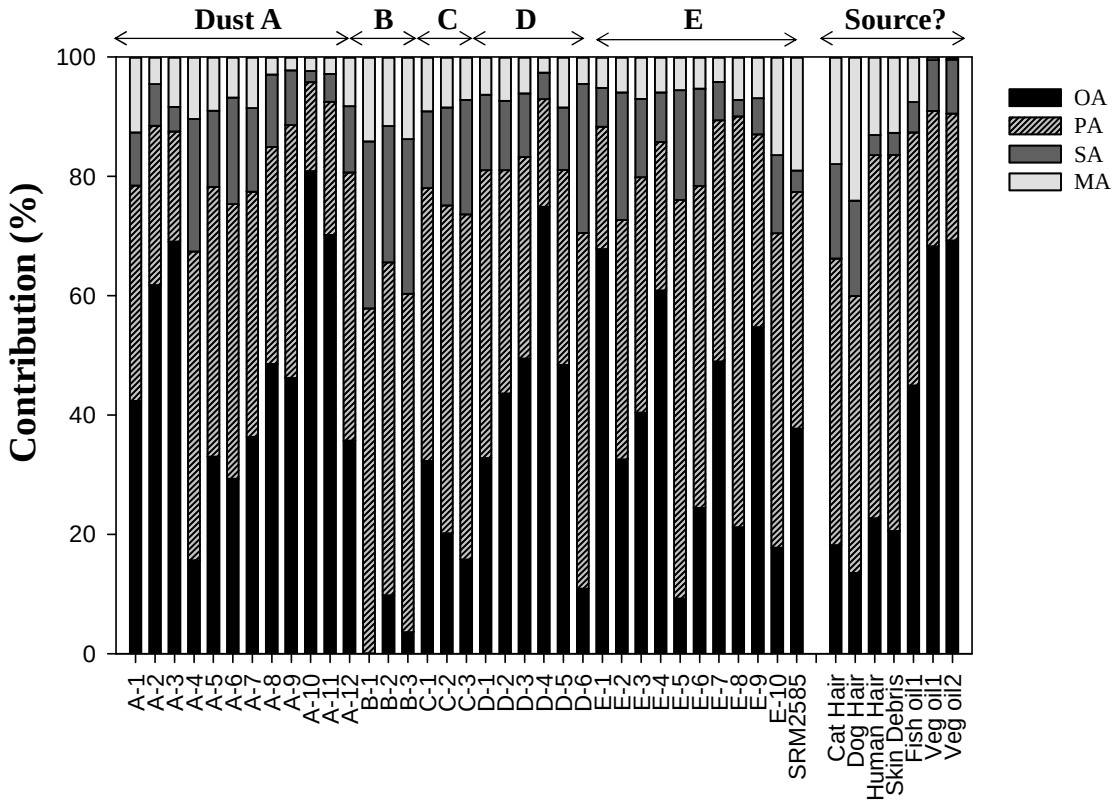

Figure 45. The contribution (%) of OA, PA, SA, and MA to the sum of the FAs in 35 house dust extracts and several possible sources.

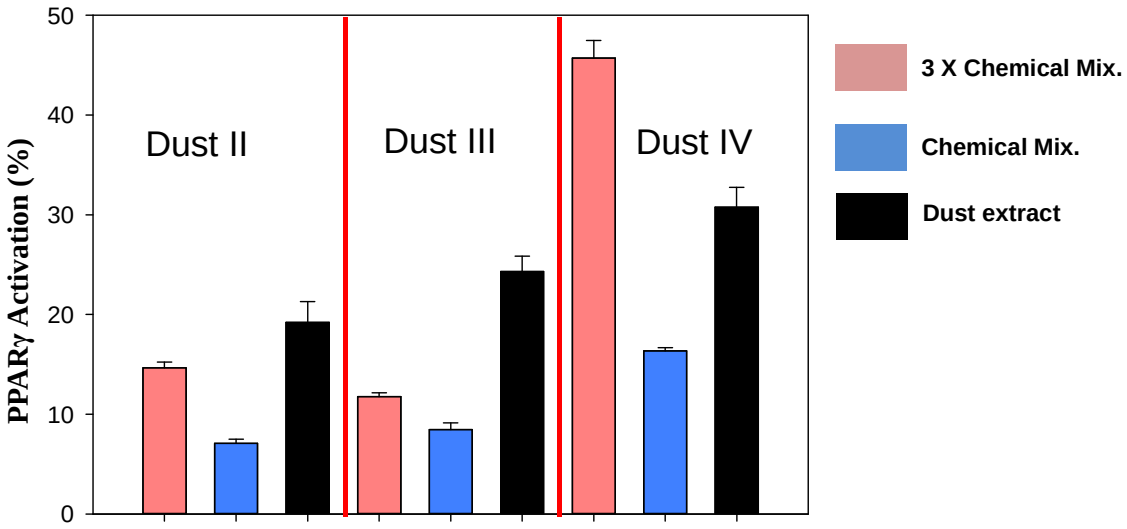

Figure 46. PPARγ activation (%) observed in the three dust extracts (~606 μg DEQ/mL) and the fatty acid mixture containing equivalent concentrations of OA, PA, SA, and MA. The fatty acid mixture was tested at the concentration measured in the dust extract and at a concentration equivalent to three times the measured concentration. Dust II and III were the dust extracts used in the NP-HPLC fractionation and Dust IV was one of the fresh dust extracts tested.

Appendix E: PPARγ activation by mixtures present in human serum

To investigate the possible effect of a mixture of SVOCs commonly measured in human serum on PPARγ activation, we prepared a mixture with the same ratio of concentrations reported in serum from previous studies (Frederiksen et al. 2010; Jonsson et al. 2001; Kannan et al. 2010; Kim and Oh 2014; Rantakokko et al. 2008; Rawn et al. 2014) (see Table 15 for mixture details). In the mixture we included TPP, MEHP, TBT, TPT, 2,4,6-TBP and BDE47 due to their frequent detection and relatively high abundance in serum, or high potency in PPARγ activation. As shown in Figure 47, the combination of the PPARγ agonists were found to activate PPARγ. The maximal activation was close to 40% by serum relevant GM concentrations. The overall dose response relationship of the mixture overlapped with TBT, and TBT appeared to be the dominant contributor. To further verify this, organotins were excluded in the mixture and no obvious activation was observed. However, the activation was observed (~10% maximal activation) if the concentration increases by 9 times. Furthermore, TPP could be the major contributor in this scenario due to its high concentration in the serum.

Overall, this study suggested that the level of those chemicals in the serum could probably activate PPARγ in vivo. However, it should be noted that TBT was measured in human serum collected in 1990 from the US, and the concentrations in the current human population may have changed due to the phase-out of TBT as the anti-fouling material (IMO, 2001) (Organisation. 2002), though it is still the byproduct of MBT and DBT and can be frequently detected in the house dust with a median of 22 ng/g dust

(ranging from <2 to 300ng/g) (Kannan et al. 2010). PPARγ activation observed after excluding organotins failed to induce any obvious PPARγ response at environmentally relevant doses. However, significant activation was observed when increasing the relevant GM concentration by 9 times and TPP seems to be the major contributor. TPP has a NOAEL value of approximately 0.4μM and the GM value of TPP in serum was reported at 0.43μM (Jonsson et al. 2001). It should be noted that few reports on TPP levels in serum are available and the concentration used in this study was only from one study with three subjects, which could increase the uncertainty of the result. Also, the measurement from the references was based on populations from different countries and the exposure might vary considerably between countries. According to several recent studies, DPP, which is the metabolite of TPP measured in human urine, can range from 1.1 to 3.4ng/mL with a GM of 1.9ng/mL (Butt et al. 2014) and could reach up to 1μM in the serum (our unpublished data), which is higher than the NOAEL of TPP. The maximum MEHP concentration measured in serum was 19.3 ng/mL (70nM) (Frederiksen et al. 2010), which was just lower than the NOAEL of MEHP (100nM) calculated in this study. Overall, no clear additive effect was observed for tested chemical mixtures in this study, which could be due to the great potency range of these chemicals in activating PPARγ. In the case of estrogen-active compounds and pharmaceuticals, significant effects were observed after mixing several weak agonists at their reported NOAEL (Pomati et al. 2006; Silva et al. 2002). Therefore, further studies on the mixture effect of various PPARγ agonists at various concentration ratios should be investigated.

Table 15. Concentrations of several known PPARγ agonists in human serum from previous studies.

Chemicals	Range Concentration	GM (ng/mL serum)	GM (nM)	NOAEL (nM)	Sampling sites	References
TBT	<1-85 ng/mL (n=32)	8.18	25.13	0.91	US	(Kannan et al. 1999)
TPT	<LOQ-0.56 ng/mL (n=300)	0.09	0.23	1.40	Finland	(Rantakokko et al. 2008)
TPP	0.13-0.15 μg/g plasma (n=3)	140	429.08	400.00	Sweden	(Jonsson et al. 2001)
TBBPA	<MDL to 713 ng/g lipid (n=76)	0.27*	0.50	50.00	South Korea	(Kim and Oh 2014)
BDE47	12-43 ng/g lipid (n=4,583)	0.14*	0.29	800.00	Canada	(Rawn et al. 2014)
MEHP	<LOD to 19.3 ng/mL (n=60)	7.88	28.31	100.00	Netherland	(Frederiksen et al. 2010)
2,4,6-TBP	5-60 ng/g lipd (n=?)	0.12*	0.36	400.00	US	Our data

*0.6% was used as the lipid content in the serum (Keller et al. 2009).

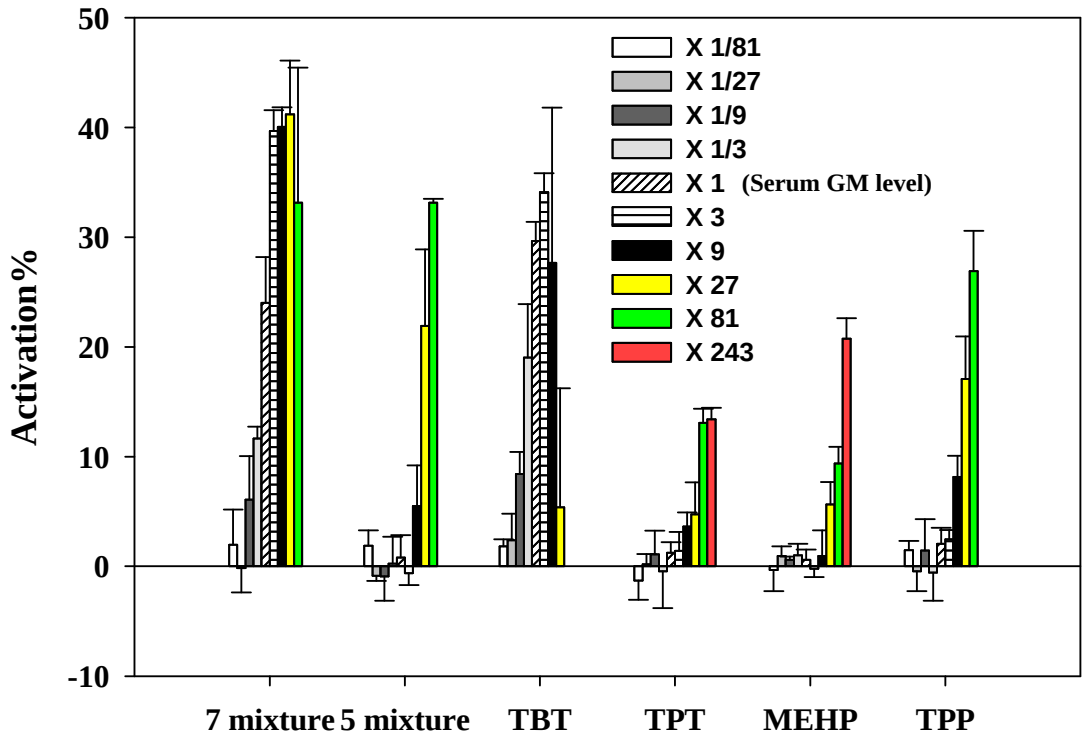

Figure 47. Dose-response relationship of PPARγ activation by several known PPARγ agonists with a fixed serum GM concentration ratio. "7 mixture" includes TBT, TPT, MEHP, TPP, BDE47, 2,4,6-TBP, and TBBPA. "5 mixture" includes other components except TBT and TPT. Values represent the average of the triplicates, and error bars represent standard deviation.

References

Albro PW. 1986. Absorption, metabolism, and excretion of di(2-ethylhexyl) phthalate by rats and mice. Environ Health Perspect 65: 293-298.

Albro PW, Thomas RO. 1973. Enzymatic hydrolysis of di-(2-ethylhexyl) phthalate by lipases. Biochimica et biophysica acta 306(3): 380-390.

Belcher SM, Cookman CJ, Patisaul HB, Stapleton HM. 2014. In vitro assessment of human nuclear hormone receptor activity and cytotoxicity of the flame retardant mixture FM 550 and its triarylphosphate and brominated components. Toxicology letters 228(2): 93-102.

Bell-Parikh LC, Ide T, Lawson JA, McNamara P, Reilly M, FitzGerald GA. 2003. Biosynthesis of 15-deoxy-delta12,14-PGJ2 and the ligation of PPARgamma. The Journal of clinical investigation 112(6): 945-955.

Berger J, Moller DE. 2002. The mechanisms of action of PPARs. Annual review of medicine 53: 409-435.

Brack W. 2003. Effect-directed analysis: a promising tool for the identification of organic toxicants in complex mixtures? Anal Bioanal Chem 377(3): 397-407.

Brack W, Klamer HJC, de Ada ML, Barcelo D. 2007. Effect-directed analysis of key toxicants in European river basins - A review. Environ Sci Pollut R 14(1): 30-38.

Brack W, Schirmer K. 2003. Effect-directed identification of oxygen and sulfur heterocycles as major polycyclic aromatic cytochrome P4501A-inducers in a contaminated sediment. Environ Sci Technol 37(14): 3062-3070.

Butt CM, Congleton J, Hoffman K, M. F, Stapleton HM. 2014. Metabolites of Organophosphate Flame Retardants and 2-Ethylhexyl Tetrabromobenzoate in Urine from Paired Mothers and Toddlers. Environ Sci Technol In Press.

Butt CM, Wang DL, Stapleton HM. 2011. Halogenated Phenolic Contaminants Inhibit the In Vitro Activity of the Thyroid-Regulating Deiodinases in Human Liver. Toxicol Sci 124(2): 339-347.

Butte W, Heinzow B. 2002. Pollutants in house dust as indicators of indoor contamination. Rev Environ Contam T 175: 1-46.

Carignan CC, Heiger-Bernays W, McClean MD, Roberts SC, Stapleton HM, Sjodin A, et al. 2013a. Flame Retardant Exposure among Collegiate United States Gymnasts. Environmental Science & Technology 47(23): 13848-13856.

Carignan CC, McClean MD, Cooper EM, Watkins DJ, Fraser AJ, Heiger-Bernays W, et al. 2013b. Predictors of tris(1,3-dichloro-2-propyl) phosphate metabolite in the urine of office workers. Environ Int 55: 56-61.

Carrière F, Grandval P, Gregory PC, Renou C, Henniges F, Sander-Struckmeier S, et al. 2005. Does the pancreas really produce much more lipase than required for fat digestion? JOP 6(3): 206-215.

Choate LM, Ranville JF, Bunge AL, Macalady DL. 2006. Dermally adhered soil: 1. Amount and particle-size distribution. Integrated environmental assessment and management 2(4): 375-384.

Collins CD, Mosquera-Vazquez M, Gomez-Eyles JL, Mayer P, Gouliarmou V, Blum E. 2013. Is there sufficient 'sink' in current bioaccessibility determinations of organic pollutants in soils? Environ Pollut 181: 128-132.

Cooper EM, Covaci A, van Nuijs ALN, Webster TF, Stapleton HM. 2011. Analysis of the flame retardant metabolites bis(1,3-dichloro-2-propyl) phosphate (BDCPP) and diphenyl phosphate (DPP) in urine using liquid chromatography-tandem mass spectrometry. Anal Bioanal Chem 401(7): 2123-2132.

Costera A, Feidt C, Dziurla MA, Monteau F, Le Bizec B, Rychen G. 2009. Bioavailability of polycyclic aromatic hydrocarbons (PAHs) from soil and hay matrices in lactating goats. Journal of agricultural and food chemistry 57(12): 5352-5357.

Covaci A, Harrad S, Abdallah MA, Ali N, Law RJ, Herzke D, et al. 2011. Novel brominated flame retardants: a review of their analysis, environmental fate and behaviour. Environment international 37(2): 532-556.

Desvergne B, Wahli W. 1999. Peroxisome proliferator-activated receptors: nuclear control of metabolism. Endocrine reviews 20(5): 649-688.

Dodson RE, Perovich LJ, Covaci A, Van den Eede N, Ionas AC, Dirtu AC, et al. 2012. After the PBDE Phase-Out: A Broad Suite of Flame Retardants in Repeat House Dust Samples from California. Environmental Science & Technology 46(24): 13056-13066.

EPA. Furniture Flame Retardancy Partnership: Environmental Profiles of Chemical Flame Retardant Alternatives; EPA 742-R-05-002A; U.S. EPA: Washington, DC, 2005.

Fallingborg J. 1999. Intraluminal pH of the human gastrointestinal tract. Danish medical bulletin 46(3): 183-196.

Fang M, Getzinger G, Copper E, Di Giulio R, Ferguson L, Stapleton H. 2014a. Effect-Directed Analysis (EDA) of Elizabeth River Porewater: Developmental Toxicity in Zebrafish (Danio rerio). Environmental Toxicology and Chemistry.

Fang M, Webster TF, Ferguson PL, Stapleton HM. 2014b. Characterizing the Peroxisome Proliferator–Activated Receptor (PPARγ) Ligand Binding Potential of Several Major Flame Retardants, Their Metabolites, and Chemical Mixtures in House Dust Environ Health Perspective In Press.

Fang M, Webster TF, Gooden D, Cooper EM, McClean MD, Carignan C, et al. 2013. Investigating a novel flame retardant known as V6: measurements in baby products, house dust, and car dust. Environ Sci Technol 47(9): 4449-4454.

Fang M, Webster TF, Stapleton HM. 2015. Activation of Human Peroxisome Proliferator-Activated Nuclear Receptors (PPARγ) by Semi-Volatile Compounds (SVOCs) and Chemical Mixtures in Indoor Dust. Submitted.

Feige JN, Gelman L, Rossi D, Zoete V, Métivier R, Tudor C, et al. 2007. The endocrine disruptor monoethyl-hexyl-phthalate is a selective peroxisome proliferator-activated receptor gamma modulator that promotes adipogenesis. J Biol Chem 282(26): 19152-19166.

Finkelstein EA, Trogdon JG, Cohen JW, Dietz W. 2009. Annual medical spending attributable to obesity: payer-and service-specific estimates. Health Aff (Millwood) 28(5): w822-831.

Frederiksen H, Jorgensen N, Andersson AM. 2010. Correlations Between Phthalate Metabolites in Urine, Serum, and Seminal Plasma from Young Danish Men Determined by Isotope Dilution Liquid Chromatography Tandem Mass Spectrometry. J Anal Toxicol 34(7): 400-410.

Fromme H, Lahrz T, Piloty M, Gebhart H, Oddoy A, Ruden H. 2004. Occurrence of phthalates and musk fragrances in indoor air and dust from apartments and kindergartens in Berlin (Germany). Indoor air 14(3): 188-195.

Gajda T, Jancso A. 2010. Organotins. Formation, Use, Speciation, and Toxicology. Metal Ions Life Sci 7: 111-151.

Gaylor MO, Harvey E, Hale RC. 2013. Polybrominated diphenyl ether (PBDE) accumulation by earthworms (Eisenia fetida) exposed to biosolids-, polyurethane foam microparticle-, and Penta-BDE-amended soils. Environmental science & technology 47(23): 13831-13839.

Gouliarmou V, Collins CD, Christiansen E, Mayer P. 2013. Sorptive physiologically based extraction of contaminated solid matrices: incorporating silicone rod as absorption sink for hydrophobic organic contaminants. Environ Sci Technol 47(2): 941-948.

Gouliarmou V, Mayer P. 2012. Sorptive bioaccessibility extraction (SBE) of soils: combining a mobilization medium with an absorption sink. Environ Sci Technol 46(19): 10682-10689.

Grün F, Blumberg B. 2009. Endocrine disrupters as obesogens. Mol Cell Endocrinol 304(1-2): 19-29.

Grün F, Watanabe H, Zamanian Z, Maeda L, Arima K, Chubacha R, et al. 2006. Endocrine-disrupting organotin compounds are potent inducers of adipogenesis in vertebrates. Mol Endocrinol 20(9): 2141-2155.

Harwood AD, Landrum PF, Weston DP, Lydy MJ. 2013. Using SPME fibers and Tenax to predict the bioavailability of pyrethroids and chlorpyrifos in field sediments. Environmental Pollution 173: 47-51.

Hauser R, Calafat AM. 2005. Phthalates and human health. Occupational and environmental medicine 62(11).

Herbstman JB, Sjodin A, Kurzon M, Lederman SA, Jones RS, Rauh V, et al. 2010. Prenatal exposure to PBDEs and neurodevelopment. Environ Health Perspect 118(5): 712-719.

Hilscherova K, Machala M, Kannan K, Blankenship AL, Giesy JP. 2000. Cell bioassays for detection of aryl hydrocarbon (AhR) and estrogen receptor (ER) mediated activity in environmental samples. Environmental science and pollution research international 7(3): 159-171.

Hites RA. 2004. Polybrominated diphenyl ethers in the environment and in people: a meta-analysis of concentrations. Environ Sci Technol 38(4): 945-956.

Hoffman K, Daniels JL, Stapleton HM. 2014a. Urinary metabolites of organophosphate flame retardants and their variability in pregnant women. Environ Int 63: 169-172.

Hoffman K, Fang M, Horman B, Patisaul HB, Garantziotis S, Birnbaum LS, et al. 2014b. Urinary Tetrabromobenzoic Acid (TBBA) as a Biomarker of Exposure to the Flame Retardant Mixture Firemaster(R) 550. Environ Health Perspect 122(9): 963-969.

Hollert H, Durr M, Holtey-Weber R, Islinger M, Brack W, Farber H, et al. 2005. Endocrine disruption of water and sediment extracts in a non-radioactive dot blot/RNAse protection-assay using isolated hepatocytes of rainbow trout. Environmental science and pollution research international 12(6): 347-360.

Hoppin JA, Brock JW, Davis BJ, Baird DD. 2002. Reproducibility of urinary phthalate metabolites in first morning urine samples. Environ Health Perspect 110(5): 515-518.

Hurst CH, Waxman DJ. 2003. Activation of PPARalpha and PPARgamma by environmental phthalate monoesters. Toxicol Sci 74(2): 297-308.

Huwe JK, Hakk H, Smith DJ, Diliberto JJ, Richardson V, Stapleton HM, et al. 2008. Comparative absorption and bioaccumulation of polybrominated diphenyl ethers following ingestion via dust and oil in male rats. Environmental Science & Technology 42(7): 2694-2700.

International Maritime Organisation. 2002. "Focus on IMO - Anti-fouling systems". http://www.imo.org/OurWork/Environment/Anti-foulingSystems/Documents/FOULING2003.pdf.

Janesick A, Blumberg B. 2011. Minireview: PPARgamma as the target of obesogens. J Steroid Biochem Mol Biol 127(1-2): 4-8.

Janesick A, Blumberg B. 2011. The Role of Environmental Obesogens in the Obesity Epidemic. In: Obesity Before Birth, Vol. 30, (Lustig RH, ed):Springer US, 383-399.

Johnson PI, Stapleton HM, Slodin A, Meeker JD. 2010. Relationships between Polybrominated Diphenyl Ether Concentrations in House Dust and Serum. Environmental Science & Technology 44(14): 5627-5632.

Jonsson OB, Dyremark E, Nilsson UL. 2001. Development of a microporous membrane liquid-liquid extractor for organophosphate esters in human blood plasma: identification of triphenyl phosphate and octyl diphenyl phosphate in donor plasma. J Chromatogr B 755(1-2): 157-164.

Kamstra JH, Hruba E, Blumberg B, Janesick A, Mandrup S, Hamers T, et al. 2014. Transcriptional and epigenetic mechanisms underlying enhanced in vitro adipocyte differentiation by the brominated flame retardant BDE-47. Environ Sci Technol 48(7): 4110-4119.

Kannan K, Senthilkumar K, Giesy JP. 1999. Occurrence of butyltin compounds in human blood. Environmental Science & Technology 33(10): 1776-1779.

Kannan K, Takahashi S, Fujiwara N, Mizukawa H, Tanabe S. 2010. Organotin compounds, including butyltins and octyltins, in house dust from Albany, New York, USA. Archives of environmental contamination and toxicology 58(4): 901-907.

Keller JM, Swarthout RF, Carlson BK, Yordy J, Guichard A, Schantz MM, et al. 2009. Comparison of five extraction methods for measuring PCBs, PBDEs, organochlorine pesticides, and lipid content in serum. Anal Bioanal Chem 393(2): 747-760.

Khim JS, Villeneuve DL, Kannan K, Lee KT, Snyder SA, Koh CH, et al. 1999. Alkylphenols, polycyclic aromatic hydrocarbons, and organochlorines in sediment from

Lake Shihwa, Korea: Instrumental and bioanalytical characterization. Environmental Toxicology and Chemistry 18(11): 2424-2432.

Kierkegaard A, De Wit CA, Asplund L, McLachlan MS, Thomas GO, Sweetman AJ, et al. 2009. A mass balance of tri-hexabrominated diphenyl ethers in lactating cows. Environmental science & technology 43(7): 2602-2607.

Kim UJ, Oh JE. 2014. Tetrabromobisphenol A and hexabromocyclododecane flame retardants in infant-mother paired serum samples, and their relationships with thyroid hormones and environmental factors. Environmental Pollution 184: 193-200.

Klosterhaus S. KA, Davis E., Klein J., Stapleton H. 2009. Characterization of organophosphorus chemicals in a PentaBDE replacement mixture and their detection in biosolids. San Francisco Estuary Institute, San Francisco, CA. 1th Annual Workshop on Brominated Flame Retardants Available at: http://wwwsfeiorg/documents/2717.

Kokatnur MG, Oalmann MC, Johnson WD, Malcom GT, Strong JP. 1979. Fatty acid composition of human adipose tissue from two anatomical sites in a biracial community. Am J Clin Nutr 32(11): 2198-2205.

Lehrke M, Lazar MA. 2005. The many faces of PPARgamma. Cell 123(6): 993-999.

Lei L, Suidan MT, Khodadoust AP, Tabak HH. 2004. Assessing the bioavailability of PAHs in field-contaminated sediment using XAD-2 assisted desorption. Environ Sci Technol 38(6): 1786-1793.

Lepom P, Berndt M, Duffek A, Warmbrunn-Suckrow E. 2013. Oral Bioaccessibility of PBDEs in Dust Using an In Vitro Gastrointestinal Model. Brominated Flame Retardant Symposium.

Lin Q, Ruuska SE, Shaw NS, Dong D, Noy N. 1999. Ligand selectivity of the peroxisome proliferator-activated receptor alpha. Biochemistry 38(1): 185-190.

Lu CX, Cheng SY. 2010. Thyroid hormone receptors regulate adipogenesis and carcinogenesis via crosstalk signaling with peroxisome proliferator-activated receptors. J Mol Endocrinol 44(3): 143-154.

Luo L, Lin S, Huang HL, Zhang SZ. 2012. Relationships between aging of PAHs and soil properties. Environ Pollut 170: 177-182.

McGee SP, Konstantinov A, Stapleton HM, Volz DC. 2013. Aryl Phosphate Esters Within a Major PentaBDE Replacement Product Induce Cardiotoxicity in Developing Zebrafish Embryos: Potential Role of the Aryl Hydrocarbon Receptor. Toxicol Sci 133(1): 144-156.

McIntyre TM, Pontsler AV, Silva AR, St Hilaire A, Xu Y, Hinshaw JC, et al. 2003. Identification of an intracellular receptor for lysophosphatidic acid (LPA): LPA is a transcellular PPARgamma agonist. Proceedings of the National Academy of Sciences of the United States of America 100(1): 131-136.

McKenna NJ, O'Malley BW. 2002. Combinatorial control of gene expression by nuclear receptors and coregulators. Cell 108(4): 465-474.

McLachlan MS. 1994. Model of the fate of hydrophobic contaminants in cows. Environmental science & technology 28(13): 2407-2414.

Meeker JD, Cooper EM, Stapleton HM, Hauser R. 2013. Urinary Metabolites of Organophosphate Flame Retardants: Temporal Variability and Correlations with House Dust Concentrations. Environ Health Persp 121(5): 580-585.

Meerts IATM, van Zanden JJ, Luijks EAC, van Leeuwen-Bol I, Marsh G, Jakobsson E, et al. 2000. Potent competitive interactions of some brominated flame retardants and related compounds with human transthyretin in vitro. Toxicol Sci 56(1): 95-104.

Michalik L, Auwerx J, Berger JP, Chatterjee VK, Glass CK, Gonzalez FJ, et al. 2006. International Union of Pharmacology. LXI. Peroxisome proliferator-activated receptors. Pharmacological reviews 58(4): 726-741.

Mid West Research Institute. 1979. Assessment of the need for limitation on triaryl and trialkyl/aryl phosphates. Report prepared for the United States Environmental Protection Agency, contract no. 68-01-4313. Mid West Research Institute, Kansas City, Mo.

Montaño M, Cocco E, Guignard C, Marsh G, Hoffmann L, Bergman A, et al. 2012. New approaches to assess the transthyretin binding capacity of bioactivated thyroid hormone disruptors. Toxicol Sci 130(1): 94-105.

Montaño M, Weiss J, Hoffmann L, Gutleb AC, Murk AJ. 2013. Metabolic activation of nonpolar sediment extracts results in enhanced thyroid hormone disrupting potency. Environ Sci Technol 47(15): 8878-8886.

MRIGlobal. 2012. Chemical Identity and Purity Screen of tert-Butylphenyl diphenyl phosphate (BPDP).

Nagorka R, Scheller C, Ullrich D. 2005. Plasticizer in house dust. Gefahrst Reinhalt L 65(3): 99-105.

Nagy L, Tontonoz P, Alvarez JG, Chen H, Evans RM. 1998. Oxidized LDL regulates macrophage gene expression through ligand activation of PPARgamma. Cell 93(2): 229-240.

Ness-Abramof R, Apovian CM. 2005. Drug-induced weight gain. Timely topics in medicine Cardiovascular diseases 9: E31.

Nolte RT, Wisely GB, Westin S, Cobb JE, Lambert MH, Kurokawa R, et al. 1998. Ligand binding and co-activator assembly of the peroxisome proliferator-activated receptor-gamma. Nature 395(6698): 137-143.

Noyes PD, Hinton DE, Stapleton HM. 2011. Accumulation and debromination of decabromodiphenyl ether (BDE-209) in juvenile fathead minnows (Pimephales promelas) induces thyroid disruption and liver alterations. Toxicol Sci 122(2): 265-274.

O'Brien J, Wilson I, Orton T, Pognan F. 2000. Investigation of the Alamar Blue (resazurin) fluorescent dye for the assessment of mammalian cell cytotoxicity. European journal of biochemistry / FEBS 267(17): 5421-5426.

Ogden CL, Carroll MD, Kit BK, Flegal KM. 2012. Prevalence of obesity and trends in body mass index among US children and adolescents, 1999-2010. Jama 307(5): 483-490.

Oomen AG, Hack A, Minekus M, Zeijdner E, Cornelis C, Schoeters G, et al. 2002. Comparison of five in vitro digestion models to study the bioaccessibility of soil contaminants. Environmental science & technology 36(15): 3326-3334.

Patisaul HB, Roberts SC, Mabrey N, McCaffrey KA, Gear RB, Braun J, et al. 2013. Accumulation and endocrine disrupting effects of the flame retardant mixture Firemaster(R) 550 in rats: an exploratory assessment. J Biochem Mol Toxicol 27(2): 124-136.

Pereira-Fernandes A, Demaegdt H, Vandermeiren K, Hectors TL, Jorens PG, Blust R, et al. 2013. Evaluation of a screening system for obesogenic compounds: screening of endocrine disrupting compounds and evaluation of the PPAR dependency of the effect. PloS one 8(10): e77481.

Pillai HK, Fang M, Beglov D, Kozakov D, Vajda S, Stapleton HM, et al. 2014. Ligand Binding and Activation of PPARgamma by Firemaster(R) 550: Effects on Adipogenesis and Osteogenesis. Environ Health Perspect.

Pomati F, Castiglioni S, Zuccato E, Fanelli R, Vigetti D, Rossetti C, et al. 2006. Effects of a complex mixture of therapeutic drugs at environmental levels on human embryonic cells. Environ Sci Technol 40(7): 2442-2447.

Qiu X, Mercado-Feliciano M, Bigsby RM, Hites RA. 2007. Measurement of polybrominated diphenyl ethers and metabolites in mouse plasma after exposure to a commercial pentabromodiphenyl ether mixture. Environ Health Perspect 115(7): 1052-1058.

Rantakokko P, Turunen A, Verkasalo PK, Kiviranta H, Mannisto S, Vartiainen T. 2008. Blood levels of organotin compounds and their relation to fish consumption in Finland. Sci Total Environ 399(1-3): 90-95.

Rawn DF, Ryan JJ, Sadler AR, Sun WF, Weber D, Laffey P, et al. 2014. Brominated flame retardant concentrations in sera from the Canadian Health Measures Survey (CHMS) from 2007 to 2009. Environ Int 63: 26-34.

Ricchi M, Odoardi MR, Carulli L, Anzivino C, Ballestri S, Pinetti A, et al. 2009. Differential effect of oleic and palmitic acid on lipid accumulation and apoptosis in cultured hepatocytes. Journal of gastroenterology and hepatology 24(5): 830-840.

Riu A, Grimaldi M, le Maire A, Bey G, Phillips K, Boulahtouf A, et al. 2011. Peroxisome Proliferator-Activated Receptor gamma Is a Target for Halogenated Analogs of Bisphenol A. Environ Health Persp 119(9): 1227-1232.

Riu A, McCollum CW, Pinto CL, Grimaldi M, Hillenweck A, Perdu E, et al. 2014. Halogenated Bisphenol-A Analogs Act as Obesogens in Zebrafish Larvae (Danio rerio). Toxicol Sci 139(1): 48-58.

Roberts SC, Macaulay LJ, Stapleton HM. 2012. In Vitro Metabolism of the Brominated Flame Retardants 2-Ethylhexyl-2,3,4,5-Tetrabromobenzoate (TBB) and Bis(2-ethylhexyl) 2,3,4,5-Tetrabromophthalate (TBPH) in Human and Rat Tissues. Chem Res Toxicol 25(7): 1435-1441.

Rossi AM, Taylor CW. 2011. Analysis of protein-ligand interactions by fluorescence polarization. Nat Protoc 6(3).

Ruby MV, Fehling KA, Paustenbach DJ, Landenberger BD, Holsapple MP. 2002. Oral bioaccessibility of dioxins/furans at low concentrations (50-350 ppt toxicity equivalent) in soil. Environ Sci Technol 36(22): 4905-4911.

Rudel RA, Camann DE, Spengler JD, Korn LR, Brody JG. 2003. Phthalates, alkylphenols, pesticides, polybrominated diphenyl ethers, and other endocrine-disrupting compounds in indoor air and dust. Environ Sci Technol 37(20): 4543-4553.

Schopfer FJ, Lin Y, Baker PR, Cui T, Garcia-Barrio M, Zhang J, et al. 2005. Nitrolinoleic acid: an endogenous peroxisome proliferator-activated receptor gamma ligand. Proceedings of the National Academy of Sciences of the United States of America 102(7): 2340-2345.

Schwarzenbach RP, Gschwend MP, Imboden MD. 2005. Environmental Organic Chemistry. Willey Interscience.

Silva E, Rajapakse N, Kortenkamp A. 2002. Something from "nothing"--eight weak estrogenic chemicals combined at concentrations below NOECs produce significant mixture effects. Environ Sci Technol 36(8): 1751-1756.

Springer C, Dere E, Hall SJ, McDonnell EV, Roberts SC, Butt CM, et al. 2012. Rodent Thyroid, Liver, and Fetal Testis Toxicity of the Monoester Metabolite of Bis-(2-ethylhexyl) Tetrabromophthalate (TBPH), a Novel Brominated Flame Retardant Present in Indoor Dust. Environ Health Persp 120(12): 1711-1719.

Stapleton HM, Allen JG, Kelly SM, Konstantinov A, Klosterhaus S, Watkins D, et al. 2008. Alternate and new brominated flame retardants detected in U.S. house dust. Environ Sci Technol 42(18): 6910-6916.

Stapleton HM, Eagle S, Sjodin A, Webster TF. 2012a. Serum PBDEs in a North Carolina toddler cohort: associations with handwipes, house dust, and socioeconomic variables. Environ Health Perspect 120(7): 1049-1054.

Stapleton HM, Klosterhaus S, Eagle S, Fuh J, Meeker JD, Blum A, et al. 2009. Detection of Organophosphate Flame Retardants in Furniture Foam and US House Dust. Environ Sci Technol 43(19): 7490-7495.

Stapleton HM, Klosterhaus S, Keller A, Ferguson PL, van Bergen S, Cooper E, et al. 2011. Identification of flame retardants in polyurethane foam collected from baby products. Environ Sci Technol 45(12): 5323-5331.

Stapleton HM, Misenheimer J, Hoffman K, Webster TF. 2014. Flame Retardant Associations Between Children's Handwipes and House Dust. Chemosphere In Press.

Stapleton HM, Misenheimer J, Hoffman K, Webster TF. 2014. Flame retardant associations between children's handwipes and house dust. Chemosphere 30(14): 00039-00033.

Stapleton HM, Sharma S, Getzinger G, Ferguson PL, Gabriel M, Webster TF, et al. 2012b. Novel and High Volume Use Flame Retardants in US Couches Reflective of the 2005 PentaBDE Phase Out. Environmental Science & Technology 46(24): 13432-13439.

Strynar MJ, Lindstrom AB. 2008. Perfluorinated compounds in house dust from Ohio and North Carolina, USA. Environmental science & technology 42(10): 3751-3756.

Suzuki G, Takigami H, Watanabe M, Takahashi S, Nose K, Asari M, et al. 2008. Identification of brominated and chlorinated phenols as potential thyroid-disrupting compounds in indoor dusts. Environmental Science & Technology 42(5): 1794-1800.

Suzuki G, Tue NM, Malarvannan G, Sudaryanto A, Takahashi S, Tanabe S, et al. 2013. Similarities in the endocrine-disrupting potencies of indoor dust and flame retardants by

using human osteosarcoma (U2OS) cell-based reporter gene assays. Environ Sci Technol 47(6): 2898-2908.

Svendsen A. 2000. Lipase protein engineering. Bba-Protein Struct M 1543(2): 223-238.

Tang-Peronard JL, Andersen HR, Jensen TK, Heitmann BL. 2011. Endocrine-disrupting chemicals and obesity development in humans: A review. Obes Rev 12(8): 622-636.

Tilston EL, Gibson GR, Collins CD. 2011. Colon extended physiologically based extraction test (CE-PBET) increases bioaccessibility of soil-bound PAH. Environ Sci Technol 45(12): 5301-5308.

Trasande L, Attina TM, Sathyanarayana S, Spanier AJ, Blustein J. 2013. Race/ethnicity-specific associations of urinary phthalates with childhood body mass in a nationally representative sample. Environ Health Perspect 121(4): 501-506.

Tue NM, Suzuki G, Takahashi S, Isobe T, Trang PT, Viet PH, et al. 2010. Evaluation of dioxin-like activities in settled house dust from Vietnamese E-waste recycling sites: relevance of polychlorinated/brominated dibenzo-p-dioxin/furans and dioxin-like PCBs. Environ Sci Technol 44(23): 9195-9200.

Tung EW, Boudreau A, Wade MG, Atlas E. 2014. Induction of adipocyte differentiation by polybrominated diphenyl ethers (PBDEs) in 3T3-L1 cells. PloS one 9(4): e94583.

U.S. EPA. (2009) Child-specific exposure factors handbook. Available: http://cfpub.epa.gov/ncea/cfm/recordisplay.cfm?deid=55145. Accessed 2012 December 17.

Van den Berg M, Birnbaum L, Bosveld AT, Brunstrom B, Cook P, Feeley M, et al. 1998. Toxic equivalency factors (TEFs) for PCBs, PCDDs, PCDFs for humans and wildlife. Environ Health Perspect 106(12): 775-792.

Van den Eede N, Dirtu AC, Neels H, Covaci A. 2011. Analytical developments and preliminary assessment of human exposure to organophosphate flame retardants from indoor dust. Environ Int 37(2): 454-461.

van der Heijden SA, Jonker MTO. 2009. PAH Bioavailability in Field Sediments: Comparing Different Methods for Predicting in Situ Bioaccumulation. Environmental science & technology 43(10): 3757-3763.

Wang H, Zhou Y, Tang C, He Y, Wu J, Chen Y, et al. 2013. Urinary phthalate metabolites are associated with body mass index and waist circumference in Chinese school children. PloS one 8(2): e56800.

Wania F, Dugani CB. 2003. Assessing the long-range transport potential of polybrominated diphenyl ethers: A comparison of four multimedia models. Environ Toxicol Chem 22(6): 1252-1261.

Watkins DJ, McClean MD, Fraser AJ, Weinberg J, Stapleton HM, Webster TF. 2013. Associations between PBDEs in office air, dust, and surface wipes. Environ Int 59: 124-132.

Webster TF, Harrad S, Millette JR, Holbrook RD, Davis JM, Stapleton HM, et al. 2009. Identifying transfer mechanisms and sources of decabromodiphenyl ether (BDE 209) in indoor environments using environmental forensic microscopy. Environ Sci Technol 43(9): 3067-3072.

WHO. 2014. Global Nutrition Targets 2025. Childhood Overweight. Policy Brief http://apps.who.int/iris/bitstream/10665/149021/2/WHO_NMH_NHD_14.6_eng.pdf?ua=1.

Wong F, Bidleman TF. 2011. Aging of Organochlorine Pesticides and Polychlorinated Biphenyls in Muck Soil: Volatilization, Bioaccessibility, and Degradation. Environmental Science & Technology 45(3): 958-963.

Yang X, Lv Z, Bian Y, Wang F, Gu C, Song Y, et al. 2013. Predicting PAHs bioavailability for earthworms by mild solvents and Tenax extraction. Journal of Environmental Chemical Engineering 1(4): 768-776.

Yu YX, Pang YP, Li C, Li JL, Zhang XY, Yu ZQ, et al. 2012. Concentrations and seasonal variations of polybrominated diphenyl ethers (PBDEs) in in- and out-house dust and human daily intake via dust ingestion corrected with bioaccessibility of PBDEs. Environ Int 42: 124-131.

Zhang JW, Zhao Y, Xu CF, Hong YN, Lu HL, Wu JP, et al. 2014. Association between serum free fatty acid levels and nonalcoholic fatty liver disease: a cross-sectional study. Scientific reports 4.

Zhang Y, Meng X, Chen L, Li D, Zhao L, Zhao Y, et al. 2014. Age and sex-specific relationships between phthalate exposures and obesity in Chinese children at puberty. PloS one 9(8): e104852.

Biography

Mingliang Fang was born in a small village in the city of Lu'an, Anhui Province, China. He received his bachelor degree (Honored) in Environmental Engineering (School of Chemical Engineering) from Xi'an Jiao Tong University in 2006 and Master of Science (Honored) in Environmental Chemistry from Pohang University of Science and Technology in 2011. During 2006-2009, he worked as an EHS (environmental, health, and safety) engineer in the drilling department affiliated to China Offshore Oil Company. After joining Duke University in 2011 as PhD student majoring Environmental Chemistry and Toxicology, he have completed many projects with diverse directions, including the identification of emerging contaminants, in vitro/in vivo metabolism as well as biomarker identification, and effect-directed analysis on complex environmental mixtures to find the causal compounds leading to the observed adverse effect. In general, his expertise is on the application of mass spectrometry and high throughput bioanalytical techniques such as in vitro and in vivo bioassays to investigate the health effects of xenobotioc chemicals or mixture exposure. To date, he has published 14 papers and 8 of them were first-authored and 4 manuscripts are still under review or to be submitted.

Fang ML, and Stapleton HM. Evaluating the Bioaccessibility of Flame Retardants in House Dust using an In Vitro Tenax Bead-Assisted Sorptive Physiologically Based Method. Environmental Science and Technology, 2014, 18;48(22):13323-30. doi: 10.1021/es503918m.

Fang ML, Webster TF, and Stapleton HM. Characterize the PPARγ Ligand Binding Potential of Several Major Flame Retardants, Their Metabolites, Indoor Dust and Bioactivated Dust. Environmental Health Perspective, 2014, doi:10.1289/ehp.1408522.

Hoffman K, Fang ML* (co-first author), Patisaul HB, Garantziotis S, Birnbaum LS, Stapleton HM. Urinary Tetrabromobenzoic Acid (TBBA) as a Biomarker of Exposure to the Flame Retardant Mixture Firemaster 550. Environmental Health Perspective, 2014 Sep;122(9):963-9. doi: 10.1289/ehp.1308028.

Fang ML, Getzinger G (co-first author), Ferguson PL, Stapleton HM. Effect-directed analysis (EDA) of Elizabeth River Porewater: Developmental Toxicity in Zebrafish (Danio rerio). Environmental Toxicology and Chemistry, 2014, Vol. 33, No. 12, pp. 2767–2774.

Pillai H, Fang ML, Beglov D, Vajda S., Stapleton HM, Webster TF, Schlezinger JJ (2014). The Flame Retardant Firemaster 550 Contains PPARγ Ligands That Induce Adipogenesis and Suppress Osteogenesis. Environmental Health Perspective, 2014, doi:10.1289/ehp.1408111.

Fang ML, Kim JC, and Chang YS. Characterizing Dechlorane Plus (DP) and its stereoisomer profile in different particle size fractions of marine sediments. Science of the Total Environment, 2014; 481:114-20.

Craig Butt, Johanna Congleton (co-first author), Kate Hoffman, Mingliang Fang, and Heather M Stapleton. Metabolites of Organophosphate Flame Retardants and 2-Ethylhexyl Tetrabromobenzoate (EH-TBB) in Urine from Paired Mothers and Toddlers. Environmental Science and Technology, 2014, 48 (17), pp 10432–10438, doi: 10.1021/es5025299.

CJ Wolf, M Fang, HM Stapleton, BD Abbott. Activation of Human Peroxisome Proliferator-Activated Receptor-Gamma (PPAR gamma) by House Dust Extracts. Birth Defects Research Part A: Clinical and Molecular Teratology 100 (5), 2014, 393-393.

Fang ML, Webster TF, Gooden DM, Cooper E., McClean MD, Carignan CC, Makey C, and Stapleton HM. Investigating a novel flame retardant known as V6: measurements in baby products, house dust, and car dust. Environmental Science and Technology. 2013 May 7;47(9):4449-54.

Fang ML, Choi SD, Baek SY, Jin GZ, Chang YS. Deposition of polychlorinated biphenyls and polybrominated diphenyl ethers in the vicinity a steel manufacturing plant. Atmospheric Environment, Volume 49, March 2012, 206-211.

Fang ML, Choi SD, Baek SY, Park H, Chang YS (2011). Atmospheric bulk deposition of polychlorinated dibenzo-p-dioxins and dibenzofurans (PCDD/Fs) in the vicinity of an iron and steel making plant. Chemosphere. 2011 Aug; 84(7):894-9.

Jin GZ, Fang ML, Kang JH, Park H, Lee SH, Chang YS (2011). Monitoring of PCBs at facilities related with PCB-containing products and wastes in South Korea. Journal of Hazardous Material. 2011 Nov 30; 196:295-301.

Wu Q, Baek SY, Fang ML, Chang YS (2010). Distribution and fate of polybrominated diphenyl ethers in indoor environments of elementary schools. Indoor Air. 2010 Jun; 20(3):263-70.